Dependency of Ly49 Recognition on Anchor Residues of Peptide Bound to MHC-I

by

Elsa Aurora Marquez

A thesis submitted in partial fulfillment of the requirements for the degree of

Doctor of Philosophy

in

IMMUNOLOGY

Department of Medical Microbiology and
Immunology University of Alberta

ABSTRACT

In rodents, Ly49s are prominent natural killer (NK) cell receptors that interact with peptide-bound class I major histocompatibility complex (MHC-I). This association generally induces inhibitory signals when MHC-I presents self-peptides, thus blocking NK cell activation against healthy cells. Inhibitory Ly49 receptors can be peptide selective in their recognition of MHC-I-peptide complexes, affording them a level of discrimination beyond detecting the presence or absence of specific MHC-I allele products. NK cell inhibitory Ly49s associate with MHC-I at a region under the MHC-I peptide binding groove, without direct contact with the peptide bound; however, specific details of peptide dependent Ly49 recognition have not been fully explored.

The mouse NK cell receptor Ly49C recognize its MHC-I ligand H-2K^{b} in a peptide selective and specific fashion. However, the molecular basis for Ly49C peptide specific recognition of H-2K^{b} has not been fully elucidated. Utilizing functional assays, we demonstrated that both the auxiliary anchor residue at position 3 (P3) and the adjacent residue at position 2 (P2), that also anchors into the peptide binding groove, influence Ly49C peptide selectivity in recognition of H-2K^{b}. In particular, we found that the Ly49C and H-2K^{b} interaction is supported by non-polar aliphatic residues at P3 and bulky non-polar aliphatic residues at P2. Previous studies in our laboratory also showed the importance of peptide anchor residues in determining recognition between a rat Ly49 receptor, Ly49i2, and its cognate ligand RT1-A1^{c}. This suggests that peptide anchor residues bound to MHC-I may be modulators of Ly49 peptide specificity in rodent models of Ly49 and MHC-I interaction.

In addition, we used functional assays to demonstrate peptide-dependent antagonism of mouse NK cell inhibition using as a model Ly49C and H-2K^b association. Partial NK cell antagonism, in other words partial depression of inhibition, was observed during the co-presentation of peptide-MHC-I (pMHC-I) complexes that support Ly49C-H-2K^b interaction and pMHC-I complexes that can bind Ly49C at an intermediate level. In contrast, a weaker antagonistic phenotype was observed by co-expression of pMHC-I complexes that confer H-2K^b and Ly49C interaction together with pMHC-I complexes that bind Ly49C at low to null levels.

Collectively, our studies show that peptides bound to H-2K^b are fundamental in the integration of NK cell signaling events that determine NK activity. Rodent Ly49 receptors can play an important role in NK cell function for the clearance of tumorigenic cells as well as virally infected cells. Given that the peptide repertoire within a cell is subjected to modifications during cell stress, such as tumorigenesis or viral infection, it is of importance to understand how Ly49 directed NK cell function is affected by the nature of the peptides bound to MHC-I.

ACKNOWLEDGEMENTS

Firstly, I want to thank my supervisor Dr. Kevin Kane for his support through my years in graduate school and to my supervisory committee, Drs. Debby Burshtyn and John Elliott, for their feedback.

The production of this thesis would not have been possible without a great team in both the Kane and Ostergaard labs, and I will always be grateful for their support inside and outside the lab.

I also want to thank friends in the department that are not only kind but are also talented scientists that I hold in high regard.

Lastly and more importantly I want to thank my family for their continuous encouragement, love and patience.

TABLE OF CONTENTS

CHAPTER **PAGE**

LIST OF FIGURES

FIGURE **DESCRIPTION** **PAGE**

LIST OF TABLES

TABLE **DESCRIPTION** **PAGE**

LIST OFABBREVIATIONS

Ab antibody

ADCC antibody-dependend cell-mediated cytotoxictiy

APC antigen presenting cell

β2m β-2-microglobulin

CD cluster of differentiation

CTLD C-type lectin-like domain

DC dendritic cell

DRiPs defective ribosomal products

ER endoplasmic reticulum

FACS fluorescence activated cell sorter

FasL Fas ligand

GM-CSF granulocyte monocyte stimulating factor

G-CSF granulocyte colony-stimulating factor

M-CSF macrophage colony-stimulating factor

GVHD graft-versus-host disease

GVL graft-versus-leukemia

HLA human leukocyte antigen

IFN-γ interferon-γ

Ig immunoglobulin

IL interleukin

IPTG isopropyl-1-thio-β-D-galactopyranoside

ITAM immunoreceptor tyrosine-based activation motif

ITIM immunoreceptor tyrosine-based inhibitory motif

KIR killer cell immunoglobulin-like receptor

LAIR leukocyte associated immunoglobulin-like receptor

LILR leukocyte immunoglobulin-like receptor

LFA-1 lymphocyte function-associated antigen 1

LRC leukocyte receptor complex

mAb monoclonal antibody

Mac-1 macrophage-1 antigen

MHC-I MHC class I

MICA MHC-I chain related A

MICB MHC-I chain related B

mRNA messenger ribonucleic acid

MS multiple sclerosis

MULT1 murine UL-16-binding-protein-like transcript

NK natural killer

NKG natural killer group

NKT natural killer T cells

NOD non-obese diabetic

PIR paired immunoglobulin-like receptor

PLC peptide loading complex

pMHC-I peptide-MHC-I

PTM post translational modification

RA rheumatoid arthritis

SHP-1 Src homology 2-domain-containing tyrosine phosphatase 1

SLE systemic lupus erythematosus

Syk Src-family tyrosine kinase

TAP transporter associated with antigen processing

TNF tumor necrosis factor

TRAIL TNF-related apoptosis-inducing ligand

ULBP UL-16 binding protein

VSV vesicular stomatitis virus

CHAPTER I

INTRODUCTION

A. The Major Histocompatibility Complex

The discrimination between self and non-self is a fundamental feature of the immune system. The expression of major histocompatibility complex molecules at the cell surface is a key aspect of self and non-self recognition. The major histocompatibility complex (MHC) is a large region in the vertebrate genome that comprises genes fundamental for the immune system. In the mouse, the MHC complex, *H-2*, is encoded on chromosome 17. In humans, the MHC complex is known as the Human Leukocyte Antigen (*HLA*) complex and it is located in chromosome 6 (1). In both mice and human, MHC genes encompass three regions: class I, class II, and class III. Genes encoded in the class I region include highly polymorphic classical class I glycoproteins and low polymorphic non-classical class I proteins (1). Classical MHC class I (MHC-I) molecules are expressed in nucleated cells and serve to present antigens to $CD8^+$ T cells and natural killer (NK) cells (2, 3). Non-classical MHC-I molecules have lower levels of expression than classical MHC-I molecules and can present antigens to a variety of cell types such as αβ and ɣδ T cells, NKT cells and NK cells (4). The class II region of the MHC codes for highly polymorphic MHC molecules expressed in professional antigen presenting cells (APCs) for the presentation of exogenous antigens to $CD4^+$ T cells (5). The class II region also includes genes required for antigen processing such as the two

subunits that form the transporter associated with antigen processing *TAP1* and *TAP2* (1). Finally, the class III region codes for additional genes involved in immune responses such as proteins necessary for complement activation (Figure 1-1) (6). Therefore, the MHC complex is a dense genetic region imperative to the development of immunity and health of the host.

B. Classical class I MHC

Glycoproteins encoded by the classical class I MHC genes, are essential in the specific recognition of self, via adaptive and innate immune $CD8^+$ T cell and NK cell receptors, respectively. Classical MHC-I molecules are expressed in nucleated cells in jawed vertebrates. For the presentation of antigens, MHC-I molecules require the non-covalent association of three components: a heavy chain, a light chain and a small peptide. First, the heavy chain is a transmembrane protein encoded by the K, D, and L loci in mouse, while it is encoded by the HLA-A, B and C loci in humans. It associates non-covalently with the second component, a light chain, also known as β-2-microglobulin (β2m), encoded in chromosome 2 and 7 in mouse and human, respectively (1). Finally, an 8 to 10 amino acid peptide associates with the heavy chain to form a heterotrimer for stable expression at the cell surface (Figure 1-2A). The heavy chain is formed by three domains: α1, α2 and the membrane proximal α3 domain. The α1 and α2 domains form the peptide binding groove with two anti-parallel α-helical walls and a β-pleated sheet floor (Figure 1-2B). Most of the polymorphisms in MHC-I molecules occur in the α1 and α2 domains; allowing the binding of a diverse repertoire of peptides (5). Polymorphisms within the peptide binding groove can influence the

identity of the peptide bound. Peptide binding to MHC-I can be restrictive and is granted to peptides that exhibit affinity for the heavy chain during complex formation in the endoplasmic reticulum (ER). While both N-terminal and C-terminal amino acids of the peptide are highly important for its association with the heavy chain; additional peptide residues that dock into cavities in the peptide binding groove are also essential for peptide binding and are known as anchor residues (Figure 1-3) (7, 8). The identity of the anchor residues of a given peptide bound to MHC-I, depend on the MHC-I allele and the identity of amino acids in pockets of the peptide binding groove (9, 10). The simultaneous expression of multiple MHC-I alleles with their distinct requirements for peptide anchor residues, increases the number of peptides that are presented to immune cells.

Depending on the identity of anchor residues that different MHC-I molecules can accept, MHC-I molecules are classified into supertypes (11-13). Interestingly, some supertypes have been conserved between species, suggesting that certain amino acids as anchor residues are favorable for the stable formation of MHC-I molecules. Peptide anchor residues can be further classified into primary and auxiliary anchor residues, both necessary for stable peptide binding (14). Primary anchor residues are usually highly conserved while auxiliary anchor residues are more variable (12). Thus, both primary and auxiliary anchor residues facilitate peptide binding to MHC-I molecules to form stable complexes at the cell surface for interaction with immune cell receptors.

C. The immunopeptidome

Peptides bound to MHC-I molecules are the refined product of endogenous or potentially exogenous proteins processed in the cell. The classical antigen processing pathway initiates with ubiquitination of cytoplasmic proteins for degradation into peptides by the proteasome (15, 16). The resulting peptides can be transported into the ER via the transporter associated with antigen processing (TAP) (17). In the ER, peptides can be trimmed by aminopeptidases and either used in the generation of MHC-I complexes or degraded entirely (18-21). At the same time, newly synthesized heavy chain associates temporarily with ER chaperones, calnexin and calreticulin, that facilitate its assembly. In addition, the thiol reductase ERp57 is recruited to aid in the formation of disulfide bonds and ensure correct folding of the heavy chain. The properly folded heavy chain forms a heterodimer with folded β2m that is recruited to associate with the peptide loading complex (PLC). PLC members include TAP, tapasin, ERp57 and calreticulin, that maintain the heterodimer at a peptide receptive conformation to facilitate peptide binding (22-27). Upon optimal peptide binding, stable MHC-I complexes egress from the ER and are transported to the cell surface (Figure 1-4).

Protein substrates for the generation of peptides can be derived from different sources. APCs, capable of endocytosis of extracellular materials, via different mechanisms, can process and release extracellular particles into the cytosol making these available for proteasomal degradation (28, 29). A supplemental source of peptides are proteins that failed transcription or translation, and these have been described as short-lived proteins that are usually products of non-coding mRNA sequences (30-32).

Finally, an additional, and major source of peptides, are defective ribosomal products (DRiPs) that result from mis-folded proteins produced from coding mRNA sequences (33, 34). Therefore, the pool of proteins available for antigen presentation, in particular at transcriptional and translational levels, can provide with an accurate representation of ongoing cellular events.

The peptide repertoire available for MHC-I binding can be influenced by the condition of the cell. During a normal and healthy state, MHC-I molecules associate with self-peptides and maintain steady-state MHC-I expression. However, cell stress resulting from viral infection or carcinogenic transformation, can lead to the presentation of either viral gene products or tumor-related proteins (35, 36). Peptide elution studies coupled with mass spectrometry analysis have made possible the identification of peptide precursors in cells subjected to stress. For instance, studies using neoplastic thymocytes revealed that 50% of the peptides eluted from MHC-I were the product of proteins involved in oncogenesis; with several proteins belonging to the PI3K-AKT-mTOR pathway, highly active in tumor cells (37, 38). In addition, due to aberrant regulation of post translational modifications (PTMs) in cancer cells, MHC-I molecules eluted from cancer cells have been shown to associate with peptides bearing PTMs in contrast to healthy cell controls. During tumorigenesis, peptides for MHC-I presentation can result from self proteins with irregular expression patterns or altered by addition of PTMs (35, 39). However, non-self peptides can also be presented on MHC-I as is the case of antigen presentation during pathogenesis.

Upon viral infection, the pool of peptides present in the cytosol can include those of viral origin. Virus entry into the host cell can release viral proteins into the cytosol and viruses use the host machinery to synthesize proteins needed for replication, making these proteins potential targets for degradation and peptide generation (40). Peptides derived from viral proteins can be loaded on the host MHC-I and can be immunogenic for T cell recognition or can also be used to "escape" T cell cytotoxicity (41-44). The ability to present non-self peptides serves to recapitulate the state of the cell and alert immune cells to respond accordingly.

The recognition of MHC-I molecules is fundamental for the health of the host. The presentation of self peptide-MHC-I (pMHC-I) complexes, or peptides presented during steady-state conditions, lead to a normal state where no immune cell activation is necessary. On the other hand, the presentation of altered-self, as is the case of peptides bearing PTM motifs due to carcinogenesis; or presentation of non-self peptides, as can occur with peptides derived from viral proteins, can lead to activation of cytotoxic cells to slow or terminate the spread of tumorigenesis or infection, respectively. Cytotoxic lymphocytes from the adaptive and innate immune system can recognize changes in MHC-I expression. Adaptive, $CD8^+$ T cells can directly recognize the peptide antigen on MHC-I, but do not respond or sense decreased levels of MHC-I, which is a strategy used by some viruses to escape $CD8^+$ T cell recognition (45-47). On the other hand, innate natural killer cells, are potent effector cells that can detect downregulation of MHC-I expression and can also recognize the peptide bound in an indirect manner (48-51). Together, both systems of recognition of MHC-I are required for the health of the host.

D. Role of natural killer cells

Natural killer (NK) cells are large granular lymphocytes that form part of the innate immune system. NK cells actively survey for virus infected and tumorigenic cells throughout lymphoid and non-lymphoid tissues. NK cells develop in the bone marrow and form 5-20% of peripheral lymphocytes in mice; while these comprise 2-10% of the total lymphocyte population in humans (52-54). In the periphery, NK cells are largely localized in the bone marrow, lymph nodes, liver, spleen, lung and blood (54, 55). Distribution between different tissues depends on homing receptors expressed on NK cells. In mouse, homing properties are described in terms of CD11b and CD27; while in humans localization of NK cells can be associated with expression of CD56 (56-58). Although the percentage of NK cells populating the periphery is low, their potent effector mechanisms are integral for mounting effective immune responses and supporting a heathy immune system.

NK cells have a broad spectrum of functional activity. Effector functions depend on the integration of activating and inhibitory signals mediated by receptors expressed at the cell surface. Upon the recognition of non-self or altered-self, NK cells can directly kill targets, produce cytokines or regulate the function of additional immune cells. NK cell cytotoxicity can take place by two routes, through degranulation or through activation of death receptors (59-62). Granules within NK cells contain perforin and granzymes, that are released onto target cells to mediate target cell membrane disruption and induce apoptosis, respectively (63). Apoptosis induced by death receptors tumor

necrosis factor-related apoptosis-inducing ligand (TRAIL) and Fas ligand (FasL) occurs by receptor recognition of ligands on target cells which can be upregulated as a result of tumor transformation (60-62, 64).

In addition to degranulation, NK cells can also release soluble pro-inflammatory cytokines such as interferon-γ (IFN-γ), tumor necrosis factor-α (TNF-α), granulocyte macrophage colony-stimulating factor (GM-CSF), granulocyte colony-stimulating factor (G-CSF), macrophage colony-stimulating factor (M-CSF), interleukin-15 (IL-15) and IL-13; as well as the anti-inflammatory cytokine IL-10 (48, 65). Given that NK cells express Fc receptors, they can also participate in the elimination of antibody coated cells by antibody-dependent cellular cytotoxicity (ADCC). Additionally, NK cells can influence the immune response by regulating other immune cells. For instance, NK cells can impact dendritic cell (DC) function by inducing DC maturation during infection (66). Finally, NK cell release of pro-inflammatory cytokines can lead to DC activation, further amplifying T cell activity, while NK cell secretion of chemokines, such as MIP-1 and RANTES, are linked to more effective adaptive immune responses against infection (66-71).

E. NK cells in health and disease

NK cells are part of the first line of defense against viral infection and oncogenic transformation. Their function depends on an integration of activating and inhibitory signals, mediated by cell surface receptors that recognize ligands on target cells. In order to escape T cell surveillance, some viruses decrease MHC-I expression; while others can cause the expression of stress ligands that engage NK activating receptors, rendering

infected cells susceptible to NK cell lysis (72, 73). NK cells are imperative against cytomegalovirus (CMV) infection in humans and mice (74-76). In addition to CMV, NK cells have been shown to play a role limiting infection by Influenza A, Sendai virus, human immunodeficiency, ebola, and hepatitis C virus (77-80).

The role of NK cells is not limited to defense against foreign pathogens, but includes detection and protection from neoplastic transformation. NK cells can be activated during oncogenesis by detecting a decrease in MHC-I expression, a phenomenon called "missing-self", where the decrease of MHC-I expression leads to NK activation (81). Additionally, cancer cells can also express activating ligands for NK cells and lead to NK cell lysis (82). Thus, NK cells can eliminate tumor cells from the circulation and are important to mount an immune response against MHC-I sufficient tumors and decrease cancer metastasis (83-88). Moreover, their potency against cancer cells can be harnessed to use as a therapeutic tool for the elimination of cancer cells (89).

Although NK cells can be highly cytotoxic upon detection of non-self or altered-self, NK cells are tolerant toward normal self, but can become pathogenic. During pregnancy, NK cells are tolerant and protect the fetus; however, pathological conditions during pregnancy such as recurrent miscarriage have been linked to NK cell reactivity (90). NK cells can also be involved in pathological conditions such as the progression of type 1 diabetes, demonstrated in NOD mice (91). In humans, NK cells can play a role in disease pathology during different stages of progression or remission in multiple sclerosis (MS), systemic lupus erythematosus (SLE) and rheumatoid arthritis (RA) (92-

94). For example, during RA, NK cells that are localized in synovium fluid of affected joints produce more IFN-ɣ compared to blood NK cells (94).

In addition, NK cells play an important role during transplantation, demonstrated by "hybrid resistance" where recipient NK cells can reject homozygous parental bone marrow transplanted into heterozygous F1 recipients (95). NK cells participate in the rejection of donor bone marrow cells in MHC mismatched bone marrow transplant, due to the lack of MHC-I ligands for inhibition of NK cell activation (96). However, NK cell mediated rejection of MHC mismatch cells can be beneficial in bone marrow transplants in leukemia patients, where alloreactive NK cells from the donor contribute to the elimination of the host cancer cells (97). Additionally, recipient NK cells are beneficial in reducing graft rejection by eliminating recipient T cells and DCs (98). The role of NK cells during health and disease can be attributed to the expression of various NK receptors that bind ligands on tissues targeted for surveillance.

F. Natural Killer cell receptors

NK cells express a diverse repertoire of receptors that allows for the recognition of healthy cells versus virus infected or tumorigenic cells. Unlike B- and T- cell receptors, NK cell receptors do not undergo gene rearrangement and are thus products of germline encoded genes. The effector functions of NK cells depend on a balance of activating and inhibitory signals mediated by receptor engagement with cognate ligand (99). Effective NK cell receptor transduction is facilitated by the formation of the immune synapse between NK effector cell and target cell that can include the

participation of adhesion molecules such as lymphocyte function-associated antigen 1 (LFA-1) and macrophage-1 antigen (Mac-1) (100, 101). At the synapse, enrichment of ligand and receptor interaction occurs and its formation is highly relevant for NK cell responses (102-106). NK cell inhibitory receptors contain an immunoreceptor tyrosine-based inhibitory motif (ITIM) in the cytoplasmic domain. Association of an inhibitory receptor with a corresponding ligand, triggers the phosphorylation of the tyrosine residue in the ITIM by a Src kinase. In turn, phosphatases containing SH2 domains are recruited to decrease phosphorylation of intracellular signaling molecules such as ZAP70, Syk, PLC□1, PLC□2, Shc, LAT, SLP76, and Vav-1, thereby increasing the threshold for NK cell activation, or halting it altogether (Figure 1-5) (107-111).

On the other hand, most activating receptors do not possess intracellular signaling domains. However, they can associate with signaling adaptor molecules via their transmembrane domain. Signaling adaptor molecules, such as DAP12 and DAP10, contain immunoreceptor tyrosine-based activation motifs (ITAM) (112). The association between activating receptors and adaptor molecules is not only necessary for signal transduction, but it can also be required for the expression of the receptor at the cell surface. Interaction between an activating receptor and its cognate ligand, leads to tyrosine phosphorylation of the ITAMs on the signaling adaptor. In turn, Syk kinases are recruited via SH2 domains and can phosphorylate downstream molecules, such as Erk1 and Erk2 that participate in the rearrangement of cytoskeletal proteins for NK cell degranulation (Figure 1-5) (113). The majority of the inhibitory and activating receptors

in murine and human NK cells are encoded in two different receptor complexes: the leukocyte receptor complex and the natural killer cell complex.

The Leukocyte receptor complex

The Leukocyte receptor complex (LRC) is encoded on chromosome 19 in humans and chromosome 7 in mice. It contains immunoglobulin (Ig) superfamily receptors that include the natural cytotoxicity receptors (NCRs), the leukocyte associated Ig-like receptors (LAIRs), the leukocyte Ig-like receptors (LILRs) and the killer-cell Ig-like receptors (KIRs). NCR receptor members include activating NKp46, NKp44 and NKp30 (114-116). While NKp46 is expressed on NK cells in humans and mice, NKp44 and NKp30 are only expressed in human NK cells (117, 118). NCRs recognize viral molecules such as hemagglutinin by NKp46 and NKp44 and their expression is important for the clearance of viral infection (119-123).

Additionally, both humans and mice express the inhibitory LAIR-1 molecule on a number of hematopoietic cells including NK cells (124, 125). The human and mouse LAIR-1 have been shown to bind collagen to inhibit NK activation. Collagen has been shown to be upregulated in tumor cells, suggesting that cancer cells might hijack LAIR-1 interaction to dampen anti-tumor NK cell responses (126, 127). The third LRC family of receptors are LILRs which include both activating and inhibitory receptors in humans (128). With the exception of LILRB1, most other LILR receptors are not known to be expressed in NK cells. LILRB1 is an inhibitory receptor that recognizes classical HLA-A, B and C molecules, as well as non-classical HLA-E and F molecules (129, 130). In

addition, LILRB1 can recognize a human cytomegalovirus (HCMV) MHC-I decoy protein, UL18 which can be detrimental for the clearance of infection (131). In mouse, the LILR family ortholog is the paired Ig-like receptor (PIR) family that contains both activating and inhibitory members that can recognize MHC-I molecules (132). PIRs are expressed on a range of immune cells such as B cells, macrophages and dendritic cells, but not on mouse NK cells (132). Finally, KIRs are the most diverse receptors in the LRC and comprise both activating and inhibitory receptors (133). KIRs recognize MHC-I molecules in an allele specific fashion and their diversity can be a result of co-evolution with their polygenic MHC-I ligands (134, 135). The precise number of KIR genes varies between individuals with anywhere between 9 and 14 genes encoded by the KIR locus (136-138).

The Natural Killer Complex

The natural killer complex (NKC) receptors are type II transmembrane glycoproteins that contain extracellular C-type lectin-like domains (CTLD). These include natural killer group (NKG) receptors, NKR-P receptors and Ly49s. NKG receptors include NKG2D, NKG2A, NKG2C, NKG2E, and NKG2F in humans and NKG2A, NKG2C, and NKG2E in mouse. NKG2D receptors are expressed as homodimers in human and mouse (139). NKG2D is an activating receptor expressed on NK cells, NKT cells, □□ T cells, $CD8^{+}$T cells and macrophages. NKG2D has been shown to play an important role during NK cell clearance of virus infection or tumorigenesis (139). The ligands for NKG2D in humans are stress-induced molecules such as MHC-I related proteins A and B (MICA and MICB), as well as UL16-binding

proteins (ULBPs) (140, 141). In mice, NKG2D binds Rae-1 and H60 family of ligands, in addition to murine UL16-binding protein-like transcript 1 (MULT1) (142, 143).

The NKG2 family of receptors, different from NKG2D, form heterodimers with CD94, a C-type lectin-like receptor also encoded in the NKC. NKG2 and CD94 heterodimers are expressed on a large population of NK cells and □□ T cells as well as on a subset of $CD8^{+}$T cells (144-147). In human, NKG2 receptors include NKG2A, NKG2C, NKG2E, and NKG2F; while mouse receptors consist of NKG2A, NKG2C, and NKG2E. Dimeric NKG2A/CD94 is an inhibitory receptor, while NKG2C/CD94, NKG2E/CD94 and NKG2H/CD94 are activating receptors. NKG2A/CD94 and NKG2C/CD94 recognize the non-classical MHC-I, HLA-E in human or $Qa\text{-}1^{b}$ in mouse (146, 148). Both HLA-E and $Qa\text{-}1^{b}$ can bind peptides derived from classical MHC-I leader sequences, displaying overall classical MHC-I expression (149, 150). The gene coding for NKG2F has a truncated extracellular region that renders it non-functional (151).

NKR-P1 receptors are mainly expressed in the mouse with NKR-P1A, NKR-P1B, NKR-P1C, NKR-P1D and NKR-P1F almost exclusively expressed in NK cells and activated $CD8^{+}$ T cells (152). In humans, only a single, non polymorphic NKR-P1 gene exists and is expressed on immature NK cells, IL-12 stimulated NK cells, and various subsets of T-cells (153-157). In mouse, NKR-P1 includes inhibitory and activating receptors, with inhibitory NKR-P1D and activating NKR-P1A, NKR-P1C, NKR-P1F and NKR-P1D receptors. The ligands for NKR-P1A and NKR-P1C are not known,

however, inhibitory NKR-P1D associates with Clr-b while activating NKR-P1F binds Clr-g (158, 159). The role of NKR-P1A in human is unclear since it it lacks a classical ITIM in its cytoplasmic domain and lacks residues in the transmembrane that would allow the association with adaptor molecules. Its cytoplasmic domain contains an ITIM-like sequence and could possibly mediate weak inhibitory functions (143, 144, 148). Lastly, Ly49 family members include both activating and inhibitory receptors (152, 160). Ly49 receptors are a multigene family predominantly expressed in rodents, while in humans only a single Ly49 region is found encoding a pseudogene (161). In mice, Ly49s are expressed on NK cells, NKT cells, a subset of T cells, B-cells, DCs and neurons (162-165). Ligands for Ly49 receptors include MHC-I molecules that can be recognized in an allele specific manner. In addition, some Ly49 receptors, such as activating Ly49H and inhibitory Ly49I, can interact with virus encoded genes that mimic MHC-I molecules such as m157, a MCMV decoy gene product (166-168).

Overall, NK cells express a broad array of activating and inhibitory receptors that influence NK function upon encounter with target cells. Within receptors from the LRC and NRC, KIRs and Ly49s have highly analogous expression and function with respect to ligand specificity and NK cell driven responses. Although structurally different, KIRs and Ly49s recognize cognate MHC-I molecules and are allele specific. Since NK cell functional dependency on Ly49 and MHC-I interaction is the topic of this thesis, I will provide more details on MHC-I association with Ly49s and what this association brings to NK cell biology.

G. Ly49 receptor expression and role in NK cell biology

Similar to KIRs, Ly49 receptors are polygenic with 16, 20, 9 and 22 genes in mouse strains C57BL/6, 129/SvJ, BALB/c, and NOD, respectively (Table 1-1) (169-172). Expression of activating and inhibitory Ly49s occurs during NK cell development, with inhibitory Ly49 expression acquired by a stochastic process. Ly49 receptor expression is essential for the development of fully functional NK cells, as demonstrated by the hyporesponsive state of NK cells that lack Ly49 receptor expression (173-176). The expression of Ly49s is necessary during NK cell education which can be influenced by MHC-I expression on hematopoietic and non-hematopoietic cells in the local environment (177, 178). The importance of MHC-I expression for NK cell education and acquisition of functional competence has been demonstrated in mice where MHC-I deficiency does not affect NK cell numbers but renders NK cells unable to respond against tumor cells that would otherwise be targets for lysis (179-181).

NK cell education can be MHC-I dependent or MHC-I independent. MHC-I dependent education can be described in terms of NK cell licensing by the arming and disarming models (182). During NK cell arming, interaction between MHC-I and MHC-I specific inhibitory receptor licenses NK cells to be functional (176, 183). NK cell disarming is mainly thought to be regulated by activating receptor signaling that leads to chronic stimulation and an anergic state that causes NK cells to be hypofunctional (182, 184). On the other hand, MHC-I independent NK cell education is thought to occur via non-MHC-I receptors or through cytokine stimulation (Figure 1-6) (185-188). NK cell education is an active process in the life of an NK cell. While education can take place

during development in the bone marrow, it can also occur in the periphery of adult hosts (176, 189, 190). The interaction of Ly49 with MHC-I is therefore not only essential during NK cell effector activity, but it is also crucial for the development of functional NK cells (191).

H. A structural view of Ly49 and MHC-I

NK cells were discovered in 1975 for their innate ability to kill cancer cells (192). Shortly after, NK cells were shown to be activated against target cells that lacked MHC-I expression; indicating NK inhibitory signaling mediated by MHC-I in MHC-I sufficient cancer cells (193). In the mouse, identification of inhibitory Ly49 receptors for MHC-I was described by Wayne Yokoyama and co-workers in 1992 (194). Since then, studies focused on Ly49 and MHC-I interaction have provided increasing evidence of the importance of their association for NK cell function.

Ly49 receptors are type II glycoproteins expressed as homodimers. Each Ly49 homodimer is formed by a CTLD, a membrane bound stalk region, a transmembrane and a cytoplasmic domain. Structurally CTLDs are composed of two anti-parallel β-sheets (β0, β1, β5 and β2, β2', β3, and β4) and two α-helices (α1 and α2) (195). Still, CTLDs structure can differ between Ly49 receptors. For instance, the Ly49C crystal structure showed that Ly49C has an additional α-helix (α3) that in other Ly49s such as Ly49A is a long loop (L3) instead (195, 196). Based on amino acid sequence of the L3/α3 region and secondary structure predictions, Ly49s can be divided into four groups: I, II, III, and IV. With the α3 region, Ly49C is the prototypical receptor for group I; while Ly49A is

the prototypical receptor for group II with the loop region in L3. Finally group III and IV receptors are Ly49B and Ly49Q, respectively. Both Ly49B and Ly49Q are predicted to acquire a random coil as L3 in group II receptors. However, phylogenetic analysis showed that due to sequence dissimilarity to group II members, and to each other, each falls into a distinct group (196, 197).

Inhibitory Ly49 receptors can recognize MHC-I molecules in an allele dependent mode with various levels of specificity (Table 1-2) (198, 199). The association between MHC-I and Ly49 has been described by mutagenesis and crystallography studies. Ly49 interaction with MHC-I occurs at a region underneath the MHC-I peptide binding groove and includes amino acids within the α1, α2 and α3 regions as well as the β2m (200-205). At the same time, amino acids within the Ly49 regions L3/α3, L5, L6, β3 and β4 participate in MHC-I interaction (Figure 1-7) (195). Ly49s have a flexible stalk that allows association with MHC-I on other cells (*in trans*) and can also bind MHC-I expressed on the NK cell itself (*in cis*) (206, 207). *Cis* interactions reduce the number of inhibitory Ly49 receptors available to bind MHC-I on other cells; thereby decreasing the potential for inhibitory signaling (176, 177, 206).

Interaction between Ly49 receptors and MHC-I molecules can occur with different stoichiometry. The Ly49A receptor has been demonstrated to associate with cognate ligand H-2D^b in a 'closed' conformation, by crystallography studies, where an Ly49A homodimer binds one H-2D^b molecule (196, 208). In addition, Ly49C can bind

H-2K^b in an 'open' conformation with bivalent stoichiometry, where one Ly49C CTLD can bind one H-2K^b molecule; similar to Ly49I interaction with H-2K^d (197, 201).

I. MHC-I peptide dependent NK cell function

NK cell receptors for MHC-I, Ly49 and KIR, in mouse and human respectively, not only discriminate between different MHC-I alleles, but they can also distinguish between different MHC-I bound peptides (49, 50, 209, 210). Inhibitory KIRs interact with MHC-I molecules at a site directly in contact with the peptide, involving peptide residues 7 and 8 that protrude upward from the peptide binding groove (211). The role of MHC-I peptide bound in KIR dependent NK cell function was described early in terms of single MHC-I peptide recognition. However, recent evidence suggests that peptides that do not support detectable KIR recognition of MHC-I, can play an active role by depressing NK cell inhibition, acting as antagonists of inhibitory KIR-MHC-I association (212).

MHC-I dependent agonistic and antagonistic phenotypes have been widely studied in T cells, in terms of T cell receptor (TCR) recognition of MHC-I (213-215). Peptides bound to MHC-I that trigger T cell activation are considered agonists; while peptide bound to MHC-I that disrupt the agonist's activating effect when co-presented with agonists are characterized as antagonist and lead to decreased T cell activation (215). Unlike agonist and antagonist phenotype in T cells, in NK cell biology an agonist peptide-MHC-I (pMHC-I) complex that interacts with inhibitory KIR leads to the NK inhibition. On the other hand, an antagonist pMHC-I complex, by itself does not interact

detectably with KIR, but when co-presented with an agonist pMHC-I, leads to a decrease in inhibition mediated by the agonist pMHC-I. As a result of peptide antagonism, NK cells can become more readily activated (212). The mechanism of NK cell antagonism has not been entirely described; however, it appears that antagonists disrupt the KIR association with agonist MHC-I complexes, leading to a decrease in phosphorylation of Vav1 signaling molecules (212). This study indicated that NK cells might be more sensitive than previously thought, by directly detecting changes in the peptides bound to MHC-I.

Rodent NK cells can also respond to changes in the peptide bound to MHC-I, in an Ly49 dependent manner. The inhibitory Ly49A receptor recognizes H-2D^{d} bearing any peptide; while rat Ly49i2 and mouse Ly49C and Ly49I are more discriminating in distinguishing the peptide bound to cognate MHC-I ligands (50, 210, 216-218). The importance of peptide discrimination relies on a mechanism where Ly49 dependent NK cell detection of self is not limited to lack of MHC-I gene products, but it extends to the peptide bound to MHC-I, allowing NK cells to detect changes in the peptide repertoire presented by MHC-I molecules.

J. Background and Rationale

Early work determining the specificity between Ly49 and MHC-I demonstrated that the CTLD region of Ly49s was required for the interaction with MHC-I (219). As for the MHC-I, α1 and α2 domains were shown to be important for Ly49 interaction; moreover, MHC-I interaction with Ly49s was supported by having MHC-I bound to a peptide (194, 220-224). Furthermore, mutagenesis studies localized in the peptide binding cleft showed that residues within this site were essential for Ly49 receptor recognition of MHC-I (225). Additional work also demonstrated the importance of the β2m in Ly49 recognition of MHC-I (203, 226). Overall these studies demonstrated that the three MHC-I components were required for Ly49 interaction, suggesting a role for Ly49s to survey for the proper folding of all three domains of MHC-I complexes.

Further studies on the role of the MHC-I bound peptide in Ly49 recognition demonstrated that amino acid at position 7 (P7) of the bound peptide contributed to H-2K^b association with Ly49C (210). Although other amino acids were tested, the poor ability of the peptide analogs to bind H-2K^b made it difficult to draw conclusions (210).

Studies in our laboratory to determine association between rat Ly49i2 and cognate ligand RT1-A1^c, showed that the amino acids comprising the B-pocket that secures the anchor residue at position 2 (P2) of the peptide bound to RT1-A1^c, influence recognition by the rat NK cell inhibitory receptor Ly49i2 (227). In addition, we showed that the specific amino acid identity of the P2 anchor residue bound to RT1-A1^c is critical to Ly49i2 recognition (218). These results suggested that both the MHC-I

primary anchor-binding pocket and its anchored residue are important to determine Ly49 recognition. Both results suggested that the B-pocket and its anchored amino acid affect the conformation below the floor of the MHC-I groove and/or β2m orientation which can affect the site of Ly49 recognition.

In mice, Ly49C recognizes H-2K^b bearing the SIINFEKL peptide, but not RGYVYQGL, AAYAYAAL, ESFSDYPPL and FAPGNYPAL (195, 210). In a study to identify peptide amino acids affecting Ly49C interaction with H-2K^b, Kärre and co-workers showed that amino acid at P7 had a partial influence in Ly49C recognition of H-2K^b. In order to identify the amino acids responsible for peptide specificity, SIINFEKL peptide analogs with substitutions at positions 1, 2, 3, 6, and 7 were created. Only peptide analogs with Ala at positions 1, 6 and 7 similarly bound H-2K^b, with only Ala substitution at P7 having a detrimental effect in Ly49C association with H-2K^b (210). However, the molecular basis of peptide dependent NK cell recognition and the impact of peptide dependent NK cell function have not been fully established. Taking in consideration our results on the role of anchor residues in inhibitory rat Ly49 recognition of MHC-I, as well as the impact that anchor residues can have on the floor of the peptide binding groove, we investigated whether anchor residues are also modulating Ly49C and H-2K^b association.

Due to the nature of anchor residues and their potency to form stable MHC-I complexes, I dedicated the first results chapter of this thesis to the process of optimizing selection of peptides and their use in forming stable H-2K^b complexes, while the second

results chapter focuses on the use of peptide analogs during functional assays in order to determine the role of individual residues of bound peptides on Ly49C interaction with H-2K^b. Finally, in the third results chapter, I analyzed the effect of co-presenting two different peptide-H-2K^b complexes on *ex vivo* NK cell function, in order to further our understanding of the role of peptide presentation on NK cell activity.

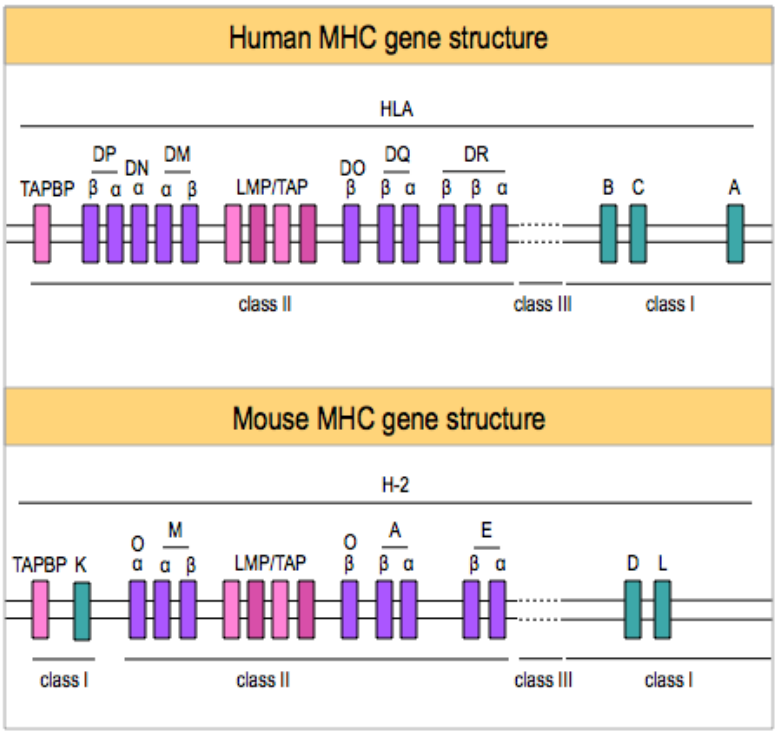

Figure 1-1. The Major Histocompatibility Complex in humans and mice. Schematic representation of genetic arrangement of the major histocompatibility complex (MHC). **(A)** In human, the MHC is known as human leukocyte antigen (HLA) while **(B)** in mice it is known as H-2. Genes in the MHC encode components of adaptive and innate immunity.

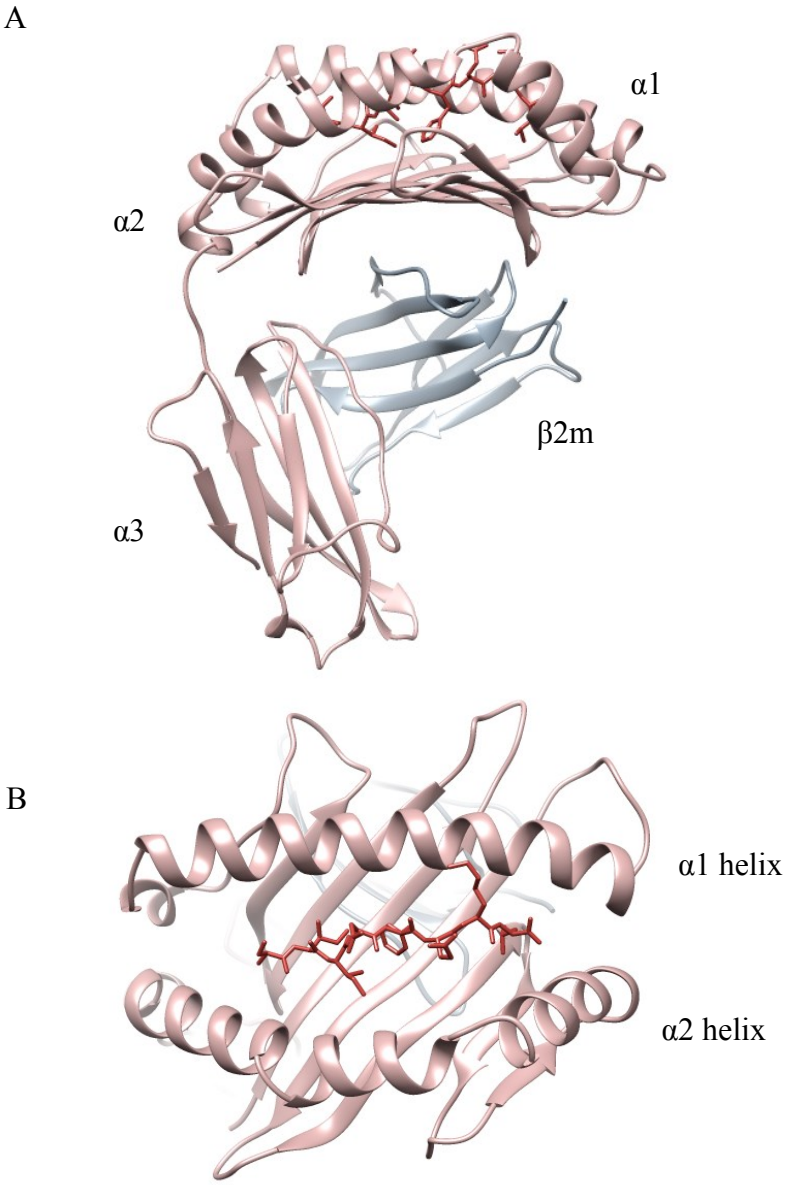

Figure 1-2. General structure of classical MHC-I molecules. (A) Side view of MHC-I heterotrimer composed of a heavy chain that non-covalently associates with a light chain, also known as β-2-microglobulin (β2m) and a small peptide. **(B)** Top view of the MHC-I molecule with a view of the peptide binding groove formed by the α1- and α2-helices and the β-pleated sheet floor, containing an 8 amino acid peptide. The heavy chain is depicted in pink ribbon, the β2m is in blue ribbon and the peptide is represented in red stick format. The figure was generated using CHIMERA UCSF software and the PDB ID coordinates 1VAC.

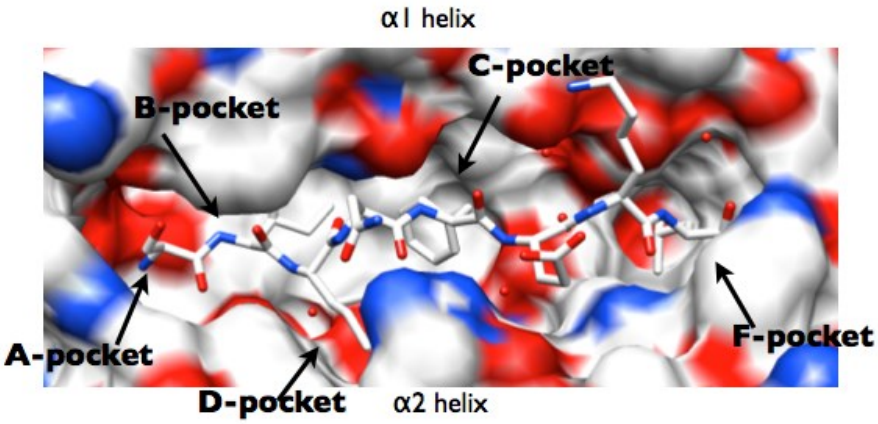

Figure 1-3. Peptide anchor residues stabilize peptide bound to MHC-I. Top view of the α1 and α2 domains of the mouse MHC-I molecule H-2K^b. A close up top view of the peptide binding groove formed by the α1 and α2 domains of mouse H-2K^b, show anchor residues docking into the A-, B-, C-, D- and F-pockets of the H-2K^b peptide binding groove. The α1 and α2 domains of H-2K^b are depicted as surface representation colored by heteroatom, the peptide is represented by stick structure colored by heteroatom. Red indicates negatively charged atoms, blue indicates positively charged atoms and white indicates neutral atoms. The figure was generated using CHIMERA UCSF software and the PDB ID coordinates 1VAC.

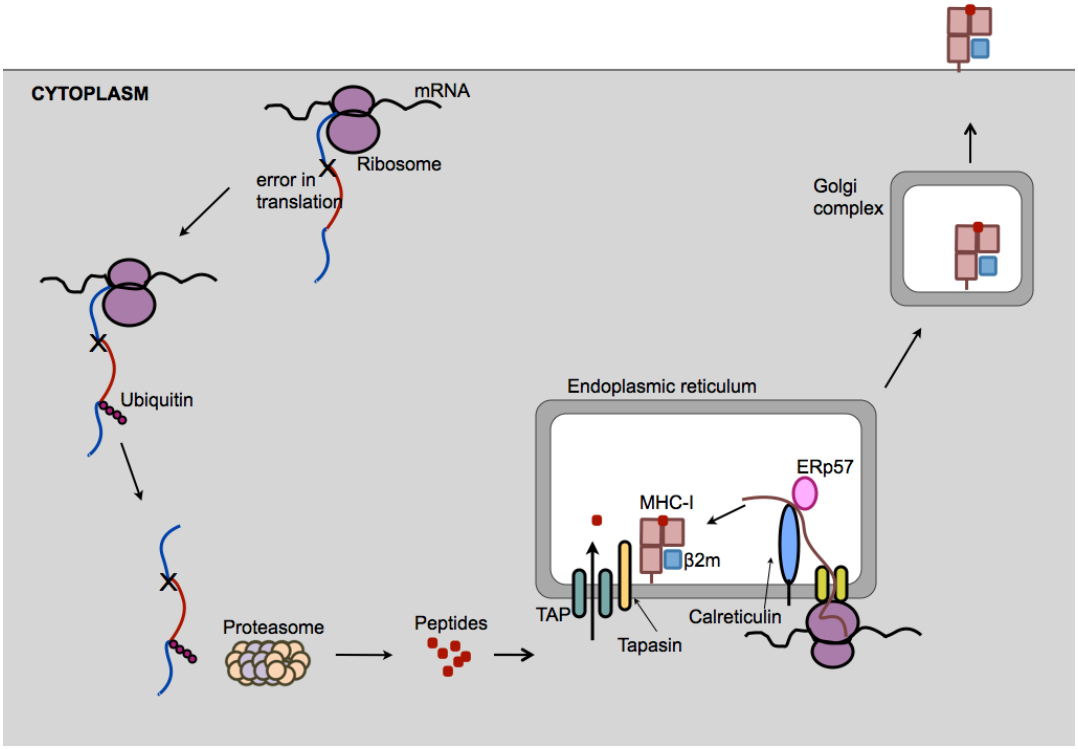

Figure 1-4. Antigen processing and presentation pathway. In the classical antigen processing pathway, proteins that undergo errors such as mis-folding, are targeted for ubiquitination and undergo proteasomal degradation that generates small peptides. Small peptides can be transported into the endoplasmic reticulum (ER) via the transporter associated with antigen processing (TAP). In the ER, peptides can be further trimmed by aminopeptidases and either used in the generation of MHC-I complexes or degraded. Simultaneously, newly synthesized heavy chain forms a heterodimer with β2m that is recruited to associate with the peptide loading complex (PLC). Components of the PLC are TAP, tapasin, ERp57 and calreticulin. The main function of the PLC is to facilitate peptide binding by maintaining the heavy chain-β2m heterodimer in a peptide receptive state. Once a suitable peptide is bound, stable MHC-I complexes are transported from the ER to the cell surface for peptide presentation.

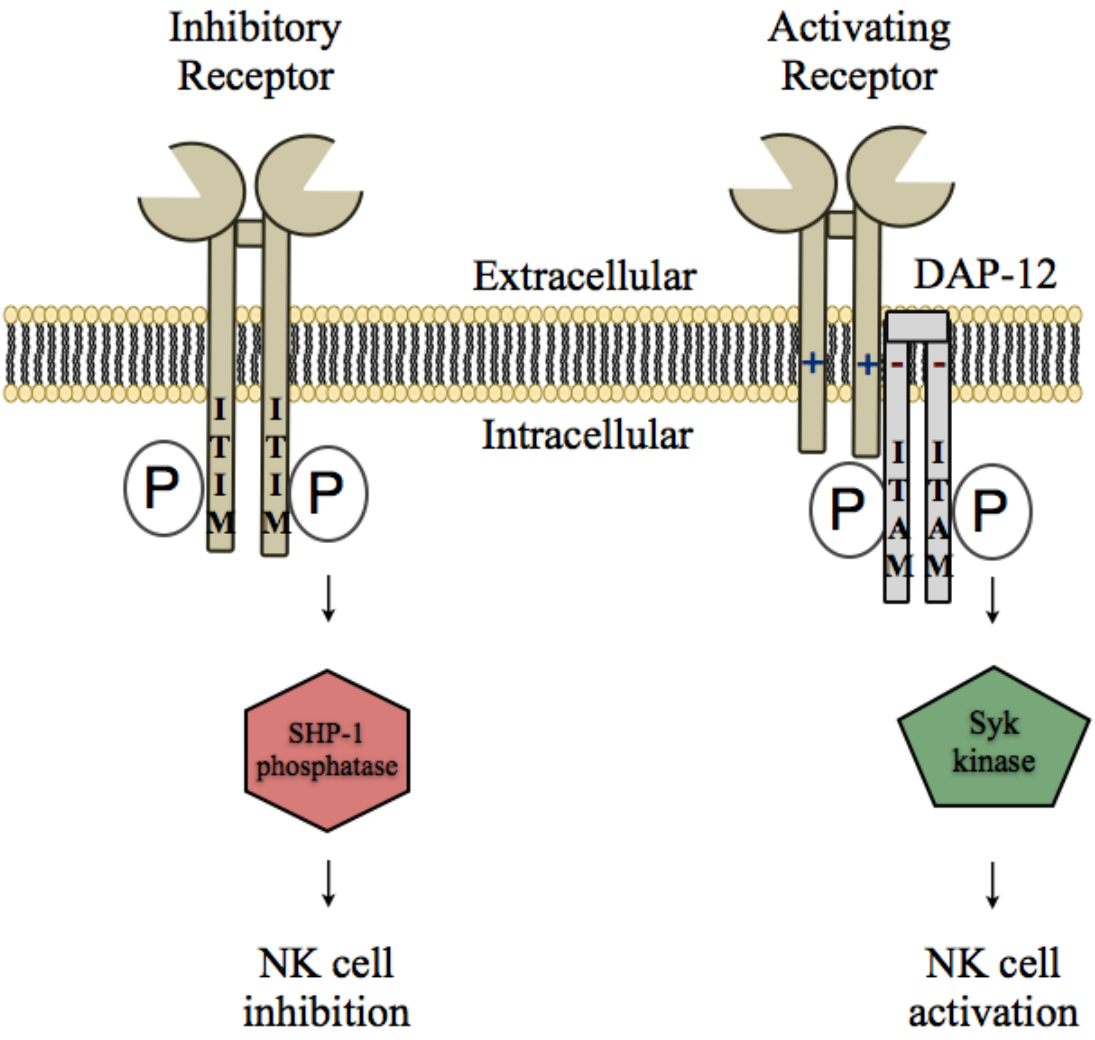

Figure 1-5. NK cell activating and inhibitory signaling. Inhibitory receptors contain immunoreceptor inhibitory motifs (ITIMs) sequences in their cytoplasmic domains. Upon receptor interaction with cognate ligand, the ITIMs become phosphorylated followed by SHP-1 recruitment leading to dephosphorylation and inhibition of NK cell activation. Activating receptors do not contain a signaling motif in their cytoplasmic domain. Nevertheless, activating receptors contain a positively charged residue in their transmembrane domains that supports the association with adaptor molecules that contain immunoreceptor tyrosine-based activating motifs (ITAMs) in their cytoplasmic domain. Upon receptor binding with ligand, ITAMs become phosphorylated followed by the recruitment of Syk kinase and a phosphorylation cascade that eventually leads to NK cell activation.

Mouse strain	Ly49 genes
C57BL/6	*q, e, x, f, d, k, h, n, i, g, l, m, c a, and b.*
129/SvJ	*q1, e, v, q2, e/c2, l/r, s, t, e/c1, r, u, u/i, i1, g. p/d, i2, p, o, and b.*
BALB/c	*q, e, y, i, g, l, c, a, and b.*
NOD	*q, e, x, f, d, u, i3, g2, p/d2, p3, i2, p2,i1, g1, p/d1, p1, w, m, h, c, a and b.*

Table 1-1. Mouse strains and Ly49 gene content. The multigene family of Ly49 receptors of mouse strains C57BL/6, 129/SvJ, BALB/c and NOD has been determined, with each strain expressing a set of Ly49 genes.

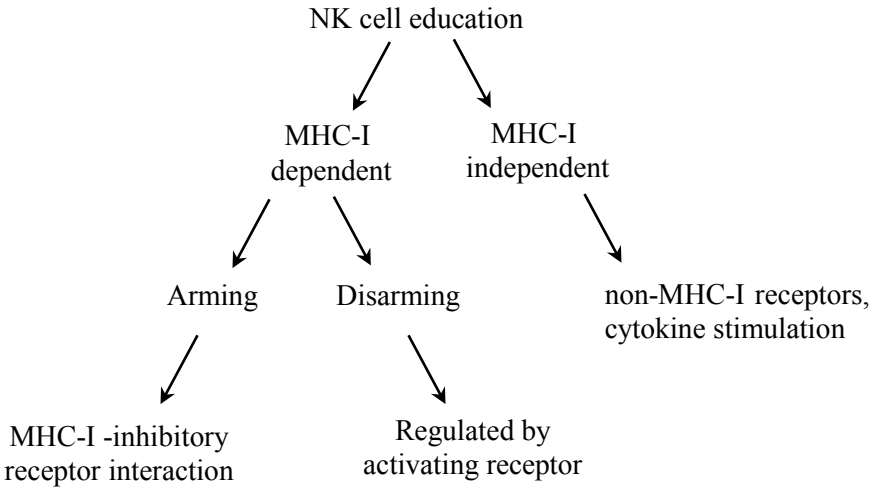

Figure 1-6. NK cell education. NK cell education is a process by which NK cells become functional and can be dependent or independent of MHC-I. MHC-I-dependent NK cell educationcan be explained by NK cell licensing described by the arming and disarming models. While NK cell arming requires NK cell MHC-I-specific inhibitory receptor interaction with cognate MHC-I, NK cell disarming is thought to be regulated by activating receptor mediated signals. On the other hand, MHC-I-independent NK cell education is thought to occur via non-MHC-I receptors or through cytokine stimulation.

RECEPTOR	ACTIVITY	LIGANDS
Ly49A	Inhibitory	H-2D $^{b, d, p, k}$, H2-M3
Ly49B	Inhibitory	unknown
Ly49C	Inhibitory	H-2K $^{b, d, k}$, H-2D$^{d, b, k}$, m157
Ly49D	Activating	H-2D^{d}
Ly49E	Inhibitory	unknown
Ly49F	Inhibitory	H-2D^{d}
Ly49G	Inhibitory	H-2D^{d}, H-2L^{d}
Ly49H	Activating	H-2D^{b}, m157
Ly49I	Inhibitory	H-2K$^{b, d, s, q, v}$, H-2D$^{b, d, s, q, v}$, m157
Ly49J	Inhibitory	H-2K^{b}
Ly49K	Activating	unknown
Ly49L	Activating	H-2K^{k}, H-2^{d}, H-2^{k}, H-2^{a}, H-2^{f}/m04
Ly49M	Activating	unknown
Ly49N	Activating	unknown
Ly49O	Inhibitory	H-2D$^{b,d, k}$, H-2L^{d}
Ly49P	Activating	H-2D^{d}, H-2D^{k}, H-2^{a}, H-2^{d}/m04
Ly49Q	Inhibitory	unknown
Ly49R	Activating	H-2D$^{d, k}$, H-2L^{d}
Ly49S	Inhibitory	unknown
Ly49T	Inhibitory	unknown
Ly49U	Activating	unknown
Ly49V	Inhibitory	H-2D$^{b, d}$, H-2K^{k}
Ly49W	Activating	H-2D^{d}, H-2K^{k}, H-2^{d}, H-2^{k}, H-2$^{f/}$m04

Table 1-2 Ligand specificity in mouse Ly49 recognition. Murine Ly49 receptors can recognize a variety of MHC-I ligands as well as viral derived products that have been shown to act as MHC-I decoy proteins.

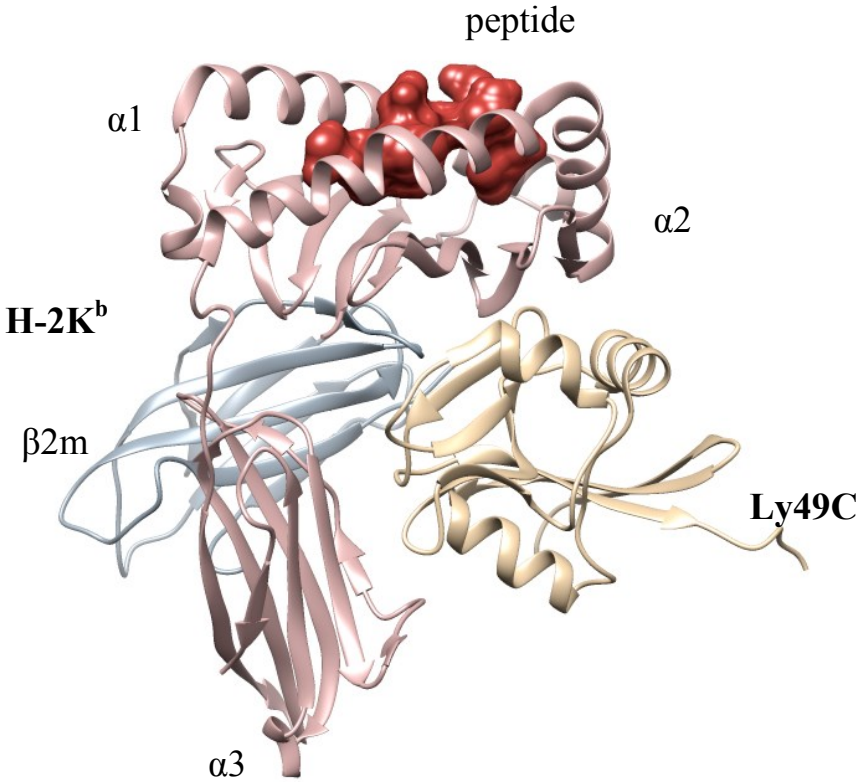

Figure 1-7. **Structural view of H-2K^b and Ly49C association.** The interface between H-2K^b and Ly49C includes H-2K^b amino acids under the peptide binding groove in the α1, α2 and α3 domains as well as in the β2m. Ly49C amino acids within the α3 and L6 regions participate in interaction with H-2K^b. The H-2K^b heavy chain is shown in pink ribbon drawing, the β2m is in grey ribbon and the peptide is in red surface drawing. The C-type lectin-like domain (CTLD) of the Ly49C monomer of the dimer is shown in gold ribbon. The figure was generated using CHIMERA UCSF software and the PDB ID coordinates 3C8K.

CHAPTER II

MATERIALS AND METHODS

Cell lines and peptides

The TAP-2 deficient RMA-S mouse T lymphoma cell line, was obtained from Dr. W. Jefferies (University of British Columbia, Vancouver, Canada) (193, 228). RNK-16 is a spontaneous F344 rat strain NK cell leukemia cell line (229). Both cell lines were maintained in RPMI supplemented with 10% FCS, L-glutamine, penicillin, streptomycin, and 50 μM 2-mercaptoethanol, unless otherwise indicated. Synthetic peptides were purchased from GenScript, each with 98% purity or higher and dissolved in DMSO.

Monoclonal antibodies and cell staining

The H-2K^b-specific monoclonal antibody (mAb), Y3 (mouse IgG2b), M1/42 (rat IgG2a), B8-24-3 (mouse IgG1a) and AF6-88.5.5.3 (mouse IgG2a) were produced in our laboratory from ammonium sulfate precipitates. Fluorescein isothiocyanate (FITC) coupled secondary anti-mouse or anti-rat antibodies were purchased from Cedarlane. Incubation with primary H-2K^b specific antibodies was done at a final concentration of 50μg/ml for 15 minutes at 4°C in Phosphate Buffered Saline (PBS) containing 2%FCS and 5mM EDTA (Staining Buffer). Following primary antibody incubation, cells are washed twice before secondary antibody is added at a 1:50 dilution in Staining Buffer. After incubation with secondary antibody, cells are washed twice with Staining Buffer

before fixing cells in PBS buffer containing 5mM EDTA and 1% formaldehyde. Stained and fixed samples were analyzed in a FACSCalibur cell analyzer (BD Biosciences).

The H-2K^b-specific mAb clone AF6-88.5.5.3 coupled to Allophycocyanin (APC) was purchased from eBioscience and used to stain RMA/S cell titration experiments in Chapter III and all subsequent H-2K^b detection experiments in Chapters IV and Chapter V, unless otherwise mentioned. RMA/S cell staining with AF6-88.5.5.3-APC was done using the mAb at a final concentration of 2µg/ml in a 15 minute incubation at 4°C in Staining Buffer. Following antibody incubation, cells are washed twice using Staining Buffer before fixing cells in PBS buffer containing 5mM EDTA and 1% formaldehyde. Stained and fixed samples were analyzed in a FACSCanto cell analyzer (BD Biosciences).

The H-2K^b-SIINFEKL-specific mAb, 25-D1.16 coupled to APC was used to detect H-2K^b-SIINFEKL complexes in Chapter V, and was purchased from eBioscience. RMA/S cell staining with 25-D1.16-APC was performed as above described for AF6-88.5.5.3-APC mAb staining. Stained and fixed samples were analyzed in a FACSCanto cell analyzer (BD Biosciences).

The 4L03311 hybridoma, producing the Ly49C specific mAb, was a gift from Suzanne Lemieux (Université du Québec, Laval, Québec, Canada). The Ly49C specific 4L03311 mAb was prepared by ammonium sulfate precipitation and PBS dialysis of the supernatant from the hybridoma grown in protein free medium. Fluorescein

isothiocyanate (FITC) coupled secondary anti-mouse antibody was purchased from Cedarlane. RNK.49W/C cells were incubated with Fc receptor blocking antibody 2.4G2, produced in our laboratory by ammonium sulfate precipitation, for 30 minutes at 4°C in Staining Buffer. Incubation with primary Ly49C specific mAb was done at a final concentration of 50µg/ml for 15 minutes at 4°C in Staining Buffer. Following 4L03311 mAb incubation, cells are washed twice before secondary antibody is added at a 1:50 dilution in Staining Buffer. After incubation with secondary antibody, cells are washed twice with Staining Buffer before fixing cells in PBS buffer containing 5mM EDTA and 1% formaldehyde. Stained and fixed samples were analyzed in a FACSCanto cell analyzer (BD Biosciences).

Antibodies against mouse CD3 and NK-1.1 for *ex vivo* C57BL/6 NK cell sorting were APC conjugated anti-NK-1.1, clone PK136 from eBioscience and PE-Cy7 conjugated anti-CD3 clone 145-2C11 from eBioscience. In addition, we used the FITC conjugated anti-Ly49C and I clone 5E6 purchased from BD Biosciences. The mouse Fc receptors antibody 2.4G2 was prepared by ammonium sulfate precipitation and PBS dialysis from the hybridoma grown in protein free medium. Staining for sorting is noted under the *Mouse NK cell separation* section of this chapter.

RMA/S stabilization assay and peptide titration assays.

RMA/S cells were incubated at 26°C in AIMV serum free media supplemented with 0.05μM mercaptoethanol and 1mM glutamine for 16 hours (230). Peptide was added to RMA/S cells peptide concentrations of 100μM for initial peptide screen. Peptide titration started at a concentration of 100μM to 0.00001μM in ten fold serial dilutions. Incubation with peptide was conducted for 15 minutes in the presence of Brefeldin A (BFA, Invitrogen) to block transport of newly synthesized MHC-I molecules to the cell surface (231, 232). RMA/S cells were washed three times using AIMV media to discard of any excess of peptide and were further incubated at 37°C for 4 hours to test stabilization of H-2K^b. Peptide binding to H-2K^b was analyzed by surface staining of H-2K^b. As a negative control we do not add any peptide to the RMA/S cells, resulting in low staining profiles after FACS analysis. On the other hand, we use the H-2K^b specific OVA peptide, SIINFEKL, as a positive control, where we observe a high H-2K^b expression by staining with H-2K^b specific antibodies.

Production of recombinant mouse β2m for cell culture.

Soluble mouse β2m, consisting of amino acids residues 1-99, was produced using BL21 (DE3) *E.coli* (Stratagene) (BL21.β2m) cells for protein expression. BL21.β2m cells were inoculated in an overnight culture using LB-Ampicillin growth media, with Ampicillin at a concentration of 50μg/ml incubated at 37°C with a shaker speed of 250RPM. The following day, 10ml of overnight cultured cells were used to inoculate 1L of LB-Amp growth media until reaching optical density (O.D.) of 0.6. Protein induction was carried out by adding isopropyl-1 thio-beta-D-galactopyranoside

(IPTG) to a final concentration of 1mM for 4 hours at 37°C shaking at 250RPM. BL21.β2m cells were harvested by centrifugation at 4°C with a speed of 4000RPM in a high speed centrifuge. After a 30 minute incubation with 50mg/ml lysozyme, 1mM MgCl, 5mg/ml DNAse, 1% Triton and 1mM DTT, inclusion bodies were purified by several rounds of sonication and washed with 100µM Tris buffer containing 100mM NaCl, 5mM EDTA, 0.1% Triton and 10µM DTT, until the supernatant was clear and the pellet was white, indicating the removal of DNA and cell debri. Pelleted inclusion bodies were dissolved in a 8M Urea buffer with 1µM DTT for 30 minutes and centrifuged to discard insoluble particles. Solubilized protein was used for an *in vitro* folding reaction by slow dilution into L-Arginine buffer using the glutathione redox system with 5µM reduced glutathione and 0.5µM oxidized glutathione for 24 hours at 4°C. Protein was then concentrated by ultrafiltration and dialyzed into 100mM Tris 100mM NaCl buffer for size exclusion chromatography using a Sepharose 26/76 column (GE Healthcare) connected to an AKTA protein purification system. Fractions corresponding to the molecular weight of β2m were pooled, concentrated, dialyzed into PBS buffer at pH7.4 and filter sterilized for cell culture.

Protein Analysis.

Protein concentration was determined using nanodrop (Thermo). Protein was analyzed by SDS-PAGE using 5µg of protein boiled in 2X SDS-PAGE sample buffer under reducing conditions and run on a 12% polyacrylamide minigel. Proteins were visualized by staining the gel with Coomassie Blue (Biorad).

Structural Analysis

Molecular graphics were compiled using the UCSF Chimera software (Resource for Biocomputing, Visualization, and Informatics, University of California, San Francisco (http://www.cgl.ucsf.edu/chimera). Protein Data Bank (PDB) ID codes used were 1VAC for H-2K^{b}-SIINFEKL, 2ZSW for H-2K^{b}-RAYIFANI, 2VAA for H-2K^{b}-RGYVYQGL and 3C8K for H-2K^{b}-SIINFEKL-Ly49C co-crystal structure.

Generation of RNK-16 cells expressing chimeric Ly49W/C

The cDNA encoding the intracellular and transmembrane domain of Ly49W^{NOD} (residues 1-66) fused with the extracellular domain of Ly49C$^{C57BL/6}$ (residues 67-261) was generated using two rounds of PCR amplification. For the first round, we amplified the transmembrane and cytoplasmic region of Ly49W^{NOD} using the 5' primer 5'-CCGCTCGAGATGAGTGAGCAGGAGGTCACTTTC that included a XhoI restriction site; and the 3' primer 5'-AGTTTTTTTTGTTGATCATACTGAAAAATTTTTGTC ACAAGCACTGAGACAAT that included a overhang sequence to bind the 5' extracellular region of Ly49C$^{C57BL/6}$. The PCR product was run on an agarose gel, purified and used as the 5' primer for the second round of PCR amplification with the 3' primer 5'-TGTGTTGATTATACTGAAAAATCTTTGTCACAAGCACTGAGACAAT that included the EcoRI restriction site. The final PCR product, chimeric Ly49W/C, was subcloned into the pCIneo vector and then into BSRαEN for transfection of RNK-16 cells. Stable RNK-16 cell transfectants expressing the chimeric Ly49W/C receptor (RNK.49W/C) were produced by electroporation and maintained in RPMI media with 10%FCS, L-glutamine, penicillin, streptomycin and 2-ME under antibiotic selection

with 10mg/ml G418. (Geneticin, invitrogen). Expression of chimeric Ly49W/C on RNK-16 cells was confirmed by cell surface staining with the 4L03311 (anti-Ly49C) mAb and analyzed by flow cytometry using FACSCanto cell analyzer gating on live cells.

Cytotoxicity Assays

RMA-S cells were cultured for 16 hours at 26°C in serum free AIMV media, supplemented with L-glutamine and 2-ME. The cells were then incubated with peptide for 15 minutes and 10µg/ml of BFA at 26°C, followed by three washes to eliminate unbound peptide. Peptide-loaded RMA-S cells were labeled with 100-150 µCi of ^{51}Cr (^{51}Chromium Radionuclide, Perkin Elmer) for 1 hour at 37°C and washed extensively. Effector RNK.49W/C cells were incubated without selective antibiotic G418 (Geneticin, Invitrogen) 48 hours prior to the assay and washed using serum free AIMV media. Cytotoxicity assays were carried out for 4 hours at 37°C with varying effector to target (E:T) cell ratios in 96-well V-bottom microtitre plates. Following the 4 hour incubation, microtitre plates were centrifuged to acquire 25µl of supernatant and transfer to a 95-well flexi-plate with 100µl of scintillant (OptiPhase 'SuperMix', Wallac, Loughborough, England). Flexi-plates were incubated in a plate shaker for 10 minutes at 900RPM, and further analyzed in a beta counter (MicroBeta, Wallac, Loughborough, England). Percent specific lysis was calculated as [(experimental release) – (spontaneous release)/(total release) – (spontaneous release)] x 100. All cytotoxicity assays were performed in triplicate in a minimum of three independent experiments.

Statistical Analysis

Comparison between groups at the 12.5:1 E:T ratio was performed using a paired, two-tailed T-test with a p value <0.05 for statistical significance (ns= not significant, *p<0.05, **p<0.005).

Prediction of peptide binding affinities to H-2K^b using NetMHCpan

The server NetMHCpan can be used to predict the affinity between specific MHC-I molecules and peptides bound, expressed in nM IC_{50} values (233). In order to predict the affinity of a given peptide for a MHC-I complex, the peptide sequence is uploaded or pasted into the submission box, followed by selection of peptide length. From a drop-down menu, we then select the species/loci of MHC-I, as well as the allele from an additional drop-down menu; where we used the "mouse (H-2)" and "H-2K^b" options correspondingly. Furthermore, options to set a threshold for strong and weak binders were set to IC_{50} of 10nM and IC_{50} of 500nM, respectively.

Sequential peptide loading

Stabilization of H-2K^b on RMA-S cells was performed by incubating cells at 26°C for 16 hours in AIMV serum free medium supplemented with L-glutamine and 2-ME and 10μg/ml of mouse recombinant β2m. Peptide loading was performed by adding the SIINFEKL peptide at a concentration of 0.005μM for 10 minutes at 26°C in the presence of 10μg/ml BFA. Cells were washed three times followed by resuspension in culture media and loading of a second peptide at concentrations of 10μM or 1μM. Cells were washed further and while a fraction of the cells were used to label with ^{51}Cr for

cytotoxicity assays, the rest of the cells were resuspended in media and incubated at 37°C for 5 hours. Stable H-2K^b complexes were then detected by flow cytometry gating on live cells using the H-2K^b specific antibody AF6-88.5.5.3-APC. Flow cytometry experiments were performed in triplicate.

Animals

Female C57BL/6 (H-2^b) mice were purchased from Charles Rivers Laboratories. All animal experiments were approved by the Animal Welfare and Policy Committee of the University of Alberta (Edmonton, Canada).

Mouse NK cell separation

We homogenized C57BL/6 female mice spleens, lysed red blood cells using ammonium chloride, and blocked Fc receptors using the 2.4G2 antibody. In order to select for NK cells expressing Ly49C, we incubated the cell suspension with anti-CD3, anti-NK1.1 and anti-Ly49C&I and sorted for CD3$^-$NK1.1$^+$Ly49C&I$^+$ NK cells in FACSAria (BD Biosciences). This cell population will include NK cells that express Ly49C and Ly49I. We have optimized CD3$^-$NK1.1$^+$Ly49C&I$^+$ cell growth using RPMI supplemented with 10%FCS, L-glu, penicillin, streptomycin, 2-ME and further supplemented with 1000U/ml of recombinant mouse IL-2, produced in our laboratory. Cells were seeded at a cell concentration of 50,000 cells/ml in 500µl of media, plated l in a 48-well plate. After three days in culture, we change media by gently removing non-adherent cells and replenishing growth RPMI media supplemented as previously mentioned. The cells remain in culture for an additional three days and then used for

functional assays. Cells were collected by carefully removing non-adherent cells and resuspended in serum free AIMV media supplemented with L-glu and 2-ME. Cells were washed three times using AIMV media to remove any trace of IL-2. On the day of the functional assay, we aliquot cells out to stain them with anti-Ly49C&I antibody to check for cell surface expression levels. This test assures that the receptor is being expressed.

CHAPTER III

PEPTIDE SEQUENCE REQUIREMENTS FOR EFFICIENT H-2K^b BINDING AT THE CELL SURFACE

A. Introduction

The class I major histocompatibility complex I (MHC-I) molecule is a trimeric cell surface protein expressed on all nucleated cells (234). MHC-I expression is essential for the distinction between self and non-self to adaptive immune T cells and innate immune natural killer (NK) cells. MHC-I molecules are composed of a heavy chain, a non-covalently associated β2-microglobulin (β2m), and a non-covalently bound peptide. The heavy chain of MHC-I molecules encompasses three domains: α1, α2, and α3. The α1 and α2 domains form the peptide binding groove where an 8 to 10 amino acid peptide can bind (7). To maintain the stability of MHC-I complexes, peptides dock into the pockets formed in the peptide binding groove via their anchor residues. Amino acids within the pockets of the peptide binding groove vary from different MHC-I alleles, and, therefore, so do the peptide anchor residues that fit in the pockets of the groove. The expression of stable MHC-I complexes with bound peptides at the cell surface is imperative for the determination of self or non-self by immune cells and responses thereof.

The antigen processing pathway is the cellular mechanism that regulates peptide binding to MHC-I and the subsequent stable expression of MHC-I complexes at the cell

surface (235). The classical antigen processing pathway often initiates with ubiquitination of cytoplasmic proteins for degradation into peptides in the proteasome (236). The resulting peptides can be transported into the endoplasmic reticulum (ER) via the transporter associated with antigen processing (TAP) (26). The peptides can then be trimmed by aminopeptidases in the ER and either used in the generation of MHC-I complexes or degraded entirely (20, 21). At the same time, newly synthesized MHC-I heavy chain interacts with chaperone proteins that facilitate its folding and its association with β2m in the ER (27). The heavy chain-β2m heterodimer subsequently interacts with other ER resident proteins that form the peptide loading complex (PLC) in preparation for peptide loading (237). PLC members include TAP, tapasin, ERp57 and calreticulin that maintain the heavy chain at a peptide receptive conformation to facilitate peptide binding (24, 238, 239). Upon formation of stable complexes, MHC-I molecules are transported to the cell surface where it can display the peptide or antigen.

Peptides bound to MHC-I are generally derived from endogenous proteins (240). In healthy cells, peptide precursors are proteins that are normally expressed in cells at steady state. However, during a viral infection or oncogenic transformation, peptides can originate from viral gene products or cancer related proteins (37, 241, 242). As such, immune cells can identify the health of any given cell by the peptides expressed by its MHC-I complexes, and respond accordingly. The identification of peptides bound to MHC-I molecules has greatly improved our understanding of peptide-specific recognition by cytotoxic T lymphocytes (CTLs) and NK cells. In the mouse, peptide identification has been in part achieved by MHC-I immunoprecipitation and peptide

elution studies, allowing the isolated peptides to be further analyzed and sequenced using mass spectrometry (243). Therefore, the sequences of multiple MHC-I peptides are known and can be used to investigate their particular roles in the context of MHC-I presentation to CTLs, as well as NK cells.

As the main focus of my project is to study specific interactions between peptide-MHC-I complexes and the NK cell inhibitory Ly49C receptor in a murine model, I first identified peptides that can be loaded exogenously onto murine MHC-I molecule H-2K^b, a ligand for Ly49C NK cell receptor (197). H-2K^b bound peptides are generally 8 amino acids in length with primary anchor residues at positions 5 (P5) and position 8 (P8), and an auxiliary anchor residue at position 3 (P3). The identity of primary anchor residues is highly conserved with P5 having aromatic residues Phe or Tyr; while P8 residues are non-polar aliphatic amino acids with Leu being the most prominent followed by Val, Ile and Met. Still conserved, auxiliary anchor residues can have more variability than primary anchor residues with aromatic amino acids at P3 such as Phe and Tyr or non-polar aliphatic residues such as Ile (244). Peptides used in this study have the mentioned canonical primary anchor residues, which make them ideal candidates for optimal peptide binding to H-2K^b. In addition, we selected H-2K^b peptides derived from self proteins as well as those derived from viral and cancer related proteins, in order to define their individual influence on Ly49C-mediated NK cell function.

B. Results

Detection of peptides bound to H-2K^b at the cell surface is dependent on peptide sequence

Mouse MHC-I molecule H-2K^b typically binds an 8 to 9 amino acid peptide on the peptide binding groove formed by the α1 and α2 domains of the H-2K^b heavy chain. Pockets formed in the H-2K^b peptide binding platform accommodate peptide anchor residues at P5 and P8, and auxiliary anchor residues at P3. Although peptide amino acid P2 is not considered an anchor residue, it still docks into the B-pocket of the H-2K^b molecule and can also be important for peptide binding (245). The importance of primary and auxiliary anchor residues in binding to H-2K^b has been clearly demonstrated by the use of Ala residue variants of the H-2K^b specific OVA peptide SIINFEKL (14, 246). Using RMA/S stabilization assays, peptides SIANFEKL, SIINAEKL and SIINFEKA have been shown unable to bind to H-2K^b (246). RMA/S cells are a mouse T cell lymphoma that lack the TAP-2 subunit of TAP and are thus incapable of transporting peptides in the cytosol to the ER for MHC-I binding (230). Due to this deficiency, RMA/S cell express low levels of peptide-empty MHC-I which can be upregulated by decreasing cell culture temperature to 26°C. Peptide-empty MHC-I molecules can be stabilized by addition of MHC-I-specific peptide, tested by incubating cells at 37°C for 4 hours and detected by flow cytometry. Peptides that do not bind MHC-I will result in low MHC-I expression profiles after the 4-hour stabilization assay, while peptides that bind MHC-I will have an increased MHC-I staining profile (230).

Using a set of peptides specific for H-2K^b, we investigated their efficacy to bind and stabilize H-2K^b on RMA/S cells. Peptides used in this study have canonical primary and auxiliary anchor residues for H-2K^b binding, and could thus potentially bind and stabilize H-2K^b on RMA/S cells. We selected a panel of 14 peptides that have been identified in other studies as being processed from self-, viral- or cancer-related proteins. We can group peptides into two categories depending on the identity of the auxiliary anchor residue at P3 as peptides with non-polar aliphatic residues Ile, Val, Met and Pro, and peptides with aromatic residues Tyr and Phe (Table 3-1A, 3-1B). For the initial screen of peptide binding, RMA/S cells were incubated with each peptide at a saturating concentration of 100μM where a plateau in H-2K^b expression on RMA/S cells can be reached in peptide titration experiments (247). We determined peptide binding to H-2K^b by flow cytometric analysis upon completion of RMA/S stabilization assays for 4 hours. The graphed results are expressed as mean fluorescence intensity ($MFI=MFI_{RMA/S + peptide} - MFI_{RMA/S + no peptide}$). For the detection of H-2K^b at the cell surface, we first used the H-2K^b specific antibody Y3 (248). We found that 9 out of the 14 peptides tested showed an increase in H-2K^b expression for the duration of the assay. From the group of seven peptides with non-polar aliphatic auxiliary anchor residues at P3, three peptides: TSINFVKI, TTIHYKYM and KSPWFTTL did not show an increase in H-2K^b staining as compared to the positive control, SIINFEKL. All other peptides, KIITYRNL, KVITFIDL and YAMIYRNL, had similar H-2K^b expression at the cell surface as induced by SIINFEKL (Figure 3-1A). From the seven peptides with aromatic R groups at P3, peptides EQYKFYSV and AQYKFIYV did not increase H-2K^b staining profile compared to the positive control RGYVYQGL. The remaining peptides of this group,

AAYAYAAL, ANYDFITV, ISFKFDHL and INFDFPKL, had similar levels of H-2K^b staining on RMA/S cells as compared to RGYVYQGL (Figure 3-1B). The peptides used in this study are known to bind H-2K^b from peptide elution studies, with some of these peptides also tested for CTL recognition analysis (249-258). Since different peptides have been shown to influence or modify determinants recognized by MHC-I specific antibodies, we examined H-2K^b expression by staining with three additional antibodies, beyond Y3 (247).

Different H-2K^b specific antibodies have similar recognition of H-2K^b-peptide complexes

Utilizing three additional antibodies that recognize H-2K^b, AF6-88.5.5.3, B8-24-3 and M1/42, we further corroborated our flow cytometric analysis using the Y3 antibody. The H-2K^b epitopes recognized by mAbs Y3, AF6-88.5.5.3 and B8-24-3 have been identified within the α1 and α2 domains of the H-2K^b heavy chain; while, the M1/42 mAb recognizes an epitope in the heavy chain that is dependent on stably bound β2m (Figure 3-2) (259-262). We analyzed AF6-88.5.5.3, B8-24-3 and M1/42 antibody staining profile to identify peptides that can bind H-2K^b, but might have been disregarded as H-2K^b "binders" by Y3 antibody staining, since peptides can change H-2K^b antibody determinants for antibody recognition. For each panel of peptides, we used SIINFEKL and RGYVYQGL as positive controls of H-2K^b binding for the group of peptides with non-polar aliphatic auxiliary anchor residues and peptides with aromatic auxiliary anchor residues, respectively.

Using the AF6-88.5.5.3 antibody, we found a similar H-2K^b staining pattern compared to the Y3 antibody staining with different peptides. The plotted graphs are expressed as mean fluorescence intensity (MFI=$MFI_{RMA/S+peptide}$ - $MFI_{RMA/S + no\ peptide}$). In the peptide group with non-polar aliphatic P3 residues, TSINFVKI, TTIHYKYM, and KSPWFTTL had low fluorescent intensities compared to the positive control SIINFEKL, while KIITYRNL, KVITFIDL, and YAMIYRNL appeared to have similar H-2K^b expression to SIINFEKL (Figure 3-3A). Similar to Y3 staining, peptides with aromatic side chains at P3, AQYKFIYV and EQYKFYSV, show reduced H-2K^b staining in contrast to RGYVYQGL staining. However, peptides AAYAYAAL, ANYDFITV, ISFKFDHL, and INFDFPKL generated H-2K^b fluorescent intensities at similar levels as RGYVYQGL (Figure 3-3B).

Additionally, we used a third H-2K^b specific antibody, B8-24-3, to detect peptide binding to H-2K^b on RMA/S cells. The plotted results are expressed as mean fluorescence intensity (MFI=$MFI_{RMA/S + peptide}$ - $MFI_{RMA/S + no\ peptide}$). In the set of peptides with non-polar aliphatic auxiliary anchor residues at P3, peptides TSINFVKI, TTIHYKYM, and KSPWFTTL had low fluorescent intensities, while KIITYRNL, KVITFIDL, and YAMIYRNL had similar fluorescent intensities as cells incubated with SIINFEKL (Figure 3-4A). Peptides with aromatic side chains at P3, AQYKFIYV, and EQYKFYSV did not exhibit an increase in H-2K^b expression, whereas peptides AAYAYAAL, ANYDFITV, ISFKFDHL, and INFDFPKL closely resembled the substantial H-2K^b staining profile as RGYVYQGL (Figure 3-4B).

Finally, staining with the M1/42 antibody, which recognizes an epitope on the heavy chain dependent on properly bound β2m, we found a similar pattern as observed by staining with the previous three antibodies. The plotted results are expressed as mean fluorescence intensity ($MFI=MFI_{RMA/S+peptide} - MFI_{RMA/S + no\ peptide}$). Some peptides in the non-polar aliphatic P3 residue category, TSINFVKI, TTIHYKYM, and KSPWFTTL showed lower fluorescent intensities compared to SIINFEKL, while, KIITYRNL, KVITFIDL, and YAMIYRNL showed comparable H-2K^b expression to SIINFEKL (Figure 3-5A). In the group of peptides with aromatic side chains at P3, EQYKFYSV and AQYKFIYV showed decreased H-2K^b staining as compared to RGYVYQGL. On the other hand, peptides AAYAYAAL, ANYDFITV, ISFKFDHL, and INFDFPKL exhibited comparable levels of H-2K^b expression to RGYVYQGL with AAYAYAAL having even higher fluorescent intensity (Figure 3-5B). These results obtained by staining with 4 distinct antibodies, that can recognize different H-2K^b epitopes, confirm that all the peptides tested, either do or do not stabilize H-2K^b during the 4-hour stabilization assay, and that peptides are not completely changing H-2K^b epitopes recognized by the 4 antibodies employed in this study.

Recombinant mouse β2m does not assist in overcoming poor stabilization of H-2K^b by peptides

As demonstrated by the RMA/S stabilization experiments, a lack of exogenous peptide decreases H-2K^b complex formation, demonstrating the importance of the peptide bound to MHC-I in securing MHC-I complex integrity. It has been suggested that, during the RMA/S stabilization assay, "empty" MHC-I and β2m dissociate before

reaching the cell surface during intracellular transportation due to the absence of peptide. We therefore provided an excess of recombinant mouse β2m during the RMA/S assay to have possibly an increased amount of MHC-I-β2m heterodimers for peptide loading. We generated recombinant mouse β2m and used it at various concentrations for RMA/S culture at 26°C for 16 hours prior to peptide loading (Figure 3-6A, 3-6B). Peptides were loaded in the same manner as described in the previous section at a final concentration of 100μM. Upon addition of mouse recombinant β2m, the total amount of stable H-2K^b was increased with all peptides. However, peptides that had shown low efficacy in stabilizing H-2K^b, remained having low binding efficiency to H-2K^b compared to the positive control SIINFEKL. The plotted results are expressed as mean fluorescence intensity ($MFI=MFI_{RMA/S + peptide} - MFI_{RMA/S + no peptide}$) (Figure 3-7A, 3-7B). This suggests that peptides yielding low H-2K^b stabilization cannot be assisted by excess of recombinant mouse β2m in cell culture during the 4-hour stabilization assay.

Determining peptide concentrations yielding similar H-2K^b upregulation.

Next, using peptides that stabilize H-2K^b: SIINFEKL, KIITYRNL, KVITFIDL, YAMIYRNL, RGYVYQGL, AAYAYAAL, ANYDFITV, INFDFPKL, and ISFKFDHL, we examined H-2K^b expression using RMA/S stabilization assays in the presence of serial dilutions of individual peptides. Results from these experiments can show at what concentration each peptide reaches saturation levels for H-2K^b binding. The saturating level is the concentration of peptide that is required to reach a plateau in a curve plotting H-2K^b expression levels on RMA/S cells and individual peptide concentrations. At the same time, we were able to further define the concentration of

each peptide necessary to yield similar H-2K^b expression on RMA/S cells. In experiments examining functional differences resulting from expression of different H-2K^b-peptide complexes on RMA/S cells, it is essential to display and maintain these complexes at similar levels.

We measured H-2K^b expression on RMA/S cells following peptide titration experiments with the peptides SIINFEKL, KIITYRNL, KVITFIDL, YAMIYRNL, RGYVYQGL, AAYAYAAL, ANYDFITV, INFDFPKL, and ISFKFDHL. The graphed results show the relative increase in H-2K^b expression on RMA/S cells when incubated with individual peptides compared to RMA/S incubated with no peptide (MFI plotted=$MFI_{RMA/S + peptide}$ - $MFI_{RMA/S + no peptide}$). We used the APC conjugated AF6-88.5.5.3 antibody to analyze RMA/S cell H-2K^b expression in our peptide titration experiments. In the group of peptides with non-polar aliphatic auxiliary anchor residues at P3, SIINFEKL, KIITYRNL, KVITFIDL, and YAMIYRNL, have similar titration curves and reaching a saturation point at a peptide concentration of 1μM. Peptides SIINFEKL and KIITYRNL highly resemble each other in their binding to H-2K^b. The lowest or baseline levels of H-2K^b expression is observed from 0.00001μM to 0.001μM; thereon followed by a rapid increase in H-2K^b expression until reaching a peptide concentration of 1μM. The SIINFEKL and KIITYRNL peptide induced H-2K^b expression is steady from 1μM to 100μM (Figure 3-8). Peptides KVITFIDL and YAMIYRNL also share high resemblance in their binding to H-2K^b as observed in H-2K^b expression on RMA/S cells. The lowest and baseline H-2K^b expression is observed from 0.00001μM to 0.01μM; followed by a fast increase in H-2K^b expression until

reaching a peptide concentration of 10μM where H-2K^b expression is steady on to 100μM peptide concentration. As compared to SIINFEKL and KIITYRNL, KVITFIDL and YAMIYRNL have lower baselines at the concentrations of 0.00001μM to 0.001μM and 0.00001μM to 0.01μM respectively (Figure 3-8).

In the group of peptides with aromatic auxiliary anchor residues at P3, the RGYVYQGL peptide is used as a positive control for H-2K^b peptide-dependent stabilization. Similar to previous results, the increase in H-2K^b expression on RMA/S cells incubated with individual peptides is expressed as mean fluorescence intensity (MFI plotted=$MFI_{RMA/S + peptide}$ - $MFI_{RMA/S + no peptide}$). The INFDFPKL peptide has the lowest baseline for H-2K^b expression at the cell surface with stable H-2K^b levels from 0.00001μM to 0.01μM. The H-2K^b levels increase linearly form 0.01μM to 1μM where H-2K^b expression reaches a constant level from 1μM to 100μM. Both RGYVYQGL and ISFKFDHL peptides have similar H-2K^b stabilization profiles with lowest H-2K^b expression from 0.00001μM to 0.001μM and 0.00001μM to 0.01μM, respectively (Figure 3-9). Expression of H-2K^b continues with a rapid increase until the peptide concentration reaches 1μM for both RGYVYQGL and ISFKFDHL. Thereon, H-2K^b peptide expression is stably uniform from 1μM to 100μM. Both peptides AAYAYAAL and ANYDFITV induce low H-2K^b expression and baseline levels from 0.00001μM to 0.0001μM. The AAYAYAAL peptide increases H-2K^b expression from 0.0001μM to 1μM, reaching uniform H-2K^b expression from 1μM to 100μM peptide concentration. With the ANYDFITV peptide H-2K^b expression rapidly increases at a peptide concentration of 0.001μM to 0.01μM where it reaches a stable H-2K^b expression to the

1μM peptide concentration and moderately increases from 1μM to 100μM. The peptide baseline for individual peptides in this group is varied, with the lowest baseline using the peptide INFDFPKL, followed by RGYVYQGL, ISFKFDHL, AAYAYAAL, and ANYDFITV (Figure 3-9). As observed in the initial screen of peptide binding to H-2K^b using RMA/S stabilization assays, peptides can bind H-2K^b at different levels, showing presumed different peptide-H-2K^b binding affinities.

C. Discussion

Expression of MHC-I and display of peptide is an integral part of the immune response against foreign antigens (2). Peptides can originate from self, viral or oncogenic proteins and their binding capabilities to MHC-I are crucial in forming stable MHC-I complexes (25). Peptide anchor residues provide MHC-I complex stability from its formation in the ER to its display on the cell surface for immune cell recognition (7,8). Using RMA/S stabilization assays, we explored the characteristics of exogenous peptide binding to H-2K^b, using a set of peptides previously identified in H-2K^b peptide elution studies or peptides used to probe CTL recognition of H-2K^b. The overall purpose of this study is to identify peptides that can bind and sustain H-2K^b expression on RMA/S cells. Moreover, the identification of peptides that maintain H-2K^b expression, allowed us to pursue mouse NK cell inhibitory Ly49C receptor recognition of H-2K^b-peptide complexes, discussed in Chapter IV.

As demonstrated in this study, peptides possessing canonical anchor residues did not necessarily stabilize H-2K^b at the cell surface. Out of the panel of 14 peptides tested,

we observed stabilization of H-2K^b by 9 peptides using flow cytometry analysis with four distinct antibodies. Addition of recombinant mouse β2m did not rescue peptide binding to H-2K^b for the peptides that did not show an increase in H-2K^b at the cell surface. Still, the formation of stable H-2K^b complexes by several peptides used in this study is evidence that peptide binding to H-2K^b on RMA/S cells can be maintained.

Although we confirmed H-2K^b peptide stabilization on RMA/S, by peptides that can be further analyzed for their ability to support, or not, NK cell Ly49C receptor binding to H-2K^b; we considered the identity of anchor residues in the 14 peptides initially tested for H-2K^b binding that did or did not maintain H-2K^b stabilization on RMA/S cells. Three peptides with non-polar aliphatic auxiliary anchor residues, KSPWFTTL, TTIHYKYM, and TSINFVKI, did not stabilize H-2K^b as compared to SIINFEKL. Peptides TTIHYKYM and TSINFVKI have the less common Ile and Met as the primary anchor residue at P8 in contrast to Leu found more frequently at this position. Amino acids Met, Ile and Leu belong in the same category as non-polar aliphatic residues, and can participate in hydrophobic interactions within the F-pocket of H-2K^b. Being more prominently found at the P8 position, Leu could allow for better docking into the F-pocket due to its isobutyl group with two methyl groups in the □-carbon that may favor more extensive contacts deep within the D-pocket, in contrast, to Ile that contains a methyl group in the β-carbon instead. Finally, Met contains a S-methyl group that can be of considerable size to bind within the F-pocket, and might necessitate chaperone aid to bind to H-2K^b in the ER. A surface structure comparison between two H-2K^b crystal structures bearing peptides with either Leu or Ile at P8,

showed Leu docking into the F-pocket with possibly stronger van der Walls interactions with amino acids in the pocket as compared to Ile (Figure 3-10). On the other hand, although the KSPWFTTL peptide has a Leu at P8, the identity of the auxiliary anchor residue, Pro, may exert higher conformational rigidity that does not support binding of the peptide to H-2K^b. In the second group of peptides, with aromatic R groups at P3, EQYKFYSV and AQYKFIYV did not bind H-2K^b. Both peptides had identical primary and auxiliary anchor residues as ANYDFICV that did bind H-2K^b. The only difference in peptides facing the peptide binding groove resided in the identity of the P2 residue that docks into the B-pocket of H-2K^b. The presence of Gln at P2 might not have been favorable for stabilizing H-2K^b due to its characteristic polar and bulky side chain. In conclusion, the null H-2K^b stabilization with peptides KSPWFTTL, TTIHYKYM, TSINFVKI, EQYKFYSV and AQYKFIYV, on RMA/S cells during the 4-hour stabilization assay, could have been a result of lack of peptide binding in the first place or it could possibly be that some bound peptides can dissociate at faster rates and were therefore not recapitulated in the 4-hour stabilization assay.

The peptide loading machinery in the ER is equipped with several proteins that assist MHC-I peptide binding (22-27). On the other hand, at the cell surface, chaperone proteins that facilitate MHC-I peptide binding are not present to participate in peptide loading. Empty H-2K^b at the cell surface on RMA/S cells is thought to have a conformation suitable for peptide binding (230). However, for peptides with more suboptimal binding motifs, or anchor residues, chaperones in the ER might be necessary to facilitate their association and form stable MHC-I complex. Therefore, the binding of

peptide on H-2K^b at the cell surface relies heavily on the identity of the residues that can easily dock into the peptide binding groove.

Functional assays are an important tool to investigate the role of peptide-MHC-I complexes in cell mediated immune responses upon recognition of peptide-MHC-I on RMA/S cells. A great advantage of using RMA/S cells as targets is the flexibility in controlling the peptide loaded onto MHC-I molecules. The disadvantage of using this cell line is that not all peptides can be loaded, restricting the panel of available peptides. An alternative approach to study H-2K^b peptide immunogenicity in cells is to express single chain trimers where the β2m is linked to the heavy chain by a glycine linker and the β2m is subsequently linked to the peptide in the groove of the heavy chain. The single chain trimers can be expressed in β2m$^{-/-}$ cells for the analysis of MHC-I complex-dependent immune responses. In conclusion, characterizing the role of peptides in complex with MHC-I is essential in elucidating mechanisms of immunity against tumor and virus peptides. With this study, we have shown that exogenous peptide binding to H-2K^b can be restrictive even when peptides possess canonical anchor residues, demonstrated after a 4-hour stabilization assay. Still, using RMA/S stabilization assays to probe peptide binding, we found a pool of peptides that can efficiently bind H-2K^b for 4 hours as demonstrated by H-2K^b specific antibody staining. Furthermore, using RMA/S cells with peptide-loaded H-2K^b can be a useful and effective method to study mouse NK cell recognition by Ly49 receptors, as demonstrated in Chapter IV of this thesis. The work to identify peptide binding to H-2K^b presented in this chapter can also

be used to test additional peptides for their ability to bind H-2K^b in the following chapter.

A

Peptide Name	Peptide Sequence	Peptide origin
pOVA	SI**I**N**F**EK**L**	Chicken Ovalbumin (256-264)
pKB3	KI**I**T**Y**RN**L**	PCI domain-containing protein 2 (318-325)
pKB1	KV**I**T**F**ID**L**	GTP binding protein I (246-253)
mdm100	YA**M**I**Y**RN**L**	E3 ubiquitin-protein ligase mdm2 (100-107)
p15E	KS**P**W**F**TT**L**	MuLV env p15E (542-549)
p53	TT**I**H**Y**KY**M**	p53 (224-231)
p79	TS**I**N**F**VK**I**	Ribonucleotide reductase Su (P79) (524-531)

B

Peptide Name	Peptide Sequence	Peptide origin
pAFV	AN**Y**D**F**IC**V**	MMTV env gp70 (446-453)
pVSV	RG**Y**V**Y**QG**L**	Vesicular Stomatitis Virus NP (52-59)
CPα1	IS**F**K**F**DH**L**	F-actin capping protein alpha1 (93-100)
p54	IN**F**D**F**PK**L**	RNA helicase p54 (407-414)
mMLRQ	EQ**Y**K**F**YS**V**	NADH-ubiquinone oxidoreductase (61-68)
PTP	AQ**Y**K**F**IY**V**	PTP-1c (SHP-1) phosphatase (503-510)
Synthetic	AA**Y**A**Y**AA**L**	Synthetic peptide

Table 3-1. Amino acid sequence and origin of H-2K^b specific peptides. (A) H-2K^b binding peptides with non-polar, aliphatic auxiliary anchor residues and **(B)** H-2K^b binding peptides with aromatic auxiliary anchor residues at P3. Bold only amino acids indicate primary anchor residues at P5 and P8. Bold and underlined indicate auxiliary anchor residues at P3.

A

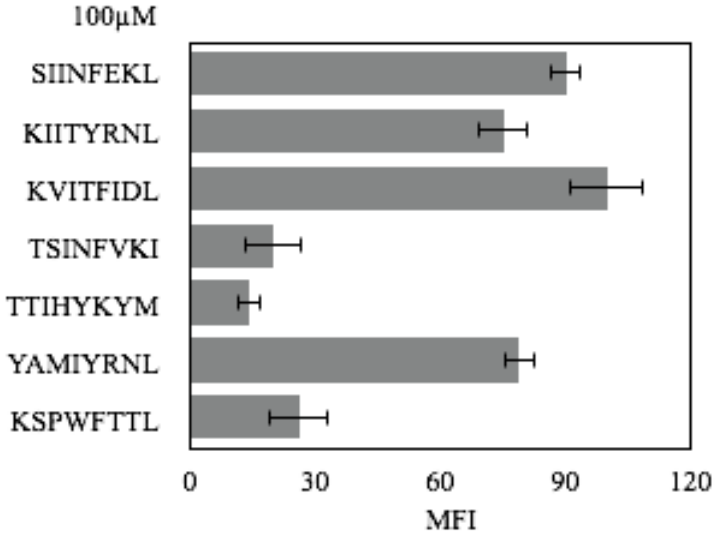
100μM
SIINFEKL
KIITYRNL
KVITFIDL
TSINFVKI
TTIHYKYM
YAMIYRNL
KSPWFTTL
0
30
60
90
120
MFI

B

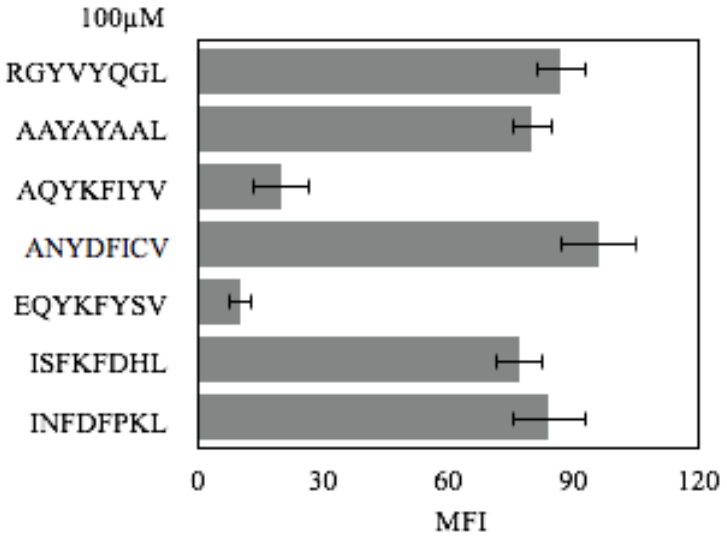
100μM
RGYVYQGL
AAYAYAAL
AQYKFIYV
ANYDFICV
EQYKFYSV
ISFKFDHL
INFDFPKL
0
30
60
90
120
MFI

Figure 3-1. Differential peptide binding to H-2K^b on RMA/S cells using the Y3 antibody. (A) Seven different peptides with non polar aliphatic auxiliary anchor residues were exogenously loaded on "empty" H-2K^b expressed on RMA/S cells at a concentration of 100μM. Detection of stabilized H-2K^b on RMA/S was done using the H-2K^b specific antibody, Y3. **(B)** Seven different peptides with aromatic auxiliary anchor residues were exogenously loaded on H-2K^b expressed on RMA/S cells at a concentration of 100μM. Detection of H-2K^b on RMA/S was done using the H-2K^b specific primary antibody Y3, followed by a secondary flourescently labeled antibody and analyzed in FACSCalibur cell analyzer. Results are the mean of three independent experiments. Error bars indicate SD.

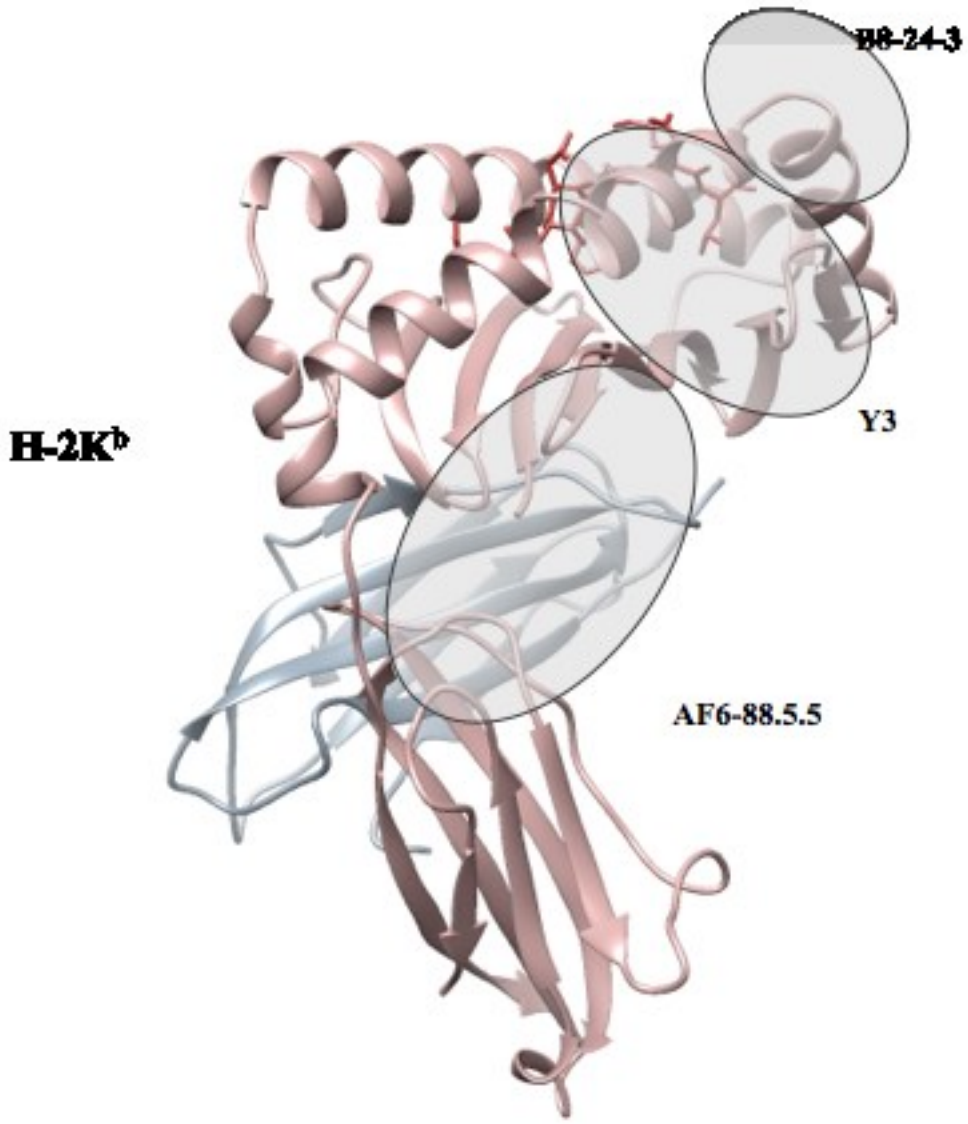

Figure 3-2. Mapping of determinants recognized by H-2K^b specific antibodies. The epitopes on H-2K^b recognized by Y3, AF6-88.5.5.3 and B8-24-3 have been mapped to regions within the heavy chain of the H-2K^b molecule. The M1/42 antibody recognizes an epitope in the heavy chain that is dependent on stably bound β2m, but epitope has not been identified.

A

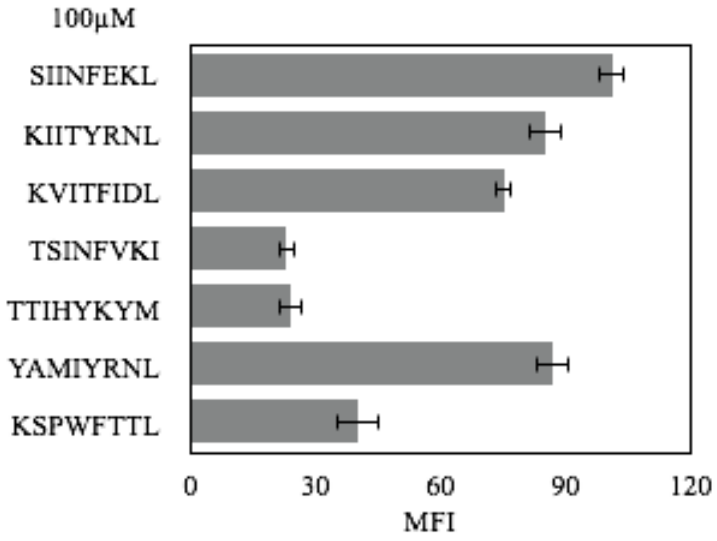
100μM
SIINFEKL
KIITYRNL
KVITFIDL
TSINFVKI
TTIHYKYM
YAMIYRNL
KSPWFTTL
0
30
60
90
120
MFI

B

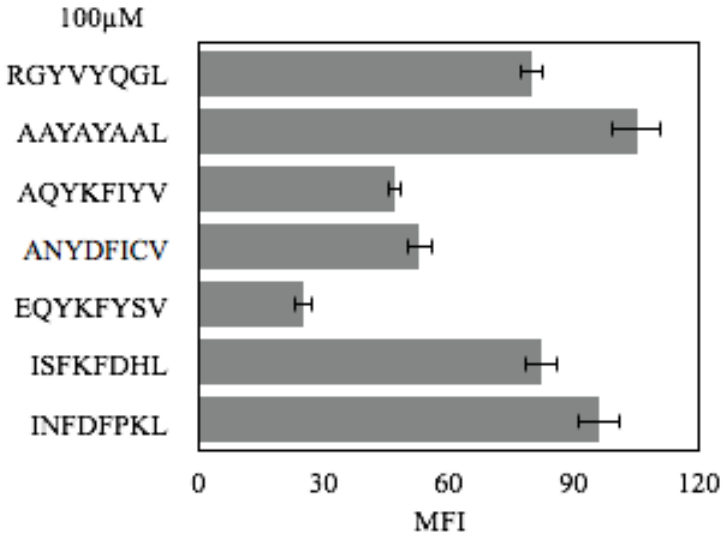
100μM
RGYVYQGL
AAYAYAAL
AQYKFIYV
ANYDFICV
EQYKFYSV
ISFKFDHL
INFDFPKL
0
30
60
90
120
MFI

Figure 3-3. Differential peptide binding to H-2K^b on RMA/S cells using an H-2K^b specific antibody AF6-88.5.5.3. (A) Seven different peptides with non polar aliphatic auxiliary anchor residues were exogenously loaded on H-2K^b expressed on RMA/S cells at a concentration of 100μM. Detection of stabilized H-2K^b on RMA/S was done using the H-2K^b specific antibody AF6-88.5.5.3 **(B)** Seven different peptides with aromatic auxiliary anchor residues were exogenously loaded on H-2K^b expressed on RMA/S cells at a concentration of 100μM. Detection of H-2K^b on RMA/S was done using the H-2K^b specific primary antibody AF6-88.5.5.3, followed by a secondary flourescently labeled antibody and analyzed in FACSCalibur cell analyzer. Results are the mean of three independent experiments. Error bars indicate SD.

A

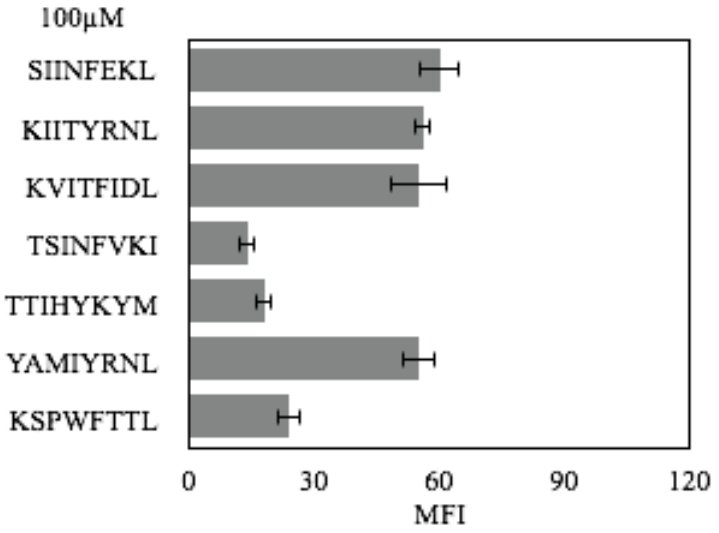
100µM
SIINFEKL
KIITYRNL
KVITFIDL
TSINFVKI
TTIHYKYM
YAMIYRNL
KSPWFTTL
0
30
60
90
120
MFI

B

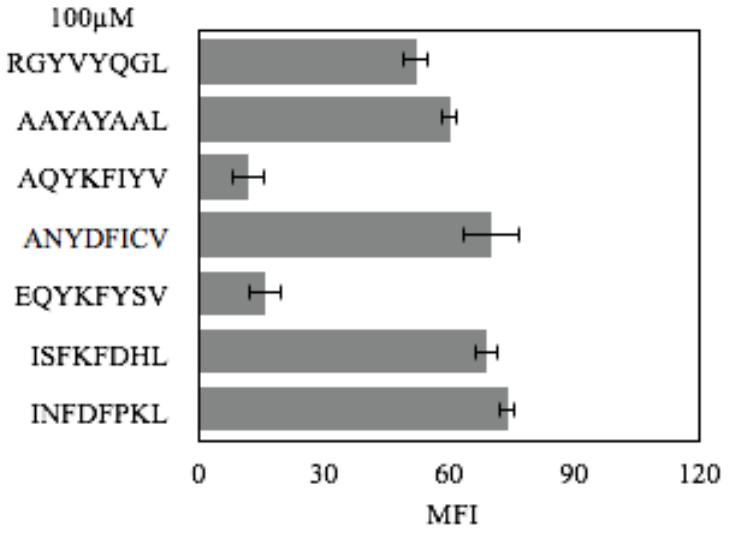
100µM
RGYVYQGL
AAYAYAAL
AQYKFIYV
ANYDFICV
EQYKFYSV
ISFKFDHL
INFDFPKL
0
30
60
90
120
MFI

Figure 3-4. Differential peptide binding to H-2K^b on RMA/S cells using a H-2K^b specific antibody, B8-24-3. (A) Seven different peptides with non polar aliphatic auxiliary anchor residues were exogenously loaded on H-2K^b expressed on RMA/S cells at a concentration of 100μM. Detection of stabilized H-2K^b on RMA/S was done using the H-2K^b specific antibody. **(B)** Seven different peptides with aromatic auxiliary anchor residues were exogenously loaded on H-2K^b expressed on RMA/S cells at a concentration of 100μM. Detection of H-2K^b on RMA/S was done using the H-2K^b specific primary antibody B8-24-3, followed by a secondary flourescently labeled antibody and analyzed in FACSCalibur cell analyzer. Results are the mean of three independent experiments. Error bars indicate SD.

A

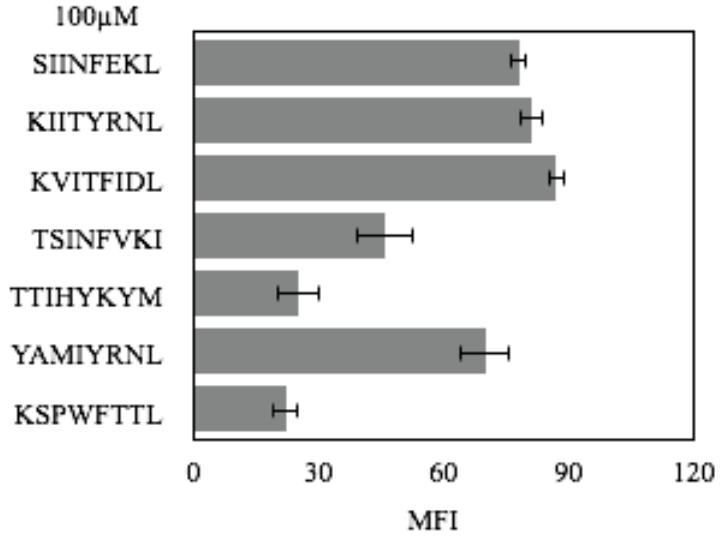
100μM
SIINFEKL
KIITYRNL
KVITFIDL
TSINFVKI
TTIHYKYM
YAMIYRNL
KSPWFTTL
0
30
60
90
120
MFI

B

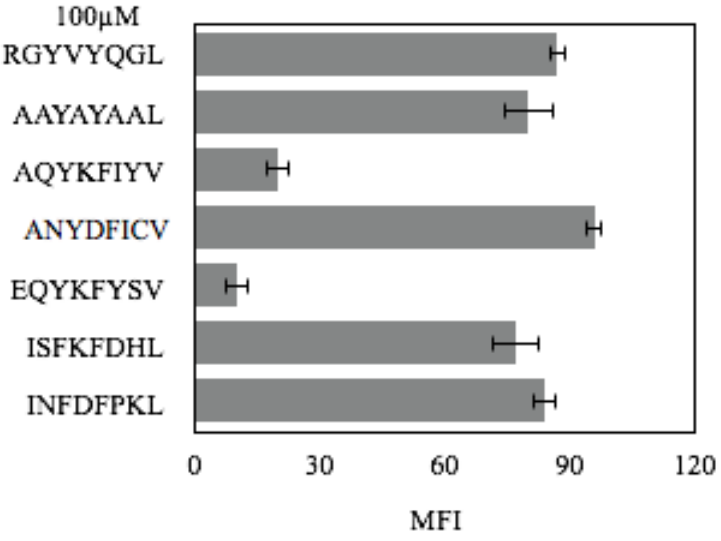
100μM
RGYVYQGL
AAYAYAAL
AQYKFIYV
ANYDFICV
EQYKFYSV
ISFKFDHL
INFDFPKL
0
30
60
90
120
MFI

Figure 3-5. Differential peptide binding to H-2K^b on RMA/S cells using the M1/42, β2m dependent antibody. (A) Seven different peptides with non polar aliphatic auxiliary anchor residues were exogenously loaded on H-2K^b expressed on RMA/S cells at a concentration of 100μM**.** Detection of stabilized H-2K^b on RMA/S was done using the H-2K^b antibody M1/42. **(B)** Seven different peptides with aromatic auxiliary anchor residues were exogenously loaded on H-2K^b expressed on RMA/S cells at a concentration of 100μM. Detection of H-2K^b on RMA/S was done using the H-2K^b specific primary antibody M1/42, followed by a secondary flourescently labeled antibody and analyzed in FACSCalibur cell analyzer. Results are the mean of three independent experiments. Error bars indicate SD.

A

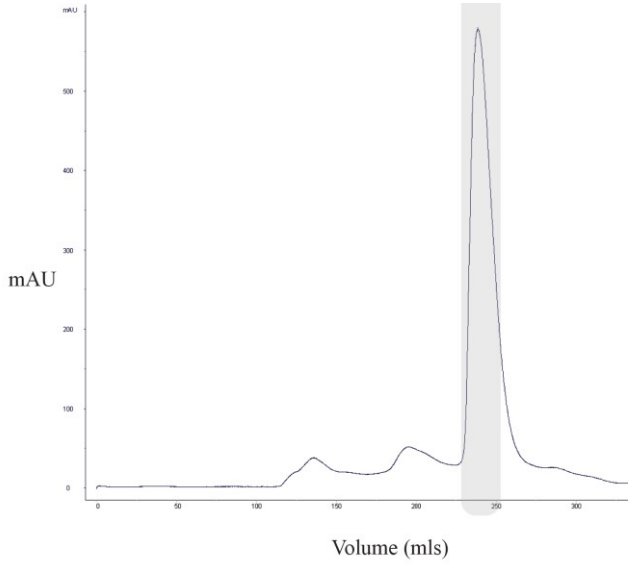

B

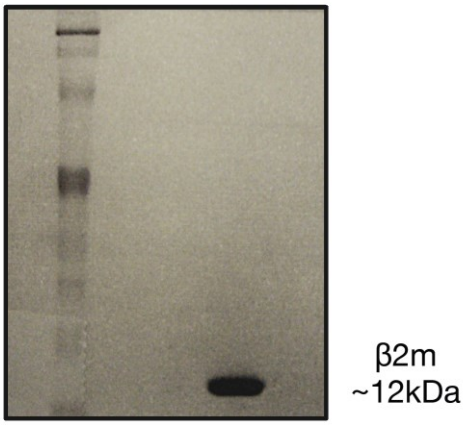

Figure 3-6. Purification of recombinant mouse β2m. (A) Size exclusion chromatogram of mouse β2m purification. **(B)** SDS-PAGE Coomasie Blue picture of recombinant mouse β2m at the expected molecular weight.

A

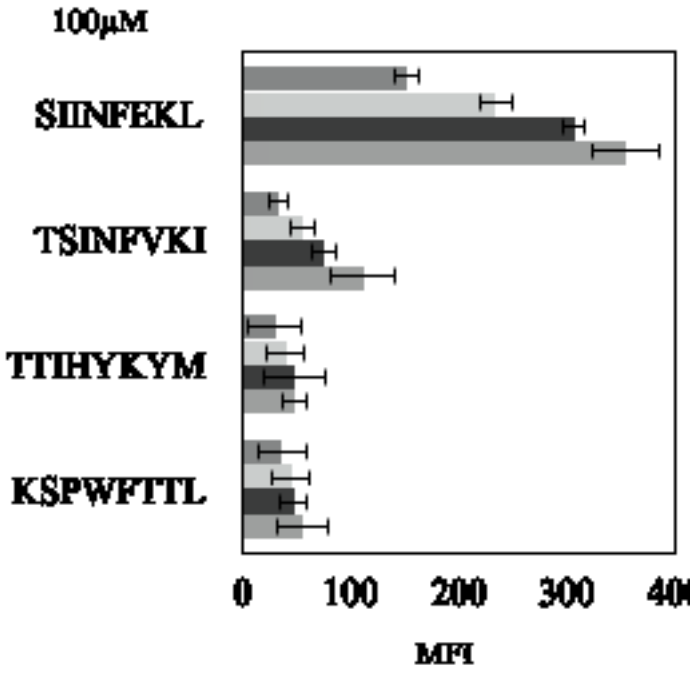
100μM
SIINFEKL
TSINFVKI
TTIHYKYM
KSPWFTTL
0
100
200
300
MFI

B

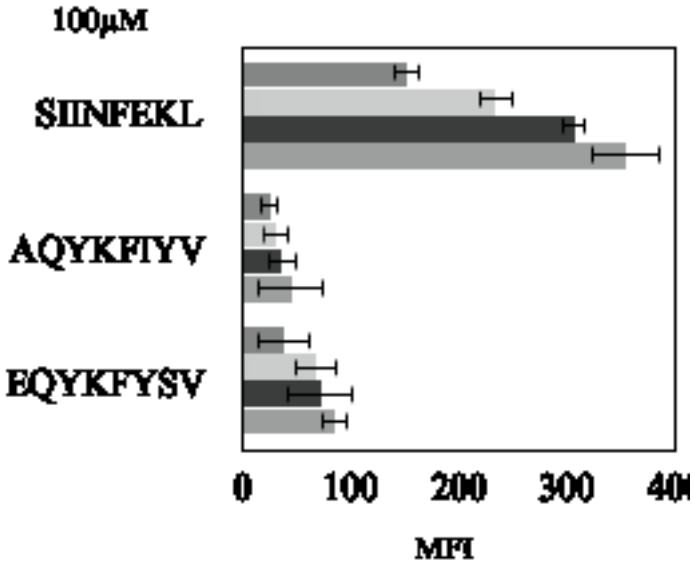
100μM
SIINFEKL
AQYKFIYV
EQYKFYSV
0
100
200
300
MFI

Figure 3-7. Recombinant mouse β2m does not aid in the stabilization of peptide-H-2K^b complexes where the peptide has low "affinity" for H-2K^b. RMA/S cells incubated with different amounts of recombinant mouse β2m, and loaded with peptides that did not show detectable H-2K^b stabilization on RMA/S cells. RMA/S were further incubated with 100μM of **(A)** peptides with non-polar aliphatic auxiliary anchor residues at P3 and **(B)** peptides with aromatic amino acids at P3. Detection of H-2K^b on RMA/S was done using the H-2K^b specific primary antibody Y3, followed by a secondary flourescently labeled antibody and analyzed in FACSCalibur cell analyzer. Results are the mean of three independent experiments. Error bars indicate SD.

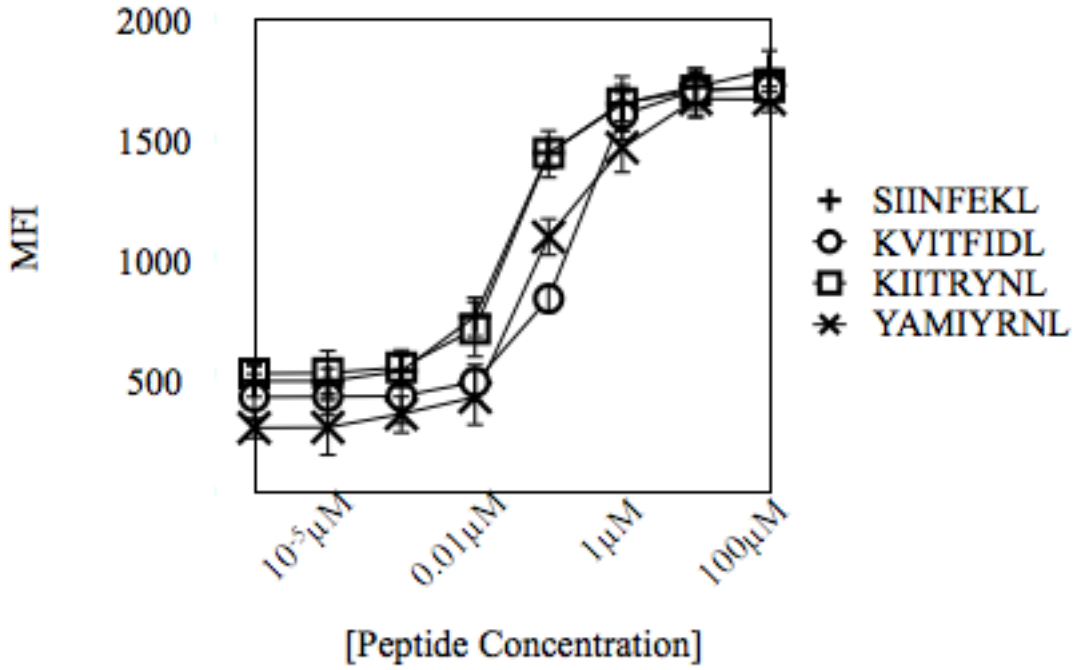

Figure 3-8. Peptide titration assays to determine similar H-2K^b expression on RMA/S cells using peptides with non-polar aliphatic P3 residues. H-2K^b expression on RMA/S cells incubated with the indicated peptides at concentrations ranging from 100µM to 10^{-6}µM in 10-fold dilution series. Detection of H-2K^b on RMA/S was done using the H-2K^b specific APC conjugated antibody AF6-88.5.5.3 and analyzed in FACSCanto cell analyzer. Results are the mean of three independent experiments. Error bars indicate SD.

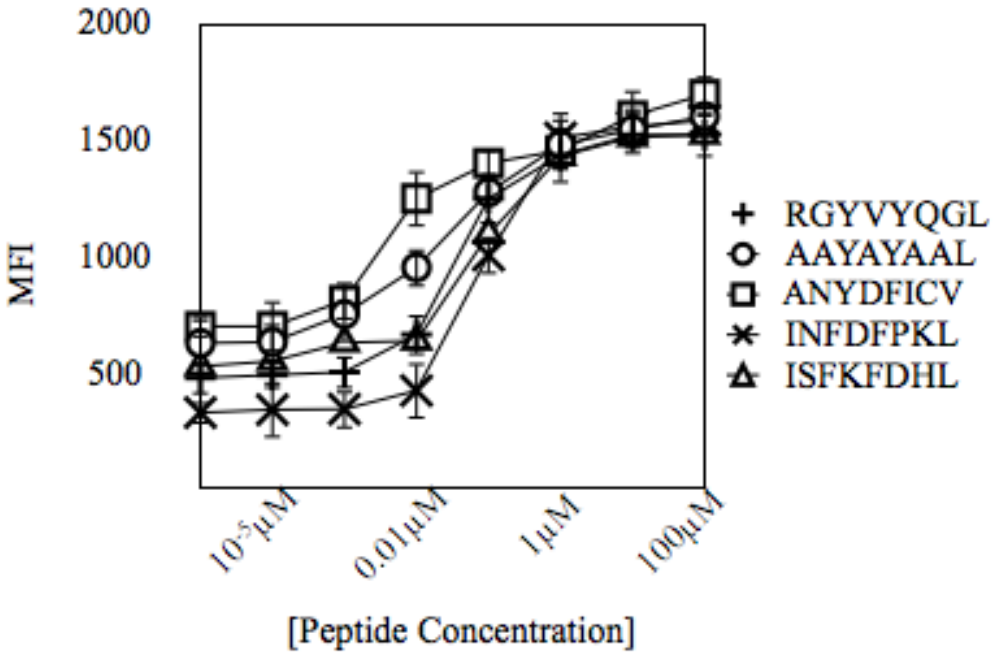

Figure 3-9. Peptide titration assays to determine similar H-2K^b expression on RMA/S cells using peptides with aromatic P3 residues. H-2K^b expression on RMA/S cells incubated with the indicated peptides at concentrations ranging from 100µM to 10^{-5}µM in 10-fold dilution series. Detection of H-2K^b on RMA/S was done using the H-2K^b specific APC conjugated antibody AF6-88.5.5.3 and analyzed in FACSCanto cell analyzer. Results are the mean of three independent experiments. Error bars indicate SD.

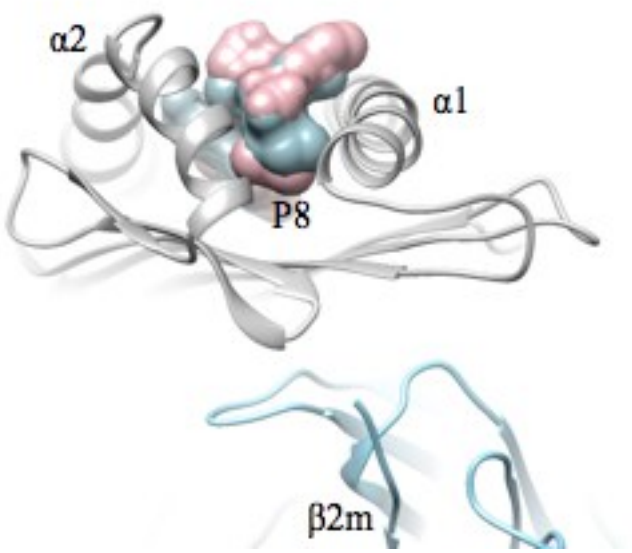

Figure 3-10. Structural comparison of P8 anchor residue identities in the F-pocket of the H-2K^b peptide binding groove. Surface view of the peptide bound to H-2K^b showing a greater area of the F-pocket occupied by P8 anchor residue Leu in SIINFEKL as compared to Ile in RAYIFANI. The H-2K^b heavy chain is in grey ribbon, the β2m in blue ribbon. Peptide residues are in filled surface drawing with SIINFEKL in pink and RAYIFANI in green.

CHAPTER IV

AMINO ACIDS AT POSITIONS 2 AND 3 OF THE H-2K^b BOUND PEPTIDE DICTATE LY49C RECOGNITION OF H-2K^b

A. Introduction

Natural killer (NK) cells play an important role in the clearance of tumor cells and virally infected cells via the release of cytotoxic molecules and the secretion of IFN-γ (48, 54, 263). NK cell activity depends on the integration of signals mediated by activating and inhibitory receptors. Examples of inhibitory receptors include Ly49s in rodents and killer-cell Ig-like receptors (KIRs) in humans (99). Inhibitory receptors expressed on NK cells interact with peptide-bound class I major histocompatibility complex (MHC-I) molecules to maintain NK cell tolerance to self. Although structurally distinct, Ly49 and KIR have analogous functions, and can recognize MHC-I in an allele specific manner (264).

Ly49 and KIR receptors can be peptide selective in their recognition of MHC-I-peptide complexes. In other words, some MHC-I bound peptides, but not all, support receptor recognition (50, 209, 218, 265, 266). This suggests that Ly49 and KIR can have a level of ligand specificity that extends beyond simply detecting the presence or absence of an MHC-I allele product, but includes the MHC-I bound peptide as well. The peptide repertoire for MHC-I binding can be modified by viral infection and tumorigenic transformation (267, 268). NK cells may subsequently detect such modifications as

changes in the self peptide pool normally displayed on MHC-I, thus altering the balance of inhibitory and activating signals, and consequently alter NK cell activity. For instance, mouse Ly49C and Ly49I, as well as rat Ly49i2, are inhibitory NK cell receptors that recognize MHC-I in a peptide selective manner. Previous studies using Ly49C and the cognate ligand H-2K^{b} have shown that the identity of the peptide at position 7 (P7) directly influences receptor-ligand interaction. In addition, we showed that peptide selective recognition of the rat MHC-I molecule, RT1-A1^{c}, by Ly49i2, is determined by the identity of the position 2 (P2) anchor residue of peptide bound to RT1-A1^{c} (218). Peptide anchor residues dock into pockets formed in the peptide binding groove, driving peptide affinity for MHC-I and affecting the topology of the peptide binding platform (245).

The mouse Ly49C peptide selective recognition of H-2K^{b} has been reported to be partially dependent on peptide amino acid at P7. Residues at P7 protrude from the peptide binding groove and interact with amino acids in the α1-helix of H-2K^{b} . Although this made a great headway in determining peptide specific recognition of MHC-I molecules by Ly49 receptors, we further probed the role of auxiliary anchor residues and/or buried residues of the MHC-I bound peptides determine peptide specificity of Ly49 receptors. In this report, we show that the identity of the peptide auxiliary anchor residue P3, and the adjacent P2 residue, both buried in the peptide binding groove, can greatly influence Ly49C peptide selectivity in recognition of H-2K^{b}. This indicates that not only in rat, but also in mice, Ly49 recognition can be determined

by peptide residues bound in specific buried locations in the peptide binding groove, and suggests this may be a fundamental feature of Ly49 recognition of MHC-I ligands.

B. Results

Ly49W/C chimeric receptors are peptide specific for recognition of H-2K^b

The mouse inhibitory Ly49C NK cell receptor binds H-2K^b complexed with certain, but not all, bound peptides, showing peptide selectivity in MHC-I recognition that is independent of MHC-I stabilization. We postulated from our work with the inhibitory rat Ly49i2 that the identity of a peptide anchor residue would be important in determining peptide selectivity of Ly49C recognition of H-2K^b. Peptides that bind H-2K^b have two conserved primary anchor residues, aromatic amino acids at P5 and aliphatic amino acids at P8, and a more variable auxiliary anchor residue at P3 (244, 269). Based on the pattern of Ly49C recognition of H-2K^b bound with different peptides, we suspected that Ly49C binding maybe influenced by the identity of the P3 auxiliary anchor residue.

Peptide dependent recognition of H-2K^b by Ly49C was addressed using functional assays. As the target cells, we used RMA/S cells loaded with different peptides using the approach described in the previous chapter. As the effector cells, we used the RNK-16 rat leukemia cell line. Since RMA/S cells are not a natural target for RNK-16 lysis, we transfected RNK-16 cells to stably express a chimeric receptor, Ly49W/C, that retains inhibitory Ly49C specificity, while responses are mediated through the activating Ly49W cytoplasmic and transmembrane domains. Thus upon

contact with ligand on RMA/S, we can obtain a functional readout of receptor and ligand interactions (Figure 4-1A).

Electroporation of RNK-16 cells with BSRαEN.Ly49W/C yielded three positive clones, 2G5, 2H7 and 5G2, with slightly different cell surface expression levels of chimeric receptor detected by staining with anti-Ly49C antibody, 4L03311 (Figure 4-1B). Clones were tested for their ability to lyse RMA/S cells, discussed in the previous chapter, loaded with H-2K^b specific peptides. We included the SIINFEKL peptide as a positive control for Ly49W/C recognition, where we expected high percent specific lysis. On the other hand, the peptide RGYVYQGL, that does not support Ly49C recognition of H-2K^b was utilized as a negative control for Ly49W/C recognition, which results in low percent specific lysis (197). Additionally, we used RMA/S cells with no peptide loaded, as a negative control for the downregulation of H-2K^b and thus expecting low percent specific lysis. In examining the peptide specific killing of RMA/S cells, we had a broad window between our positive and negative controls that would allow us to denote small differences between peptides tested in further experiments, where we only change one amino acid within the peptide bound to H-2K^b. The three clones tested showed MHC-I and H-2K^b-peptide specific Ly49C recognition others have observed using *ex vivo* NK cells, where H-2K^b-SIINFEKL leads to recognition, H-2K^b-RGYVYQGL does not support recognition, as well as a loss of H-2K^b represented by RMA/S incubated in the absence of peptide . The trend for recognition was similar in clones 2G5, 2H7, and 5G2 that expressed the chimeric receptor. Clone 5G2 had the narrowest range between our positive and negative controls and showed lower

cytotoxicity against target cells as compared to clones 2G5 and 2H7 (Figure 4-2A). Although clone 2G5 showed a marked difference between positive and negative controls, we observed higher specific lysis of negative control targets compared to clones 5G2 and 2H7 (Figure 4-2B). Finally, clone 2H7 showed the more favorable combination of pronounced contrast between positive and negative controls, as well as the expected low cytotoxicity towards RMA/S cells incubated with the RGYVYQGL peptide or no peptide for the loss of H-2K^b expression (Figure 4-2C). The similar pattern of peptide-specific cytotoxicity between these three clones demonstrated that, rather than uniquely clone-specific, this is a phenotype consistent among clones expressing the chimeric receptor. Therefore, we used 2H7 clones for our cytotoxicity studies elucidating Ly49W/C recognition of H-2K^b bearing different peptides on RMA/S cells.

Identity of the peptide auxiliary anchor residue at P3 correlates with Ly49C recognition of H-2K^b

We initially tested various peptides in our cytotoxicity assays and looked for a pattern of Ly49W/C recognition of H-2K^b bearing different peptides on RMA/S cells, focusing on the primary anchor and auxiliary anchor residues (Table 4-1). Additionally, in parallel to cytotoxic assays, we performed RMA/S stabilization assays as described in Chapter III, in order to corroborate H-2K^b peptide dependent expression. The group of peptides with non-polar aliphatic auxiliary anchor residues at P3, stabilize H-2K^b on RMA/S cells at similar levels (Figure 4-3A). Probing Ly49W/C recognition of H-2K^b, by cytotoxicity assays, showed that RMA/S cells loaded with peptides with non-polar aliphatic P3 residues, including SIINFEKL, KVITFIDL, KIITYRNL and YAMIYRNL,

similarly support Ly49W/C and H-2K^b association (Figure 4-3B, 3C). On the other hand, although capable of yielding similar H-2K^b expression on RMA/S cells (Figure 4-4A), peptides bearing aromatic residues at P3 such as ISFKFDHL, INFDFPKL ANYDFICV and RGYVYQGL, did not or poorly supported H-2K^b recognition by Ly49W/C (Figure 4-4B, 4C). As expected, we did not observe a correlation in the identity of primary anchor residues and H-2K^b recognition by Ly49W/C. In contrast, we observed a division within the peptides, where peptides containing an Ile or Met at the P3 auxiliary anchor position granted H-2K^b recognition by Ly49W/C (Figure 4-3), but those containing a Tyr or Phe at P3 did not, or did poorly (Figure 4-4) (Table 4-2). In line with previous studies by Franksson *et al*., our results suggest that there are distinctions in Ly49W/C recognition of H-2K^b-peptide complexes (210).

Aliphatic residues at P3 are supportive of Ly49W/C recognition of H-2K^b

We tested Ala substituted SIINFEKL variants at each residue individually to examine Ly49W/C recognition and compare to what others have observed as far as variant stabilization of H-2K^b and Ly49C recognition. As previously shown by other groups, SIINFEKL analogs bearing Ala at the positions P1, P2, P3, P5, and P8 did not stably bind H-2K^b compared to the unchanged SIINFEKL peptide (Figure 4-5) (246). However, P4, P6, and P7 Ala SIINFEKL variants created stable H-2K^b complexes and were tested for Ly49W/C recognition of H-2K^b (Figure 4-5). At the same time as cytotoxicity experiments to probe Ly49W/C peptide dependent recognition of H-2K^b, we performed RMA/S stabilization assays with P4, P6, and P7 Ala SIINFEKL variants to verify H-2K^b expression on RMA/S cells (Figure 4-6A). Compared to SIINFEKL,

Ala peptide analogs SIIAFEKL and SIINFAKL did not show a reduction in Ly49W/C recognition, while SIINFEAL showed a modest decrease in recognition as previously demonstrated (Figure 4-6C, 6D).

Since Ala substitutions at the auxiliary anchor residue P3 did not yield stable H-2K^b complexes, we substituted a Val or a Tyr for the Ile at P3 of SIINFEKL, a peptide highly supportive of Ly49W/C recognition, while allowing the other peptide residues of SIINFEKL to remain unchanged. Therefore, SIINFEKL peptide variants, SIVNFEKL and SIYNFEKL, were used to investigate the role of P3 in H-2K^b recognition by Ly49W/C using cytotoxicity assays. In parallel to killing assays, we also carried out RMA/S stabilization assays with peptides SIVNFEKL and SIYNFEKL, as well as control peptides, where all peptides yielded H-2K^b expression at similar levels (Figure 4-7A). Substituting Val for Ile at P3, SIVNFEKL, made no significant difference to H-2K^b recognition, as observed in cytotoxicity experiments; however, exchange of a Tyr for Ile, SIYNFEKL, partially reduced H-2K^b recognition as compared to the RGYVYQGL peptide or no peptide (Figure 4-7B, 7C). These results indicated that aliphatic residues Val or Ile at P3 are fully supportive of, while the aromatic and polar Tyr is detrimental to, Ly49W/C interaction with H-2K^b. The substitution of Tyr for Ile at P3 in SIINFEKL did not completely disrupt recognition, indicating that additional residue(s) may contribute to Ly49C and H-2K^b interaction as we observed with the P7 residue. Nevertheless, partial decrease in MHC-I-peptide recognition by Ly49 receptors, can be an importantfactor in determining NK cell function.

P2 and P3 peptide residues combine to drive Ly49W/C recognition of H-2K^b

We further investigated the role of peptide residues in Ly49W/C recognition of H-2K^b by comparing variants of a synthetic peptide, AAYAYAAL. Like RGYVYQGL, AAYAYAAL is not supportive of H-2K^b interaction with Ly49W/C (197). We recapitulated the identity of SIINFEKL residues that we and others have found to contribute to Ly49C recognition into the AAYAYAAL peptide to test gain of recognition. Peptides used in this assay include AIIAFAKL, AIIAFAAL, and AIIAYAAL, that bind H-2K^b at similar levels, demonstrated by RMA/S stabilization assays that were performed in parallel to cytotoxicity assays (Figure 4-8A). Interestingly, the peptide AIIAFAKL is fully supportive of Ly49W/C recognition, as is AIIAFAAL and AIIAYAAL, suggesting a pivotal role for residues that dock into the adjacent B-pocket and D-pocket of H-2K^b which might be a site important to allow for H-2K^b and Ly49W/C interaction (Figure 4-8B, 8C). To pinpoint individual effects of P2 and P3 in Ly49W/C recognition of f H-2K^b, we tested P2 and P3 Ala substitutions in the AIIAYAAL peptide. However, peptides AAIAYAAL and AIAAYAAL did not stabilize H-2K^b on RMA-S cells for the duration of the cytotoxicity assays (Figure 4-9). Therefore, our data suggests that the amino acid identity of of both P3 and P2 peptide residues are required to alter H-2K^b recognition by Ly49W/C.

An LCMV immunodominant peptide and CTL escape mutants do not support Ly49C recognition of H-2K^b

During a viral infection, the peptide repertoire in the cell is subjected to modification, resulting in presentation of viral peptides and possibly an altered array of

self peptides to T cells (267). Mouse lymphocytic choriomeningitis virus (LCMV) infection produces an immunodominant virus-derived peptide, GP1 33-41 (KAVYNFATM) that can be presented by H-2K^b and H-2D^b (270). Due to cytotoxic T lymphocyte (CTL) immunosurveillance, GP1 33-41 is subjected to mutation, thus producing CTL escape variants (45, 47, 271). Such natural peptide escape variants have not been explored in the context of Ly49 recognition. This is especially important given that the peptide-selective nature of Ly49 recognition can greatly impact NK cell function. Of the GP1 33-41 escape variants, peptides with canonical primary peptide anchor residues were able to bind H-2K^b: KAVYNYASM and KAVFNFATM at similar levels during RMA/S stabilization assays (Figure 4-10A). In the H-2K^b-KAVYNFATM crystal structure, Lys^1 sits outside the peptide binding groove with Tyr^4 as the auxiliary anchor residue, while Phe^6 and Met^9 are the primary anchor residues in comparison to octameric peptides where auxiliary anchor residues are at P3 and primary anchors are at P5 and P8 (272). We used the wildtype GP1 33-41 and CTL escape variant peptides to probe their role in Ly49W/C recognition of H-2K^b, also including the VSV derived peptide, RGYVYQGL, as a negative control. We found that the wildtype and the related escape variant peptides supported Ly49W/C recognition of H-2K^b poorly or not at all, as compared to the OVA peptide SIINFEKL (Figure 4-10B, 10C). Consistent with our previous results, regardless of its polarity in this set of peptides, the presence of a bulky residue at the auxiliary anchor residue (P4 in the case of nonameric peptides) is detrimental for Ly49W/C recognition. Thus, although GP1 mutates to escape CTL recognition, it does not enhance Ly49W/C recognition to possibly escape NK cell surveillance.

C. Discussion

Ly49 receptors interact with MHC-I molecules at a site beneath the floor of the peptide binding groove involving amino acids in the α1 and α2 domains, as well as the α3 domain and β2m, with no access to the bound peptide (195). Nevertheless, Ly49 recognition is dependent on the MHC-I bound peptide and can also be peptide selective. For instance, Ly49A recognizes H-2D^{d} when in complex with any bound peptide, while Ly49C is more discriminating between different H-2K^{b}-peptide complexes (220). A study using a limited number of SIINFEKL peptide analogs showed that amino acid at P7 had a partial influence in Ly49C recognition of H-2K^{b}. Since we have shown that the rat Ly49i2 recognizes cognate MHC-I ligand, RT1-A1^{c}, in a peptide selective manner; a process that is dependent on the P2 peptide anchor residue, we investigated whether anchor residues had an effect on Ly49C recognition of H-2K^{b} (218).

Given that the peptide repertoire in a cell can be affected by different stimuli, including viral infection or oncogenic transformation, it is important to investigate the mechanisms by which different peptides affect Ly49 recognition and, therefore, NK cell function. Utilizing functional assays that provided a positive response for Ly49C recognition via a Ly49W/C chimeric receptor, we found a correlation between the peptides that grant Ly49C recognition and the identity of the peptide auxiliary anchor residue at P3. Peptides bearing aliphatic R groups at the auxiliary anchor residue P3, supported Ly49C recognition of H-2K^{b}, while peptides containing amino acids with aromatic side chains at P3 show decreased Ly49C recognition of H-2K^{b}. In order to directly examine the role of the auxiliary anchor residue in Ly49C-H-2K^{b} interaction, we

used SIINFEKL peptide variants where we exchanged Ile at P3 to a Val, similar to Ile, or to a Tyr, found in peptides that did not facilitate Ly49W/C recognition of H-2K^b. The exchange of Ile to Tyr led to a loss of Ly49W/C recognition of H-2K^b; while Ile to Val did not have a significant effect on receptor-ligand interaction. Additionally, the AAYAYAAL peptide stabilized H-2K^b but did not support Ly49C recognition of H-2K^b. However, by substituting Ile at P3 and P2, the AIIAYAAL peptide also stabilized H-2K^b and, importantly, was fully supportive of Ly49W/C interaction. Our studies show that the identity of residues at P2 and P3 of the H-2K^b bound peptide are fundamental to Ly49W/C recognition.

A well defined role of peptide anchor residues is to form stable complexes for the presentation of peptide-MHC-I complexes at the cell surface. We have also demonstrated here that an anchor residue plays a role in determining Ly49C recognition of H-2K^b, thus expanding our understanding of the molecular basis for Ly49C peptide selectivity. Earlier studies in our laboratory demonstrated the importance of anchor residues in determining rat inhibitory Ly49i2 recognition of its cognate ligand, RT1-A1^c. We determined the role of the anchor residue at P2 of the RT1-A1^c bound peptide using peptide variants of a high affinity peptide, NPRKVTAYL, where Pro or Val at P2 supported Ly49i2 recognition, but Gln at this position completely abrogated Ly49i2 interaction with RT1-A1^c(218). Like mouse Ly49, Ly49i2 also interacts with RT1-A1^c at a site under the base of the peptide binding groove, as demonstrated by mutagenesis studies, indicating that Ly49s can indirectly detect differences in the MHC-I bound peptide (227). Taken together, our results indicate that peptide selectivity in rodent

Ly49s in both mice and rats can be attributed in part or in whole to the identities of anchor residues of the MHC-I peptide bound, and this might be a fundamental aspect of NK cell surveillance.

We demonstrated that the identities of peptide residues P2 and P3 bound in the peptide binding groove influenced Ly49C association with H-2K^b. The molecular mechanism that modulates this process might be elucidated by analyzing the crystal structure of H-2K^b bound to SIINFEKL and RGYVYQGL. Anchor residues in H-2K^b bound peptides were at P5 and P8 and an auxiliary anchor residue at P3; where P5 and P8 are inserted in a downward vertical fashion, while P3 is in a more horizontal, slanted position within the D-pocket. The P8 residue makes extensive contacts with residues in the F-pocket of H-2K^b; while, P5 docks into the C-pocket, which is adjacent to the B-pocket bearing the P2 residue. The P3 residue occupies the shallower D-pocket, which unlike other pockets that are in the floor of the groove, is partly formed by residues in the α2-helix of the peptide binding groove. When the B-pocket is occupied by a small residue at P2, such as Gly in RGYVYQGL, a water molecule can fill the B-pocket of H-2K^b and contribute to an extensive hydrogen bond network that stabilizes the core of the peptide-binding groove, which with RGYVYQGL also involves the hydroxyl group of Tyr at P5 in the C-pocket and the α-carbon of P3 (7). With the SIINFEKL peptide, Ile at P2 fully occupies the B-pocket, leaving no space for water molecules, potentially increasing the flexibility of the core of the peptide binding groove, and in turn, possibly decreasing the free energy requirements for Ly49C binding of H-2K^b (Figure 4-11) (7, 195).

The auxiliary anchor residue at P3 occupies a shallow pocket, found at the 'hinge' region joining the two segmented areas of the α2-helix, a structural component of the heavy chain that provides additional flexibility to accommodate different peptides. A bulky and polar amino acid at the auxiliary anchor residue P3, as in the RGYVYQGL peptide, occupies a larger area and gives rise to hydrogen bond formation with Glu^{152}; while in the SIINFEKL peptide, the uncharged and relatively small size of Ile results in van der Waals interactions with amino acids in the B-pocket (Figure 4-12A). Interactions at the 'hinge' region of the α2-helix, including Glu^{152}, can have an impact on solvent exposed residues in the loops that connect the antiparallel β-strands that form the platform of the groove floor (Figure 4-12B). For instance, in the H-$2K^b$-SIINFEKL complex, Arg^{111} forms a hydrogen bond with Glu^{128}, but in the H-$2K^b$-RGYVYQGL complex Arg^{111} instead shares a hydrogen bond with Glu^{102} (Figure 4-13A) (273). This difference in intramolecular interactions, can affect Ly49C binding since Arg^{111} shares van der Waals contacts with Met^{225} in Ly49C as well as salt bridges with Glu^{241} in Ly49C; and Glu^{128} forms salt bridges with Lys^{221} of Ly49C, as observed in the H-$2K^b$-SIINFEKL-Ly49C co-crystal structure (Figure 4-13B) (195). Therefore, the differences in the identity of peptide residues P2 and P3 may influence the heavy chain by promoting different hydrogen-bond networks at the core of the peptide binding groove, by affecting α-helical components that drive different intramolecular interactions, and by affecting the orientation and/or flexibility of β2m, which may be significant in determining Ly49C interaction.

As mentioned above we have proposed structural mechanisms for Ly49C interaction of H-2K^b depending on the identity of residues at P2 and P3 of the bound peptide. In addition, we briefly mentioned how flexibility of the peptide-H-2K^b complexes can modify the free energy requirement for Ly49C binding depending on the identity of anchor residues. The binding affinity between the peptide and MHC-I can be an indication of complex rigidity, where low peptide binding affinity can be equivalent to higher complex flexibility and less free energy of binding needed to modify conformational components for Ly49 binding. Therefore it is still necessary to investigate if the complexes we have observed to support Ly49C recognition of H-2K^b correlate with low H-2K^b-peptide binding affinities. Using a bioinformatics method, we determined IC_{50} values for H-2K^b and peptides tested in this study. The IC_{50} value are obtained using the algorithm NetMHCpan which takes into account the identity of anchor peptide residues and specific MHC allele information to produce quantitative predictions of the affinity between the peptide and the MHC of interest (233). Most of the peptides that have strong predicted binding affinity for H-2K^b were also in the group of peptides that did not support Ly49W/C recognition; while the majority of the predicted weaker H-2K^b peptide binders were also part of the set of peptides supporting Ly49W/C binding (Table 4-3). Although we have found a relationship between Ly49W/C recognition of H-2K^b and theoretical peptide affinity for H-2K^b, using a web based algorithm, it is still necessary to perform experimental measurements of peptide-H-2K^b affinities to corroborate if peptide binding affinities for H-2K^b are in fact a substantial factor in determining Ly49C association with H-2K^b. Therefore, the next step is to perform circular dichroism experiments of refolded H-2K^b heterotrimers with

peptides that do or do not support Ly49C recognition in order to find out the stability that each peptide provides to the heterotrimer. Circular dichroism is a technique often used to determine the thermal stability of soluble protein complexes. Using circular dichroism, we can obtain the protein complex changes in ellipticity at different temperatures and the protein complex melting temperature. Both measurements correlate with loss of secondary structure during denaturation and can be an indication of the degree of integrity each peptide provides to the MHC-I complex (274). Notably, peptide binding for H-2K^b proportionally correlates with anchor residues. Primary anchor residues are highly conserved while auxiliary anchor residues and other residues that dock into the peptide binding cleft are only partially conserved. Therefore, it is plausible that residues docking into the peptide binding groove near the N-terminal region of the peptide might be more important than previously thought for directing peptide binding affinity to H-2K^b and can be the rheostats of peptide binding affinities. Moreover, the different peptide binding affinities could have an impact on NK cell recognition by Ly49 receptors.

The peptide repertoire in a cell changes depending on its physiological state, including tumorigenic transformation and viral infection. Variations in the peptide pool could possibly have significant influences on the functionality and responsiveness of NK cells that express peptide selective receptors such as Ly49C. During LCMV infection, a virus glycoprotein derived immunodominant peptide, GP1 33-41, as well as GP1 33-41 CTL escape variant peptides that differ in amino acid sequence, can be displayed on H-2K^b, a ligand for Ly49C. To gain insight into the influence of LCMV-derived

immunodominant and immunoselected variant peptides on the recognition and function of a peptide-selective NK cell receptor, Ly49C, we tested the LCMV peptide, GP1 33-41 (KAVYNFATM), and CTL escape variants that can also stably bind to H-2K^b, KAVFNFATM and KAVYNYASM, for recognition by Ly49W/C. Given that the WT and escape mutant peptides have bulky aromatic R groups at the auxiliary anchor position, and as can be predicted from our study, we found that these peptides did not support Ly49C recognition, similar to the RGYVYQGL peptide. Notably, although two of these peptides are used to escape CTL recognition, our results suggest that the inhibitory Ly49C receptor would not engage, or poorly engage with H-2K^b bearing any of these peptides. Depending on the frequency of such wildtype or variant GP1 33-41 peptide MHC-I complexes *in vivo,* NK cell function may be affected by lowering the threshold for NK cell activation. Ultimately, *in vivo* studies may establish how important peptide-dependent NK cell responses are during the course of viral infection.

Inhibitory KIR, like Ly49 receptors, can exhibit peptide selectivity in their recognition of cognate MHC-I ligands (209). Unlike Ly49 receptors that bind cognate ligands at a site under the peptide binding groove, KIR in humans, interact with MHC-I at a polymorphic region in the α1 and α2 domains above the peptide binding groove, with access to the bound peptide, where peptide amino acids 7 and 8 influence MHC-I recognition (275-277). Despite distinct modes of MHC-I recognition, peptide selectivity characteristic of KIRs and Ly49s reflects a shared ability to detect changes in the peptide repertoire of cells.

Peptide selectivity of Ly49 recognition may afford NK cells an added level of surveillance beyond simply detecting the presence or absence of specific MHC-I allele products. This could be useful in the context of cell transformation or pathogenic infection, where the expression level of MHC-I might not change, but its peptide content may (37). In this case, Ly49 may be able to discriminate MHC-I bound with different peptide repertoires, distinguishing self from non-self and/or altered self. due to different bound peptides. Advances in mass spectrometric identification of MHC-I-bound peptides, combined with a greater understanding of peptide features that confer peptide specific recognition of MHC-I by Ly49 receptors as provided here, might facilitate prediction and manipulation of NK cell responses (243, 278, 279). In addition, the importance of peptide selectivity *in vivo* remains to be established; for example, during NK cell education or target cell transformation, processes where Ly49-MHC-I interactions are fundamental to the fate and function of NK cells (99, 280). It also remains to be determined how many more receptors in the Ly49 family are peptide selective in ligand recognition, including activating Ly49 that can recognize MHC-I (281-283). Finally, identifying anchor residues as prime drivers of Ly49 peptide selectivity, and the endogenous peptides within which they reside, can be of importance towards defining self for NK cells.

Our work using different peptide analogs demonstrated the importance of anchor residues in the recognition of H-2K^b molecules by Ly49C receptors. We have speculated on different intramolecular effects that amino acids at P2 and P3 have on the H-2K^b heavy chain that affect the site of Ly49C recognition. However, a question that

still remains is whether peptides used in our studies have high or low affinity to H-2K^b, relative to one another, and how peptide-H-2K^b affinities correlates with Ly49C-H-2K^b interaction.

A

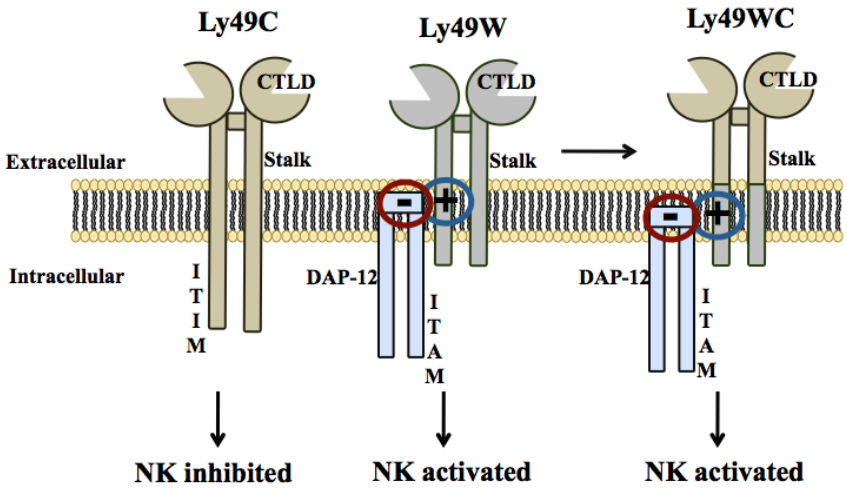

B

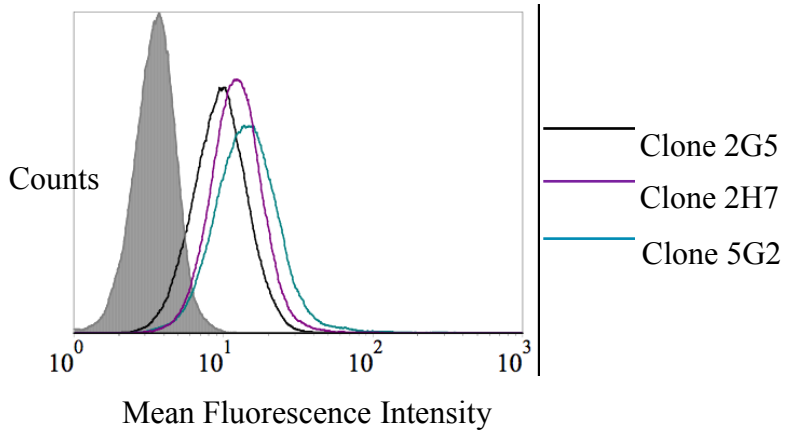

Figure 4-1. Expression of chimeric receptor Ly49W/C on RNK-16 cells. (A) Schematic representation of chimeric receptor complex with C57BL/6 inhibitory Ly49C extracellular domain and NOD activating Ly49W transmembrane and cytoplasmic domains that associate with adaptor molecule DAP12. **(B)** RNK-16 cells were stably transfected with the chimeric receptor Ly49W/C (RNK.49W/C) and generated clones 2G5, 2H7 and 5G2. Cell surface expression of Ly49W/C was detected using the Ly49C specific mAb 4L03311. Open histogram indicates 4L03311 staining and shaded histogram is the isotype control.

A

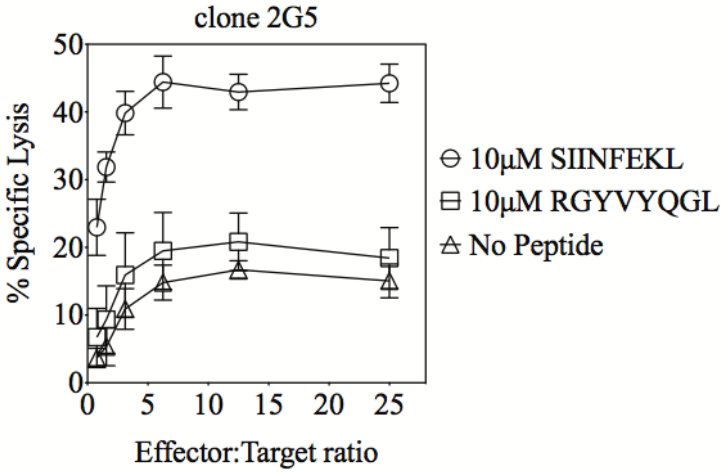
clone 2G5
% Specific Lysis
50
40
30
20
10
0
0
5
10
15
20
25
Effector:Target ratio
10μM SIINFEKL
10μM RGYVYQGL
No Peptide

B

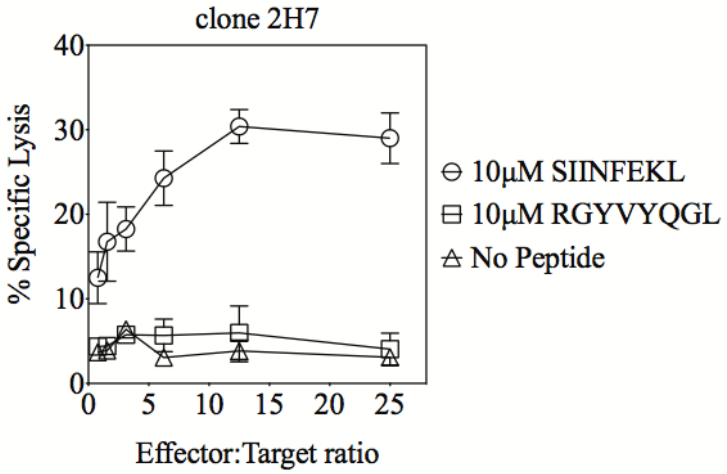
clone 2H7
% Specific Lysis
40
30
20
10
0
0
5
10
15
20
25
Effector:Target ratio
10μM SIINFEKL
10μM RGYVYQGL
No Peptide

C

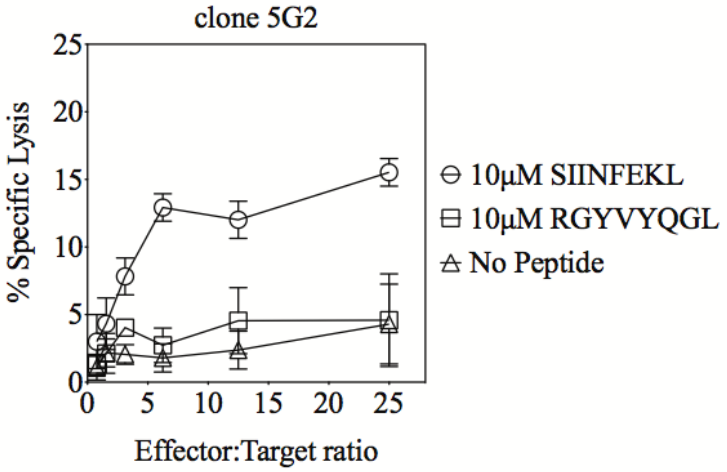
clone 5G2
% Specific Lysis
25
20
15
10
5
0
0
5
10
15
20
25
Effector:Target ratio
10μM SIINFEKL
10μM RGYVYQGL
No Peptide

Figure 4-2. Chimeric receptor Ly49W/C recognizes H-2K^b in a peptide selective manner. RNK-16 clones expressing Ly49W/C **(A)** 2G5, **(B)** 2H7 and **(C)** 5G2, were tested for their ability to lyse RMA/S cells loaded with the H-2K^b specific peptides. The SIINFEKL peptide is a positive control of Ly49W/C-H-2K^b recognition, the RGYVYQGL peptide is a negative control of Ly49W/C-H-2K^b association and the no peptide is a negative control that accounts for low levels of H-2K^b at the cell surface and therefore low Ly49W/C-H-2K^b interaction. Data represent the mean of three independent experiments, error bars represent the SD.

A

Peptide Sequence	Peptide origin
SI**I**N**F**EK**L**	Chicken Ovalbumin (256-264)
KI**I**T**Y**RN**L**	PCI domain-containing protein 2 (318-325)
KV**I**T**F**ID**L**	GTP binding protein I (246-253)
YA**M**I**Y**RN**L**	E3 ubiquitin-protein ligase mdm2 (100-107)

B

Peptide Sequence	Peptide origin
AN**Y**D**F**IC**V**	MMTV env gp70 (446-453)
RG**Y**V**Y**QG**L**	Vesicular Stomatitis Virus NP (52-59)
IS**F**K**F**DH**L**	F-actin capping protein alpha1 (93-100)
IN**F**D**F**PK**L**	RNA helicase p54 (407-414)
AA**Y**A**Y**AA**L**	Synthetic peptide

Table 4-1. Sequence and origin of H-2K^{b} specific peptides. (A) Peptides with non-polar aliphatic auxiliary anchor residues. **(B)** Peptides with aromatic auxiliary anchor residues. Bold indicates primary anchor residue, bold and underlined indicates auxiliary anchor residue.

A

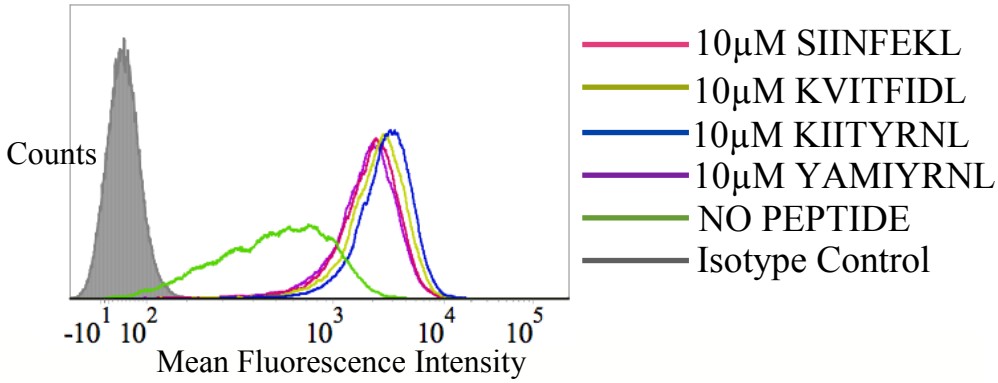
Counts
-10^1 10^2 10^3 10^4 10^5
Mean Fluorescence Intensity
10μM SIINFEKL
10μM KVITFIDL
10μM KIITYRNL
10μM YAMIYRNL
NO PEPTIDE
Isotype Control

B

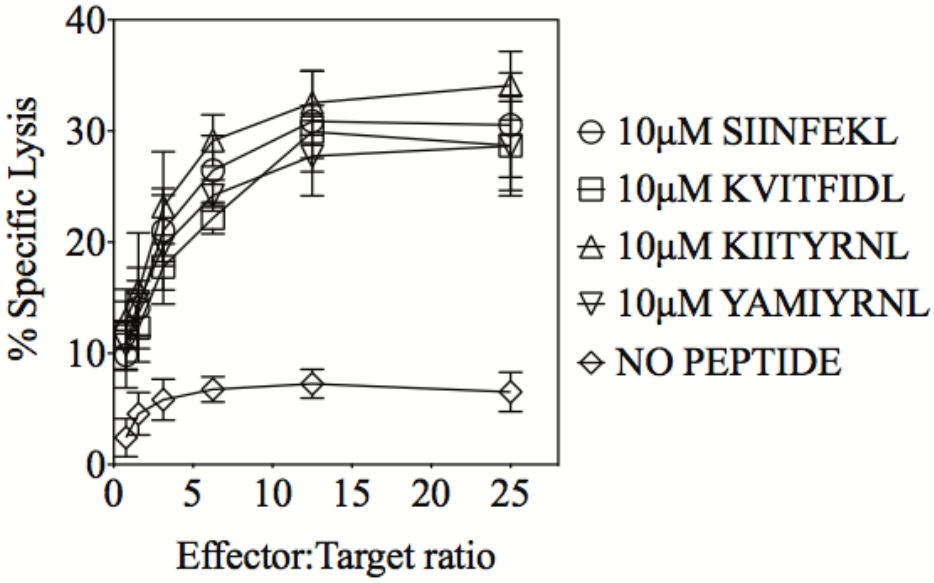
% Specific Lysis
0
10
20
30
40
0 5 10 15 20 25
Effector:Target ratio
10μM SIINFEKL
10μM KVITFIDL
10μM KIITYRNL
10μM YAMIYRNL
NO PEPTIDE

C

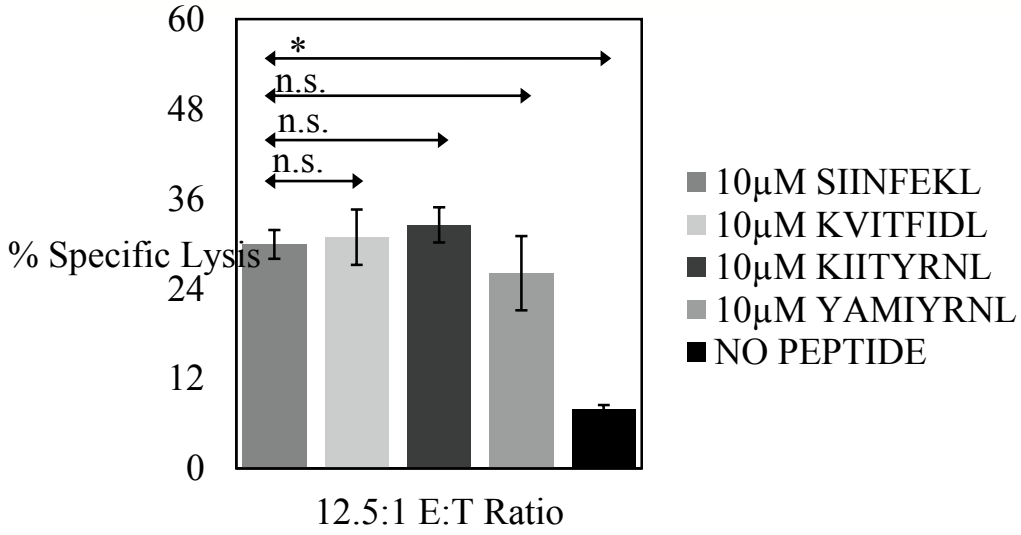
% Specific Lysis
0
12
24
36
48
60
*
n.s.
n.s.
n.s.
12.5:1 E:T Ratio
10μM SIINFEKL
10μM KVITFIDL
10μM KIITYRNL
10μM YAMIYRNL
NO PEPTIDE

Figure 4-3. Ly49C peptide dependent recognition of H-2K^b is retained in peptides with non-polar aliphatic auxiliary anchor residues. (A) RMA-S cell surface expression of H-2K^b when incubated with the indicated peptides, or no peptide. Shaded histogram corresponds to isotype control. **(B)** Percent specific lysis of RMA-S cells incubated with peptides bearing aliphatic R groups at P3, in the presence of RNK.49W/C effector cells with **(C)** statistical analysis at the 12.5:1 E:T ratio. Results plotted are the mean of three independent experiments with error bars representing SD.

A

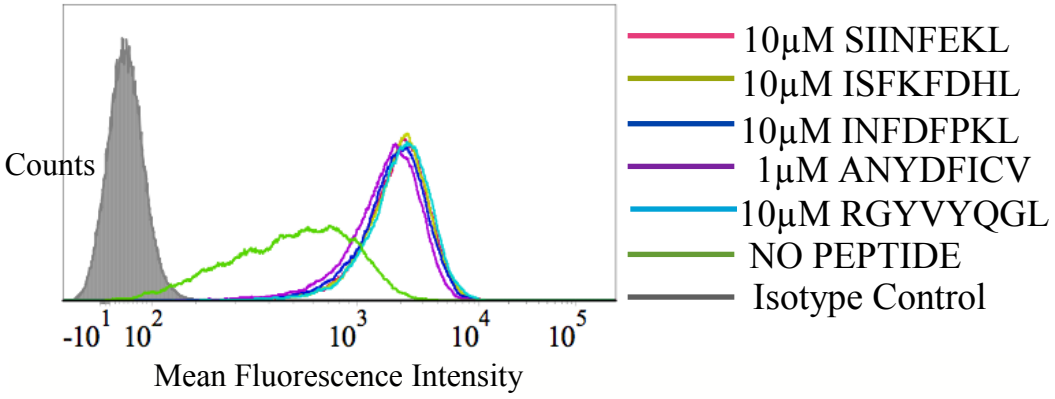
Counts
-10^1 10^2 10^3 10^4 10^5
Mean Fluorescence Intensity
10μM SIINFEKL
10μM ISFKFDHL
10μM INFDFPKL
1μM ANYDFICV
10μM RGYVYQGL
NO PEPTIDE
Isotype Control

B

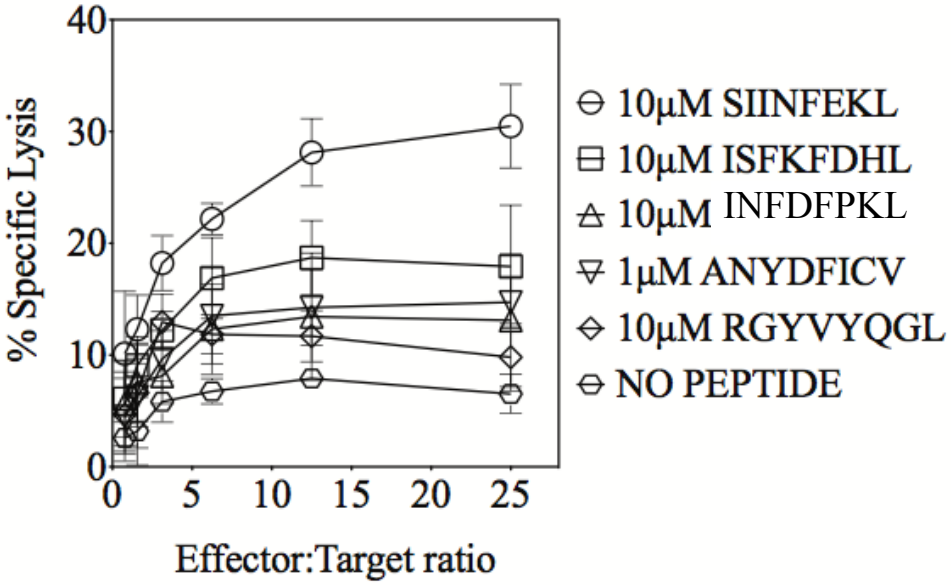
% Specific Lysis
0 10 20 30 40
0 5 10 15 20 25
Effector:Target ratio
10μM SIINFEKL
10μM ISFKFDHL
10μM INFDFPKL
1μM ANYDFICV
10μM RGYVYQGL
NO PEPTIDE

C

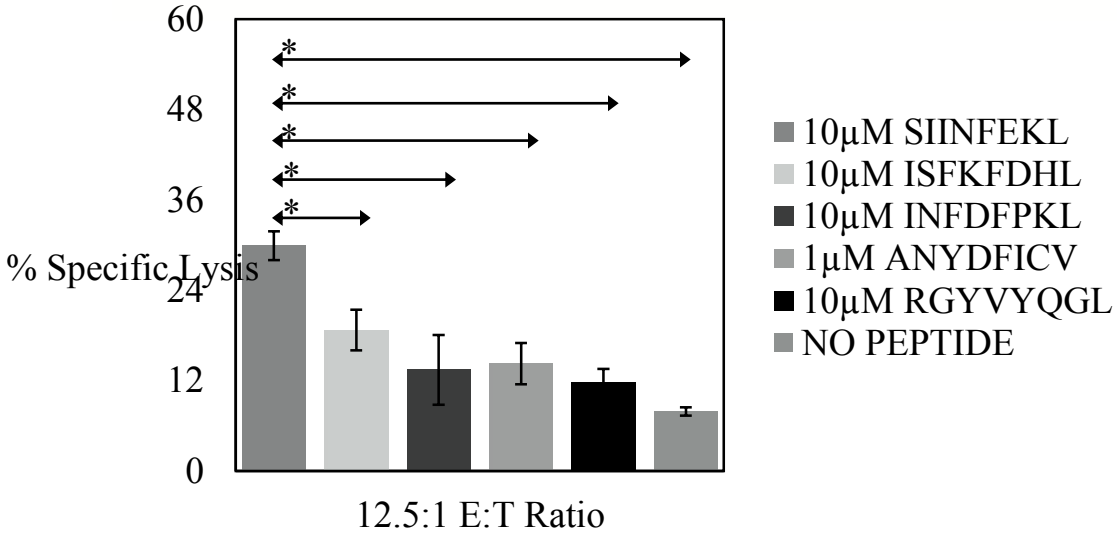
% Specific Lysis
0 12 24 36 48 60
*
12.5:1 E:T Ratio
10μM SIINFEKL
10μM ISFKFDHL
10μM INFDFPKL
1μM ANYDFICV
10μM RGYVYQGL
NO PEPTIDE

Figure 4-4. Ly49C peptide dependent recognition of H-2K^b decreases in peptides with non-polar aliphatic auxiliary anchor residues. (A) RMA-S cell surface expression of H-2K^b when incubated with the indicated peptides, or no peptide. Shaded histogram corresponds to isotype control. **(B)** Cytotoxicity assay using RMA-S cells loaded with peptides that have aromatic R groups at P3, co-incubated with RNK.49W/C cells, **(C)** including statistical analysis at the 12.5:1 E:T ratio (ns= not significant, *p<0.05, **p<0.005). Assays were performed in triplicate in three independent experiments with error bars representing the SD.

Peptide Origin	H-2K^b bound peptide sequence								% specific lysis (Ly49W/C recognition)
	1	2	**3**	4	**5**	6	7	**8**	
PCI domain protein	K	I	**I**	T	**Y**	R	N	**L**	HIGH
Chicken Ovalbumin (256-264)	S	I	**I**	N	**F**	E	K	**L**	HIGH
E3 ubiquitin-protein ligase	Y	A	**M**	I	**Y**	R	N	**L**	HIGH
GTP binding protein 1	K	V	**I**	T	**F**	I	D	**L**	HIGH
F-actin capping protein	I	S	**F**	K	**F**	D	H	**L**	MED
MMTV env gp70	A	N	**Y**	D	**F**	I	C	**V**	MED
RNA helicase p54 (407-414)	I	N	**F**	D	**F**	P	K	**L**	LOW
VSV NP peptide	R	G	**Y**	V	**Y**	Q	G	**L**	LOW
Synthetic K^b binding peptide	A	A	**Y**	A	**Y**	A	A	**L**	LOW

Table 4-2. Peptide dependent Ly49W/C recognition of H-2K^b. Peptides containing non-polar aliphatic auxiliary anchor residues at P3 support Ly49W/C association with H-2K^b as demonstrated by cytotoxicity assays. On the other hand peptides with aromatic residues at P3 are not highly supportive of Ly49W/C and H-2K^b interaction. For peptide amino acid sequence, bold indicates primary anchor residues at P5 and P8, bold and underlined indicates P3 auxiliary anchor residue.

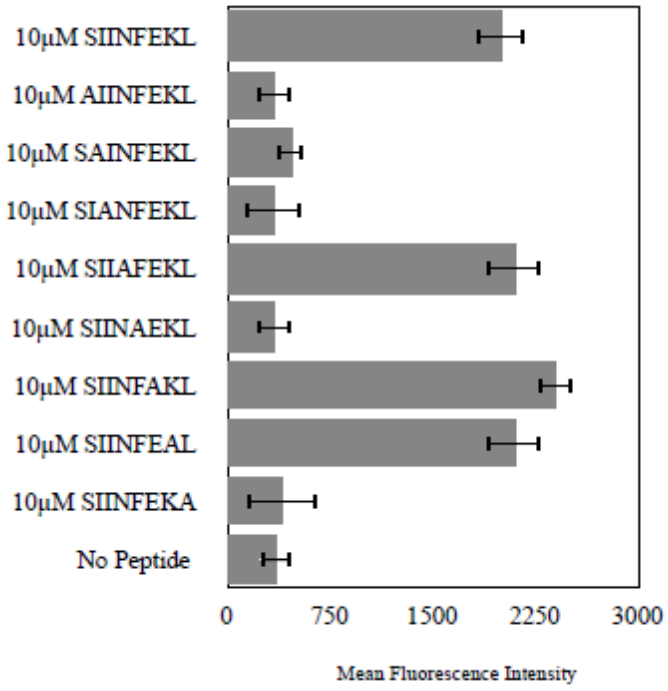

Figure 4-5. H-2K^b stabilization using Alanine SIINFEKL variants. RMA/S stabilization assay using 10μM of the indicated SIINFEKL Ala variant peptide. Cell surface expression of H-2K^b was detected using the APC conjugated AF6-88.5.5.3 antibody. Assays were conducted in triplicate in three independent experiments. Error bars indicate SD.

A

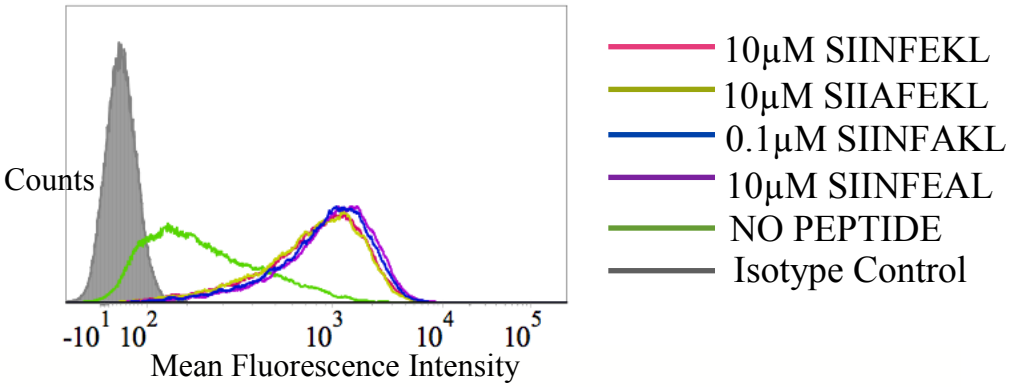
Counts
-10^1 10^2 10^3 10^4 10^5
Mean Fluorescence Intensity
10μM SIINFEKL
10μM SIIAFEKL
0.1μM SIINFAKL
10μM SIINFEAL
NO PEPTIDE
Isotype Control

B

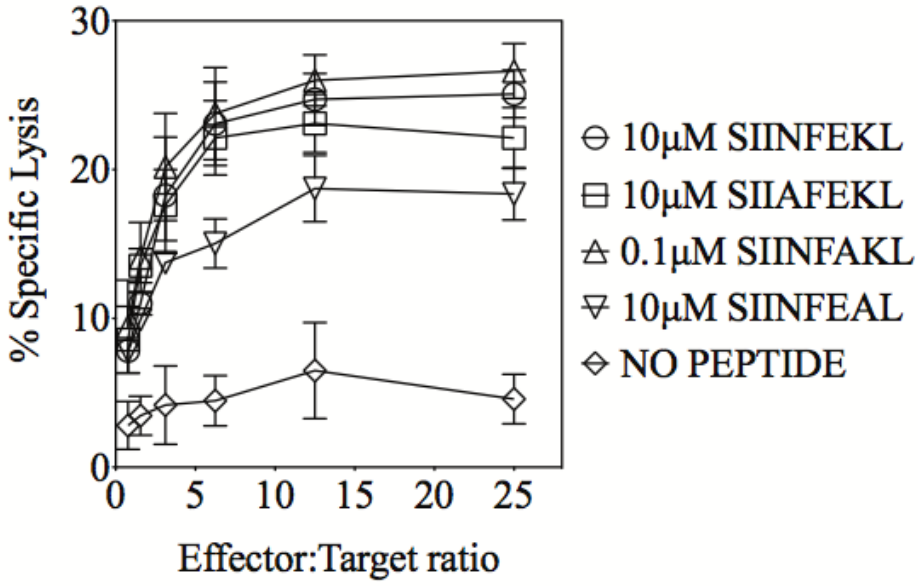
% Specific Lysis
0
10
20
30
0 5 10 15 20 25
Effector:Target ratio
10μM SIINFEKL
10μM SIIAFEKL
0.1μM SIINFAKL
10μM SIINFEAL
NO PEPTIDE

C

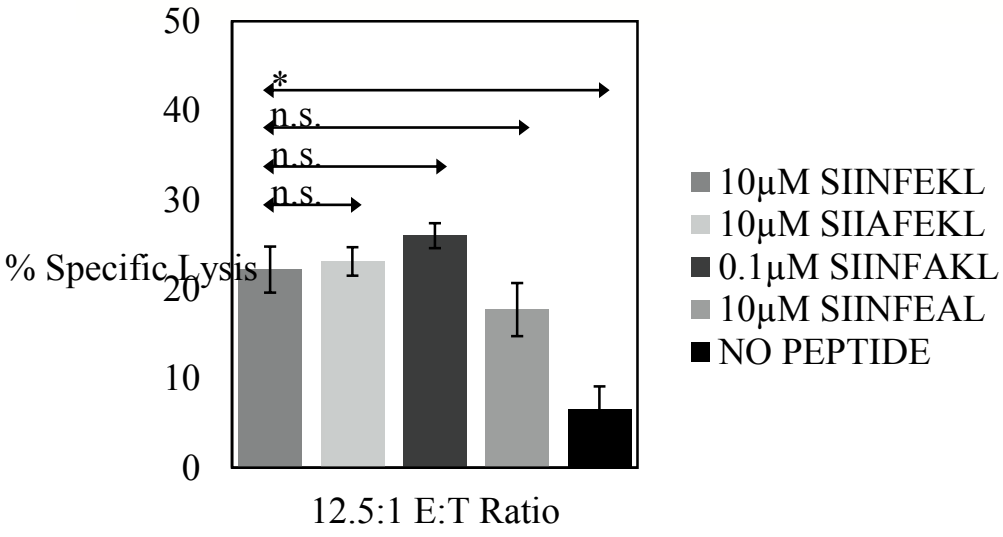
% Specific Lysis
0
10
20
30
40
50
*
n.s.
n.s.
n.s.
12.5:1 E:T Ratio
10μM SIINFEKL
10μM SIIAFEKL
0.1μM SIINFAKL
10μM SIINFEAL
NO PEPTIDE

Figure 4-6. Solvent exposed residues of the H-2K^b bound peptide do not influence Ly49C recognition. (A) Expression of H-2K^b on RMA/S incubated with the indicated SIINFEKL peptide variants. **(B)** Cytotoxicity assay using RNK.49W/C effector cells and RMA-S targets incubated with the indicated SIINFEKL variants and **(C)** statistical analysis at the 12.5:1 E:T ratio (ns= not significant, *p<0.05, **p<0.005). Assays were conducted in triplicate in three independent experiments. Error bars indicate SD.

A

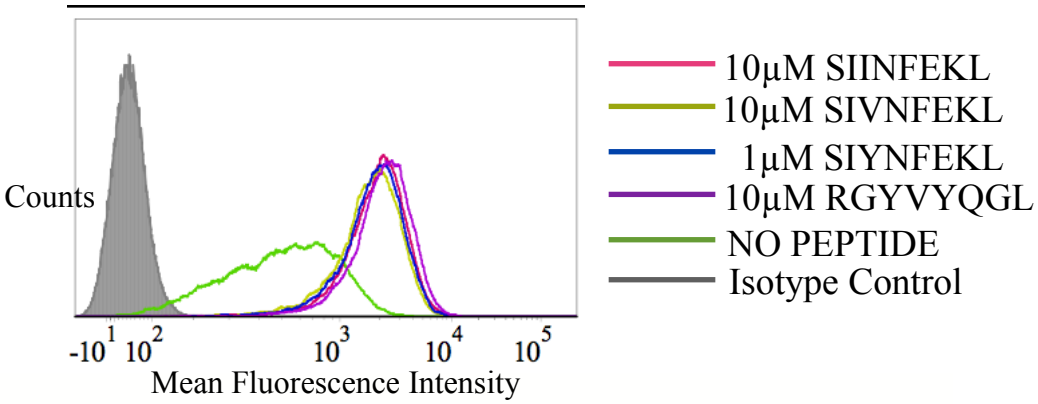
Counts
-10^1 10^2 10^3 10^4 10^5
Mean Fluorescence Intensity
10μM SIINFEKL
10μM SIVNFEKL
1μM SIYNFEKL
10μM RGYVYQGL
NO PEPTIDE
Isotype Control

B

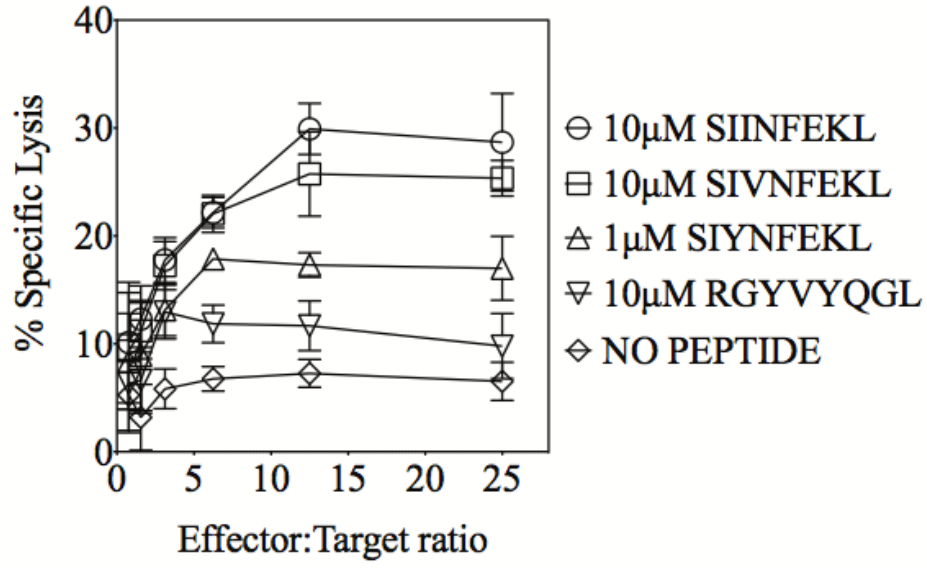
% Specific Lysis
0 10 20 30 40
0 5 10 15 20 25
Effector:Target ratio
10μM SIINFEKL
10μM SIVNFEKL
1μM SIYNFEKL
10μM RGYVYQGL
NO PEPTIDE

C

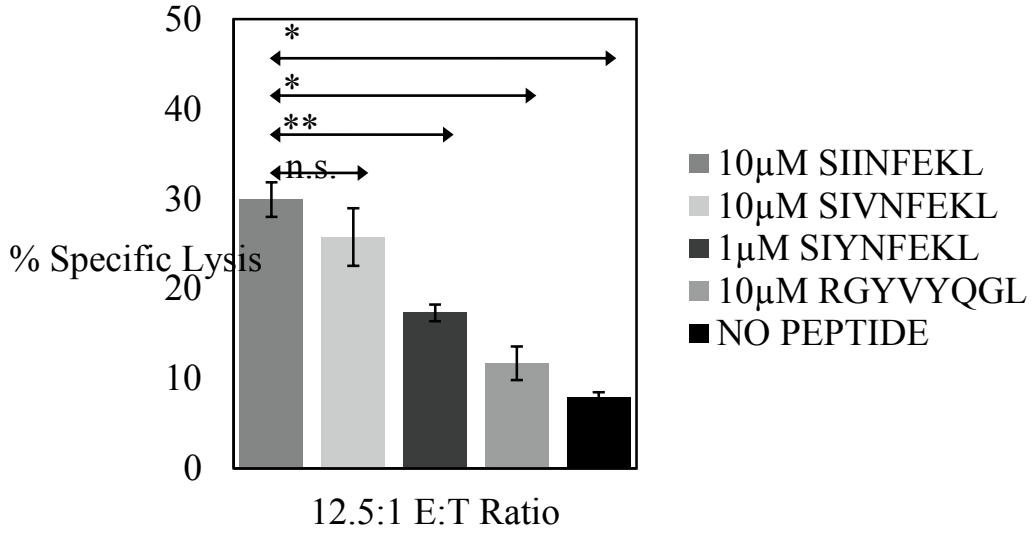
% Specific Lysis
0 10 20 30 40 50
*
*
**
n.s.
12.5:1 E:T Ratio
10μM SIINFEKL
10μM SIVNFEKL
1μM SIYNFEKL
10μM RGYVYQGL
NO PEPTIDE

Figure 4-7. **Peptide amino acid substitution demonstrates that auxiliary anchor residue P3 is an important factor in determining Ly49C recognition. (A)** Expression of H-2K^{b} on RMA/S cells co-incubated with the listed peptides **(B)** Cytotoxic assay using RNK.49W/C effector cells and RMA-S targets incubated with the indicated SIINFEKL variants (SIVNFEKL and SIYNFEKL) and RGYVYQGL, and **(C)** statistical analysis at the 12.5:1 E:T ratio (ns= not significant, *p<0.05, **p<0.005). Assays were conducted in triplicate in three independent experiments. Error bars indicate SD.

A

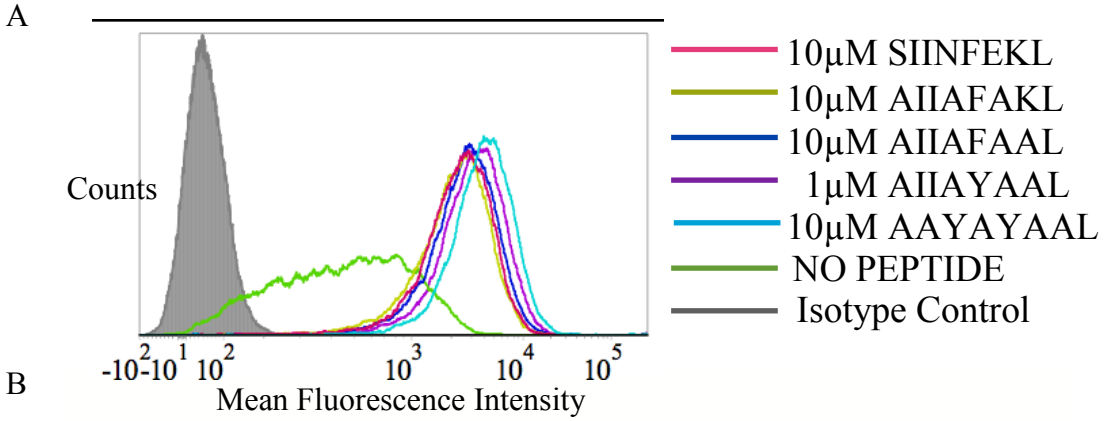
Counts
-10^2 -10^1 10^2 10^3 10^4 10^5
Mean Fluorescence Intensity
10μM SIINFEKL
10μM AIIAFAKL
10μM AIIAFAAL
1μM AIIAYAAL
10μM AAYAYAAL
NO PEPTIDE
Isotype Control

B

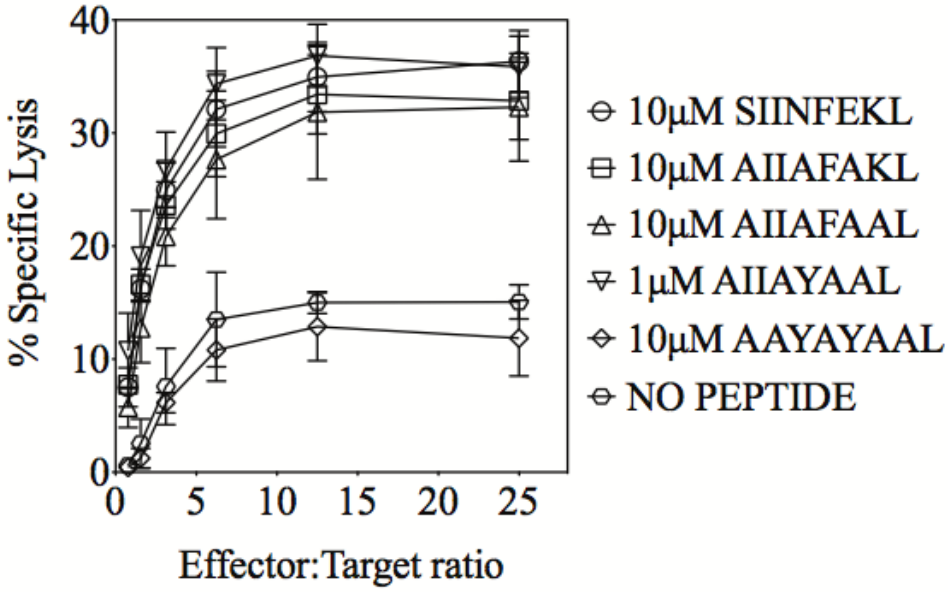
% Specific Lysis
0
10
20
30
40
0 5 10 15 20 25
Effector:Target ratio
10μM SIINFEKL
10μM AIIAFAKL
10μM AIIAFAAL
1μM AIIAYAAL
10μM AAYAYAAL
NO PEPTIDE

C

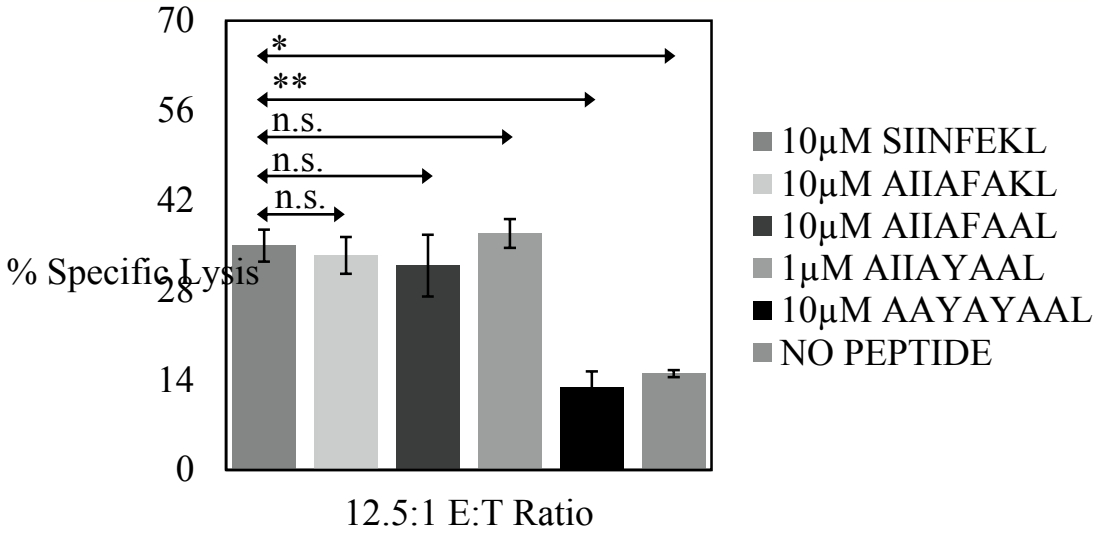
% Specific Lysis
0
14
28
42
56
70
*
**
n.s.
n.s.
n.s.
12.5:1 E:T Ratio
10μM SIINFEKL
10μM AIIAFAKL
10μM AIIAFAAL
1μM AIIAYAAL
10μM AAYAYAAL
NO PEPTIDE

Figure 4-8. Peptide residues P2 and P3 determine Ly49C recognition of H-2K^b. (A) Expression of H-2K^b incubated with the indicated peptides. **(B)** Percent cytotoxicity of RMA-S targets loaded with the indicated peptides incubated with RNK.49W/C effectors, **(B)** including statistical analysis at the 12.5:1 E:T ratio (ns= not significant, *p<0.05, **p<0.005). Results were obtained in triplicate during three independent experiments. Error bars represent the SD.

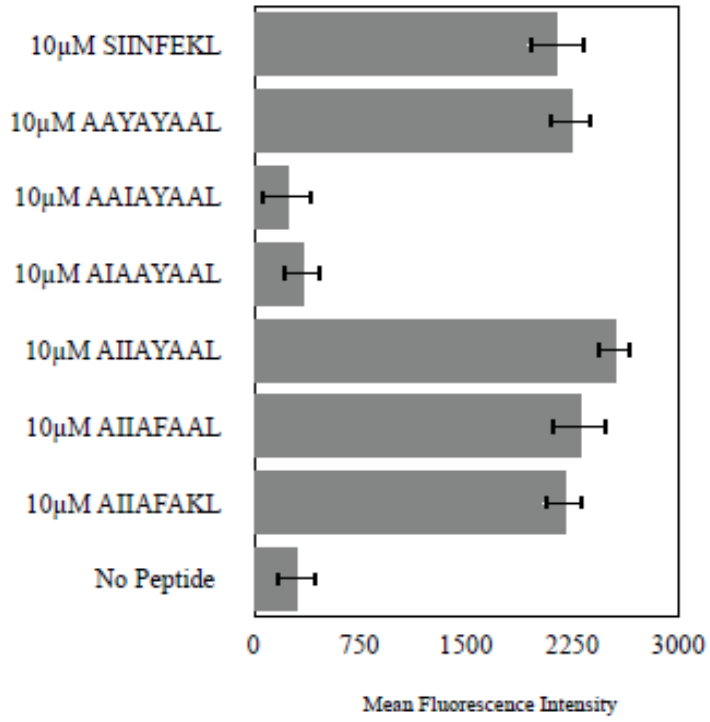

Figure 4-9. H-2K^b stabilization using AAYAYAAL peptide variants to recapitulate SIINFEKL anchor residues. RMA/S stabilization assay using 10μM of the indicated peptide. Cell surface expression of H-2K^b was detected using the APC conjugated AF6-88.5.5.3 antibody. Assays were conducted in triplicate in three independent experiments. Error bars indicate SD.

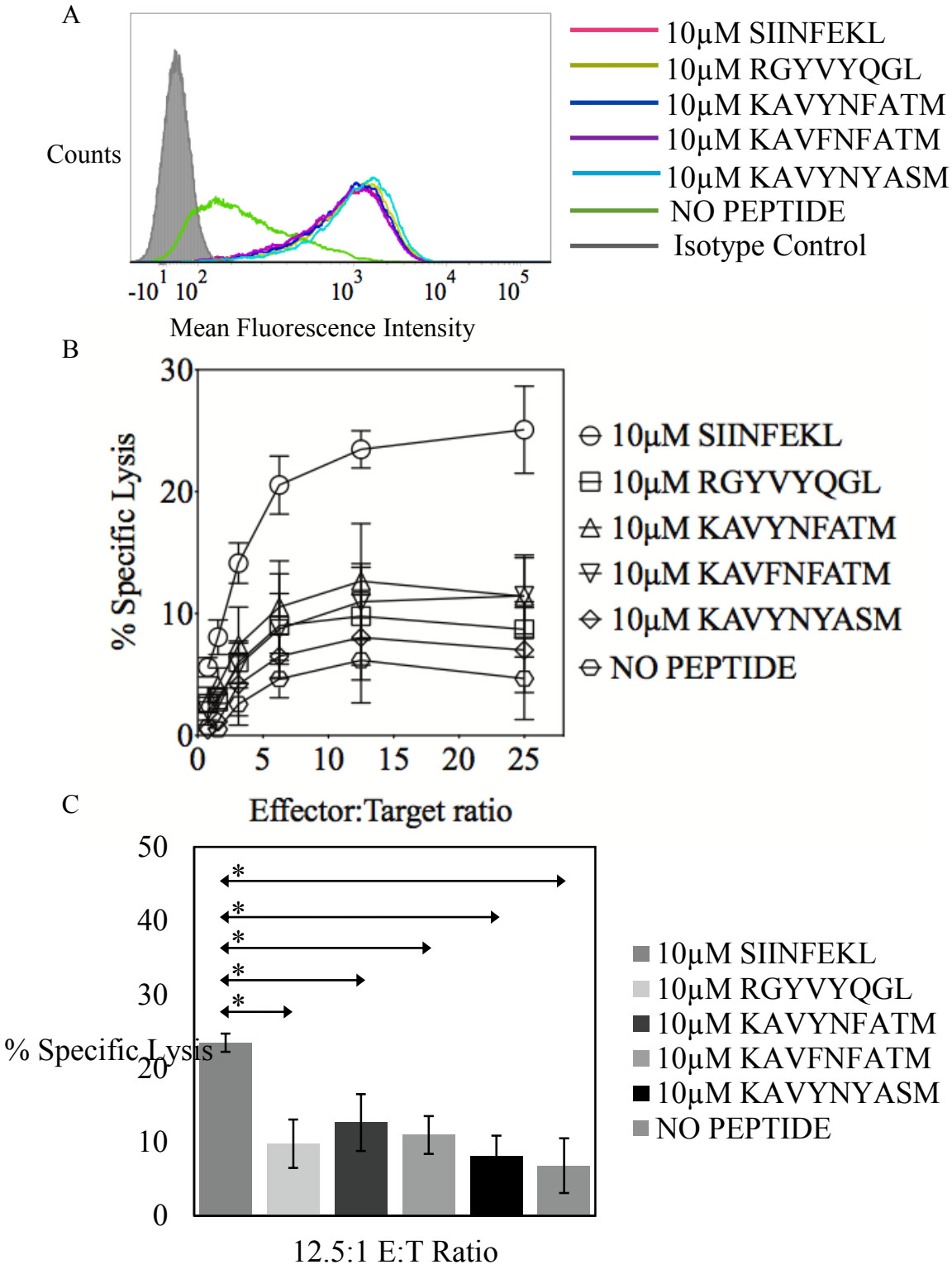
A
Counts
-10^1 10^2 10^3 10^4 10^5
Mean Fluorescence Intensity
10μM SIINFEKL
10μM RGYVVYQGL
10μM KAVYNFATM
10μM KAVFNFATM
10μM KAVYNYASM
NO PEPTIDE
Isotype Control
B
% Specific Lysis
0 10 20 30
0 5 10 15 20 25
Effector:Target ratio
10μM SIINFEKL
10μM RGYVVYQGL
10μM KAVYNFATM
10μM KAVFNFATM
10μM KAVYNYASM
NO PEPTIDE
C
% Specific Lysis
0 10 20 30 40 50
12.5:1 E:T Ratio
10μM SIINFEKL
10μM RGYVVYQGL
10μM KAVYNFATM
10μM KAVFNFATM
10μM KAVYNYASM
NO PEPTIDE

Figure 4-10. **LCMV immunodominant peptide and escape mutants are not recognized by Ly49W/C receptors when bound to H-2K^{b}**. **(A)** Profile of H-2K^{b} expression on RMA/S cells incubarted with indicated peptides. **(B)** Percent specific lysis of RMA-S cells incubated with LCMV derived immunodominant and immunoselective peptides in the presence of RNK.49W/C effector cells with **(C)** statistical analysis at the 12.5:1 E:T ratio (*p<0.05, **p<0.005). Experiments were performed in triplicate during three independent experiments. Error bars represent SD.

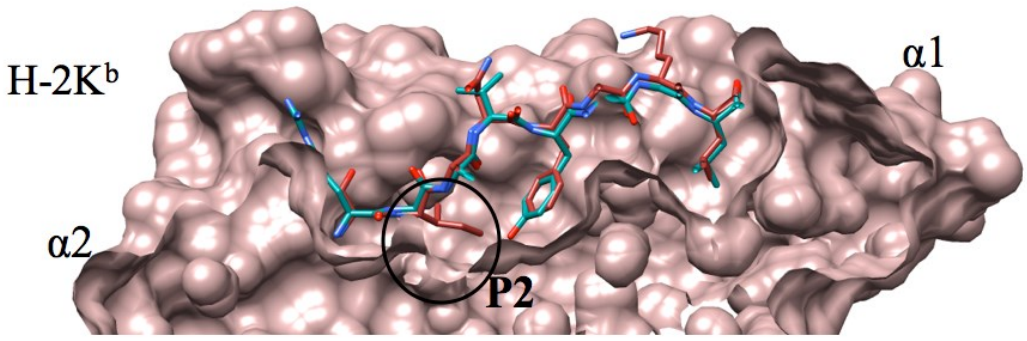

Figure 4-11. **Structural analysis of peptide amino acid docking into the B-pocket of H-2K^{b}**. The H-2K^{b} bound peptide amino acid at position 2 (P2) docks into the B-pocket of H-2K^{b}. Comparison between P2 of H-2K^{b}-SIINFEKL and H-2K^{b}-RGYVYQGL, complexes that support or not Ly49C-H-2K^{b} interaction, respectively, show notable differences in the crystal structure. The presence of a small residue at P2, such as Gly in H-2K^{b}-RGYVYQGL, allows for a water molecule to occupy the B-pocket of H-2K^{b}, supporting extensive hydrogen bond interactions at the core of the peptide binding groove. On the other hand, in H-2K^{b}-SIINFEKL, Ile at P2 fully occupies the B-pocket, with no water molecules observed in the B-pocket, resulting in lack of extensive hydrogen bond networks that could increase H-2K^{b} heavy chain flexibility. A greater degree of heavy chain flexibility can facilitate H-2K^{b} molecular displacement necessary for Ly49C association. In the figure, the H-2K^{b} heavy chain is shown in pink surface drawing, the SIINFEKL peptide is in dark red, the RGYVYQGL peptide is in teal. The figure was generated using CHIMERA UCSF software and PDB IDs IVAC for H-2K^{b}-SIINFEKL and 1KPU for H-2K^{b}-RGYVYQGL.

A

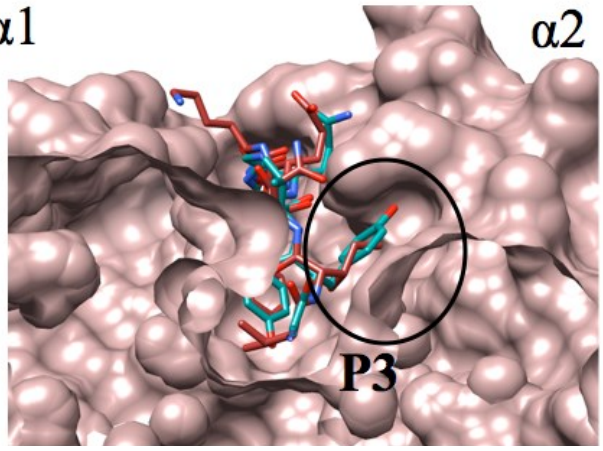

B

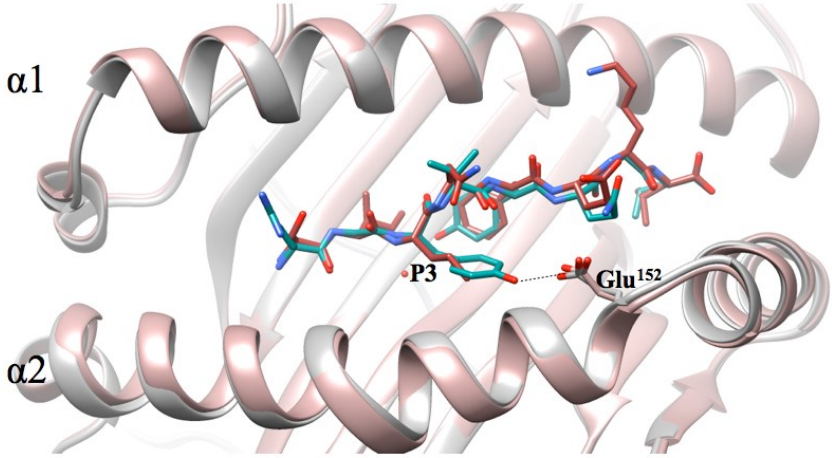

Figure 4-12. **Structural analysis of peptide amino acid docking into the D-pocket of H-2K^b**. **(A)** The auxiliary anchor residue at position 3 (P3) docks into the shallow D-pocket of H-2K^b formed by residues within the α2-helix. Comparison of P3 in H-2K^b-SIINFEKL and H-2K^b-RGYVYQGL, complexes that support or not Ly49C-H-2K^b interaction, respectively, shows different interactions within the D-pocket of H-2K^b. Shown in the surface representation of H-2K^b, the D-pocket is fully occupied by Tyr with RGYVYQGL, while Ile is relatively smaller and does not allow for extensive interactions within amino acids in the D-pocket as compared to Tyr. **(B)** In addition, the Tyr at P3 in RGYVYQGL, also yields hydrogen bond formation with Glu^{152} in the α2-helix of H-2K^b, whereas in the SIINFEKL peptide, the uncharged Ile only results in van der Waals interactions with amino acids in the B-pocket. In the figure, the H-2K^b-SIINFEKL heavy chain is shown in pink ribbon, the H-2K^b-RGYVYQGL heavy chain is shown in grey ribbon, the SIINFEKL peptide is in dark red, the RGYVYQGL peptide is in teal. The figures were generated using CHIMERA UCSF software and PDB IDs IVAC for H-2K^b-SIINFEKL and 1KPU for H-2K^b-RGYVYQGL.

A

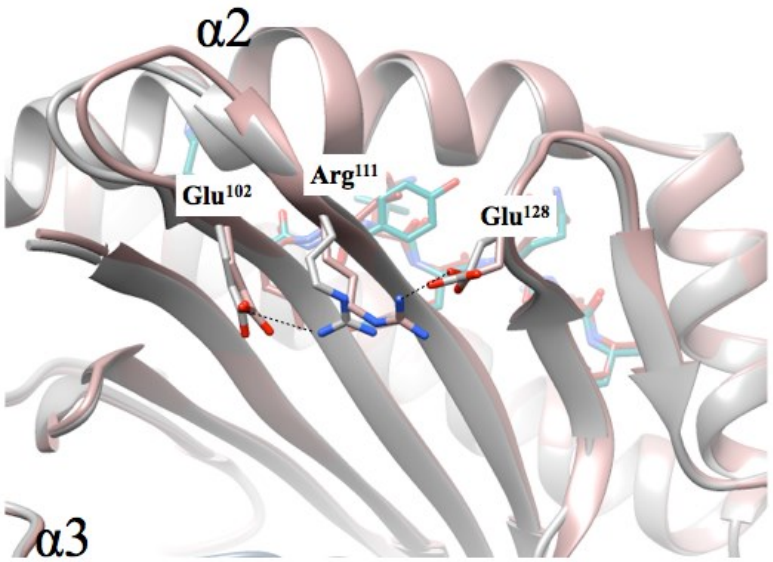
α2
Glu102
Arg111
Glu128
α3

B

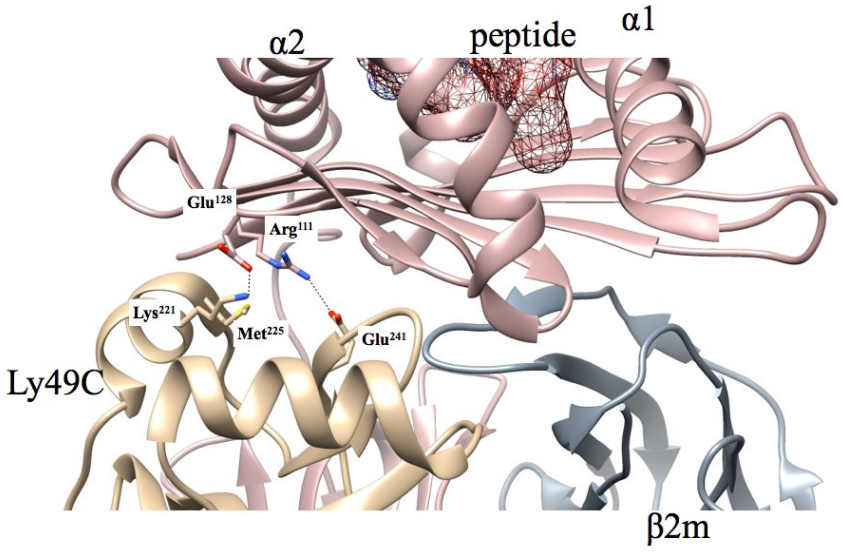
α2
peptide
α1
Glu128
Arg111
Lys221
Met225
Glu241
Ly49C
β2m

Figure 4-13. **H-2K^b peptide dependent intramolecular interactions that potentially affect H-2K^b and Ly49C association. (A)** Comparison between H-2K^b-RGYVYQGL and H-2K^b-SIINFEKL residues Arg^{111} and Glu^{128}, that participate in Ly49C interaction, shows that in the H-2K^b-SIINFEKL complex, Arg^{111} forms a hydrogen bond with Glu^{128}, but in the H-2K^b-RGYVYQGL complex Arg^{111} instead shares a hydrogen bond with Glu^{102} . Differences in intramolecular interactions within the H-2K^b that are affected by the peptide bound, can be an important factor for the support of receptor and ligand association. In the figure, the H-2K^b-SIINFEKL heavy chain is shown in pink ribbon, the H-2K^b-RGYVYQGL heavy chain is shown in grey ribbon. The SIINFEKL peptide is in dark red and the RGYVYQGL peptide is in teal. Hydrogen bonds are represented in black dashed lines. **(B)** In the co-crystal structure of H-2K^b-SIINFEKL and Ly49C, Arg^{111} in H-2K^b-SIINFEKL shares van der Waals contacts with Met^{225} in Ly49C as well as salt bridges with Glu^{241} in Ly49C. In addition, Glu^{128} in H-2K^b-SIINFEKL forms salt bridges with Lys^{221} of Ly49C. In the figure, the H-2K^b-SIINFEKL heavy chain is shown in pink ribbon, the β2m in blue ribbon and the SIINFEKL peptide is in dark red. The CTLD of the Ly49C monomer is shown in gold ribbon. The figures were generated using CHIMERA UCSF software and PDB IDs IVAC for H-2K^b-SIINFEKL, 1KPU for H-2K^b-RGYVYQGL and 3C8K for H-2K^b-SIINFEKL-Ly49C.

A

Peptide Sequence	**Peptide origin**	**IC_{50} for association with H-2K^b (nM)**
SI**I**NF**F**EK**L**	Chicken Ovalbumin (256-264)	392.3601
KI**I**T**Y**RN**L**	PCI domain-containing protein 2 (318-325)	404.9105
KV**I**T**F**ID**L**	GTP binding protein I (246-253)	498.5564
YA**M**I**Y**RN**L**	E3 ubiquitin-protein ligase mdm2 (100-107)	126.4429

B

Peptide Sequence	**Peptide origin**	**IC_{50} for association with H-2K^b (nM)**
AN**Y**D**F**IC**V**	MMTV env gp70 (446-453)	254.4448
RG**Y**V**Y**QG**L**	Vesicular Stomatitis Virus NP (52-59)	96.0161
IS**F**K**F**DH**L**	F-actin capping protein alpha1 (93-100)	35.7493
IN**F**D**F**PK**L**	RNA helicase p54 (407-414)	62.7041
AA**Y**A**Y**AA**L**	Synthetic peptide	32.7871

Table 4-3. Predicted binding affinity of peptides to H-2K^b and Ly49W/C NK cell response. (A) IC_{50} values for peptides that support Ly49C recognition of H-2K^b and **(B)** peptides that have low Ly49C recognition profiles for H-2K^b.

CHAPTER V

TUNING MOUSE NK CELL FUNCTION BY THE MHC-I PEPTIDE

A. Introduction

Natural killer (NK) cells are crucial lymphocytes for the early detection of virally infected and transformed cells. Their effector functions depend on the integration of inhibitory and activating signals, respectively, mediated by activating and inhibitory receptors (99). Since inhibitory signals generally dominate over activating signals, overcoming the threshold of inhibition is an important regulatory step for the activation of NK cells (284). Prominent NK cell receptors include the killer Ig-like receptors (KIRs) in humans and the Ly49s in rodents. Although structurally different, KIRs belonging to the Ig-like superfamily and Ly49s to the C-type lectin superfamily, these have analogous function (204, 285). Both receptor systems include activating and inhibitory members. Inhibitory receptors interact with peptide-bound class I major histocompatibility complex (MHC-I) allowing NK cells to detect changes in MHC-I expression as a result of cell stress.

Unlike adaptive immune cells, immune surveillance by NK cells occurs early during the initiation of infection or cell transformation, without the need of prolonged immune priming (286). Recognition of changes in the presentation of peptide-MHC-I (pMHC-I) complexes by Ly49s can influence NK cell function and is important to understand NK cell recognition of self molecules (193, 284). Peptides bound to MHC-I

are generally derived from endogenous protein sources. Upon infection or oncogenesis, the presence of virus proteins or over-expression of self or altered-self proteins changes the peptide repertoire for MHC-I binding (37). The presentation of peptides from viral proteins can occur as quickly as 4 hours after infection (2). In addition, defective ribosomal products (DRiPs) of self or altered-self proteins can also be presented rapidly. DRiPs are generated from nascent ribosome translated mRNA products that undergo error or premature termination during translation, potentially resulting in polypeptides that do not fold or assemble properly into functional proteins. Importantly, DRiPs are thought to be the major source of peptides for antigen presentation, giving a snapshot of ongoing cellular events to immune cells (33, 34). Since the peptides displayed by MHC-I are informative of the state of a cell, NK cell recognition of peptides bound to MHC-I can be an important tool for their activation upon recognition of non-self or altered-self complexes. Recognition of MHC-I by NK cells that is dependent on bound peptide may serve an important role in innate cell immune surveillance.

Our previous work, described in Chapter IV, on the role of H-2K^b-bound peptides in Ly49C recognition demonstrated the importance of peptide identity in NK cell responses. Using functional assays, our study revealed that the identity of the peptide residues that dock into the peptide binding groove near the peptide N-terminus, at P2 and P3, can impact Ly49C recognition of H-2K^b. This is particularly important when MHC-I expression remains intact during cell transformation or viral infection (268). Cell stress leading to a decrease in MHC-I, can render a cell susceptible to NK cell mediated lysis due to the decrease in ligand for inhibitory NK cell receptors, a

phenomenon known as “missing-self”. However, cell stress can also lead to changes in the peptide repertoire for MHC-I binding without disturbing MHC-I expression; a phenomenon that has not been fully characterized in Ly49 dependent NK cell function. Our studies using H-2K^b loaded with single peptides showed a peptide selective recognition of MHC-I by inhibitory Ly49C receptor. This suggests a second layer of discrimination where not only the lack of MHC-I, or “missing-self”, leads to activation, but the identity of the peptide bound to the MHC-I is also crucial for NK cell recognition. Nevertheless, how this aspect of NK cell specificity is integrated in NK cell function upon encounter with target cells that can express pMHC-I complexes, remains to be established. While peptides that fully support MHC-I association with inhibitory receptors successfully lead to inhibitory signals, the role of peptides that do not productively support the inhibitory function of NK inhibitory receptors is less clear.

In humans, KIR-dependent NK cell responses can also be modulated by the peptide bound to MHC-I. Fadda L. *et al* demonstrated that a MHC-I peptide that does not support detectable association of KIR and MHC-I, when co-presented with a peptide that supports KIR-MHC-I association, has an antagonistic effect that leads to NK cell activation (212). In NK cell biology, a pMHC-I complex that associates with an inhibitory receptor is considered an agonist complex which results in NK cell inhibition, as opposed to the cytotoxic T lymphocyte (CTL) concept of a pMHC-I agonist that results in T cell activation from a successful T cell receptor-pMHC-I association. With NK cells, an antagonistic pMHC-I is characterized as a pMHC-I complex that disrupts agonist pMHC-I association with inhibitory receptor(s), leading to NK cell activation. In

contrast, during CTL recognition of target cells, the expression of antagonistic pMHC-I leads to CTL inhibition (212, 213). At least for human NK cells, Fadda L. *et al* provided a model in which the peptide bound to MHC-I acts as a rheostat of KIR mediated NK cell activity. We therefore investigated if a similar phenomenon was observed in mice and asked whether the co-presentation of different pMHC-I complexes can modify Ly49 dependent NK responses. Knowing if murine NK cell, peptide-driven antagonism is also observed, can be useful to understand how peptides bound to MHC-I shape NK cell functions in an animal model.

B. Results

ex vivo NK cells for functional assays

The association between both human KIRs and murine Ly49s with MHC-I ligands can be peptide dependent (50, 210, 218, 276, 287). However, KIRs and Ly49s interact with their corresponding MHC-I molecules at different sites. The interface between KIRs and MHC-I include amino acids within the MHC-I α1-helix and α2-helix 2 as well as the peptide amino acids 7 and 8, which protrude out from the peptide binding cleft towards solvent (275, 288). In contrast, MHC-I interaction with Ly49 receptors occurs in a region of MHC-I under the peptide binding groove including amino acids in the α1, α2, and α3 domain as well as the β2m, with no direct contact with the bound peptide (195). Still, both receptor systems have acquired the ability to differentiate between distinct pMHC-I complexes, a feature that can be beneficial in detecting non-self or altered-self peptides on MHC-I. Moreover, peptide antagonism of human KIR inhibitory function leading to activation of human NK cells, has brought up

a novel NK activating mechanism where peptides that do not induce detectable association of MHC-I and inhibitory KIR, can function to lead to NK cell activation. Such a peptide driven antagonistic effect has not been reported in murine NK cells or with inhibitory Ly49 receptors. We investigated how the concomitant presentation of two different peptides on H-2K^b influenced recognition of inhibitory Ly49C receptor, and tested their effect on NK cell reactivity.

Using *ex vivo* NK cells, we can directly test the requirements of H-2K^b-bound peptide in overcoming the threshold of NK cell inhibition. From our previous work on peptide specific recognition of H-2K^b by Ly49C, we identified peptides that confer high, intermediate or low/null levels of recognition. Therefore, we are using Ly49C and H-2K^b association as a model, in order to study peptide antagonism in murine NK cells. In brief, NK cells used in this study were separated by sorting and enriching an NK cell population from C57BL/6 female mice spleens. NK cell enrichment from spleens was done by lysis of red blood cells, followed by blockade of Fc receptors and staining against CD3 and NK1.1 to sort for CD3$^-$NK1.1$^+$ cells. The NK1.1 marker is expressed on NK cells and NKT cells, by selecting NK1.1 positive cells, we enrich for cells expressing the marker: NK and NKT cells. The CD3 marker is found in T cells and NKT cells, therefore by negatively selecting CD3$^+$ cells, we discard T cells and NKT cells, enhancing the purity of the NK cell population (Figure 5-1A). Additionally, we used the 5E6 antibody that selected CD3$^-$NK1.1$^+$ cells expressing Ly49C and/or Ly49I inhibitory receptors (Figure 5-1A). Therefore effector cells for this study can be characterized as CD3$^-$NK1.1$^+$Ly49C&I$^+$, for enriched NK cells expressing Ly49C

and/or Ly49I receptors with a purity of 94.04% after sorting (Figure 5-1B). $CD3^-$ $NK1.1^+Ly49C\&I^+$ cells were expanded for 6 days in the presence of 1000U/ml of recombinant IL-2 before use for cytotoxicity assays. Prior to use for functional assays, IL-2 cultured $CD3^-NK1.1^+Ly49C\&I^+$ cells were stained with the anti-Ly49C&I antibody, 5E6, to examine surface expression of Ly49C&I (Figure 5-1C). By staining expanded $CD3^-NK1.1^+Ly49C\&I^+$ cells, with the 5E6 antibody, we corroborated expression of Ly49C&I, having 88.11% of gated live cells positive for Ly49C&I (Figure 5-1C). Therefore, the effector cells used in our studies are enriched for NK cells expressing both Ly49C and Ly49I. The previously mentioned strategy for the use of enriched 5E6 positive C57BL/6 NK cells has been used for functional studies focused on $H\text{-}2K^b$ and Ly49C association (210). Given that other activating and inhibitory receptors expressed on C57BL/6 NK cells do not associate with $H\text{-}2K^b$, the selection of 5E6 positive C57BL/6 $CD3^-NK1.1^+$ cells is a convenient method for sorting NK cells positive for Ly49C. For instance, activating Ly49 receptors expressed on C57BL/6 NK cells include Ly49M, Ly49N, Ly49H, Ly49K and Ly49D that do not recognize $H\text{-}2K^b$. Additional inhibitory receptors expressed on C57BL/6 NK cells include Ly49A, Ly49J, Ly49G, Ly49F, Ly49E, and Ly49B; with Ly49J presumably binding $H\text{-}2K^b$ besides Ly49C and Ly49I. Since the levels of $H\text{-}2K^b$ recognition by Ly49I are low, as compared to $H\text{-}2K^b$ recognition by Ly49C, and the frequency of Ly49I positive NK cells is also low, 5E6 positive $CD3^-NK1.1^+$ cells can allow us to detect Ly49C and $H\text{-}2K^b$ dependent NK cell activity (50).

Selection of H-2K^b peptides

Previous work in our laboratory further characterized the role of amino acids within the peptide bound to H-2K^b for Ly49C recognition (Chapter IV). We initially tested a group of peptides for their ability to support H-2K^b-Ly49C association, which resulted in different degrees of recognition by individual peptides. For instance, high levels of recognition were observed with peptides SIINFEKL and KIITYRNL, intermediate levels of association were seen with ISFKFDHL, while low to null levels of recognition were observed with peptides AAYAYAAL and RGYVYQGL. The variable degree of recognition of H-2K^b bearing different peptides can be described as a mechanism where peptides act as rheostat to influence NK cell function. In order to study the possibility of peptide antagonism, we selected SIINFEKL as the agonist peptide, since it supports Ly49C recognition of H-2K^b. Using the SIINFEKL peptide as the agonist peptide is useful due to its established role providing support to Ly49C-H-2K^b interaction. In addition, a H-2K^b-SIINFEKL-specific antibody is available and can be used to measure H-2K^b-SIINFEKL complexes in the presence or absence of a secondary pMHC-I complex. Measuring the quantity of H-2K^b-SIINFEKL levels as compared to that of second co-displayed pMHC-I complexes on the cell surface can aid in the interpretation of our cytotoxicity assays and allow us to distinguish between both agonist and secondary peptide MHC-I complexes. For the antagonist peptide, we tested two different peptides: RGYVYQGL and ISFKFDHL. For antagonism in inhibitory KIR dependent NK cell activation, the antagonistic peptide by itself showed no detectable support of KIR-MHC-I interaction, but when co-presented with an agonist peptide, it antagonized inhibitory pMHC-I complexes. Therefore, the RGYVYQGL

peptide, which does not detectably support Ly49C-H-2K^b association, can be used to probe if the same mechanism is utilized in murine NK cells when co-expressed with the agonist SIINFEKL (Table 5-1). The ISFKFDHL peptide confers an intermediate level of H-2K^b recognition by Ly49C, and can be probed to study antagonism to investigate if a low or moderate interaction is necessary between the ligand and receptor to allow for antagonism (Table 5-1). Finally, we also tested KIITYRNL, a peptide that similar to SIINFEKL, supports Ly49C recognition of H-2K^b, as a control, where H-2K^b is occupied with both peptides that support Ly49C recognition and should not lead to NK cell activation (Table 5-1). Using peptides that individually induce different levels of association between Ly49C and H-2K^b, we can uncover whether antagonist pMHC-I complexes, should we find them, are required to trigger a minimal or intermediate level of Ly49C-MHC-I interaction.

NK cell inhibition can be mediated by low SIINFEKL concentrations

In order to test peptide antagonism, we use RMA/S cells as target cells after loading them with peptide of choice and labeling with ^{51}Cr. RMA/S cells are a mouse T cell lymphoma cell line defective in TAP-2 expression. A deficiency in TAP-2 abrogates the transportation of peptides from the cytosol to the endoplasmic reticulum (ER) for loading onto MHC-I, leading to low expression levels of MHC-I. Nevertheless, incubation of RMA/S cells at 26°C for 16 hours, upregulates the amount of empty MHC-I molecules which can be stabilized by the exogenous addition of MHC-I binding peptides. In addition, the use of recombinant mouse β2m during the 26°C incubation increases the amount of MHC-I expression at the cell surface. Since we are loading

RMA/S cells with two different peptides, we produced and used mouse recombinant β2m in order to have a greater number of H-2K^b molecules to load peptides. As a method to load two different peptides, we utilized a sequential peptide loading procedure. In general, following culture at 26°C for 16 hours in the presence of recombinant mouse β2m, RMA/S are incubated with Brefeldin A (BFA) to block transport of newly synthesized MHC-I molecules from the Golgi to the cell surface. RMA/S cells are then loaded with the agonist SIINFEKL peptide followed by washes and then addition of a second peptide to be tested as antagonist or control. Advantages of using a sequential peptide loading strategy are that we avoid peptide competition for H-2K^b binding and we also keep the agonist peptide concentration constant.

For sequential peptide loading, we needed to use a low concentration of the agonist SIINFEKL peptide so that there is no SIINFEKL saturation, and we still have empty H-2K^b molecules for the loading of a second peptide. Therefore, we performed SIINFEKL peptide titrations using RMA/S cells that were cultured with 10μg/ml of recombinant mouse β2m at 26°C for 16 hours. After addition of BFA, RMA/S cells were loaded with the SIINFEKL peptide at the concentrations of 10μM, 5μM, 1μM, 0.5μM, 0.1μM, 0.05μM, 0.01μM or no peptide. Peptide-loaded RMA/S cells were labelled with ^{51}Cr and used in a 4-hour cytotoxicity assay to examine CD3$^-$ NK1.1$^+$Ly49C&I$^+$ cell responses. Expression of H-2K^b with SIINFEKL at different concentrations was assessed by flow cytometry analysis utilizing the AF6-88.5.5.3 antibody conjugated to APC. As a negative control, RMA/S incubated with no peptide, showed low levels of H-2K^b expression. H-2K^b expression on RMA/S cells is gradually

increasing upon incubation with the SIINFEKL concentrations aforementioned (Figure 5-2A). During cytotoxicity assays, we incubated effector $CD3^{-}NK1.1^{+}Ly49C\&I^{+}$ and target RMA/S cells at different effector to target cell ratios. Results from cytotoxicity experiments are described as % specific lysis reaching a "plateau" at the 0.5:1 effector to target cell ratio in cytotoxicity against targets incubated with SIINFEKL. The highest % specific lysis detected was against RMA/S cells with no peptide at 40%. Target cells with different concentrations of the SIINFEKL peptide, yielded a "titration" of RMA/S-SIINFEKL targets for $CD3^{-}NK1.1^{+}Ly49C\&I^{+}$ effectors, with the lowest effector lysis against RMA/S incubated with 10μM SIINFEKL, at 21%. Thereon, we observed a steady increase in lysis towards RMA/S cells incubated with lower SIINFEKL concentrations (Figure 5-2B). In order to direct our attention to the impact of SIINFEKL mediated inhibition by $CD3^{-}NK1.1^{+}Ly49C\&I^{+}$ cells, we normalized the experimental data presented at the 0.5:1 effector to target ratio in our cytotoxicity assays. To obtain normalized data, we set out 21% from RMA/S-SIINFEKL ($\%SL_{(RMA/S\text{-}SIINFEKL)}$) as "0% Activation" and 40% from RMA/S-NO PEPTIDE ($\%SL_{(NO\ PEPTIDE)}$) as "100% Activation". We used the % specific lysis data, from individual curves ($\%SL_{(experiment)}$), representing RMA/S incubated with different SIINFEKL concentrations at the 0.5 to 1 effector to target cell ratio and determined normalized activity using the formula: $\%\ Activity=(\%SL_{(experiment)}-\%SL_{(RMA/S\text{-}SIINFEKL)})/(\%SL_{(NO\ PEPTIDE)}-\%SL_{(RMA/S\text{-}SIINFEKL)})X100$. The normalized % activity at the 0.5:1 effector to target cell ratio was 6.5%, 0.6%, 21%, 40.5%, 52.6% and 71% for RMA/S incubated with 5μM, 1μM, 0.5μM, 0.1μM, 0.05μM and 0.01μM respectively (Figure 5-2C). In order to decide what is the concentration of SIINFEKL peptide to be used during sequential peptide loading,

we compared flow cytometry analysis of H-2K^b expression on target cells and cytotoxicity assay results. We found that using SIINFEKL at the sub-saturating concentration of 0.05μM, we have retained H-2K^b expression at the cell surface of RMA/S and still have CD3$^-$NK1.1$^+$Ly49C&I$^+$ inhibitory effects at intermediate levels (Figure 5-2A, -2B, -2C). Importantly, using sub-saturating levels of SIINFEKL can still allow us to load an additional peptide to probe peptide antagonism in murine NK cells.

Peptide preventing H-2K^b-Ly49C interaction weakly antagonizes NK inhibition

Studies using human KIR receptors and their peptide selective association with MHC-I molecules, showed that a strong agonist pMHC-I complex that interacts with KIR, can be antagonized by a pMHC-I complex that by itself does not detectably support inhibitory KIR-MHC-I association. Therefore, we used RGYVYQGL, a peptide that does not induce detectably Ly49C-H-2K^b binding, to investigate if a similar antagonistic effect is found with murine NK cells. As a peptide agonist, SIINFEKL bound to H-2K^b on RMA/S cells leads to lower CD3$^-$NK1.1$^+$Ly49C&I$^+$ cell lysis as compared to RMA/S cells incubated with no peptide (Figure 5-2B, -2C). This phenotype can therefore be attributed to the expression of agonist H-2K^b-SIINFEKL complexes, leading to inhibitory signals, dependent on Ly49C. To elucidate the effects of H-2K^b-RGYVYQGL co-expressed with H-2K^b-SIINFEKL; we used RMA/S as target cells and loaded them first with 0.05μM SIINFEKL followed by 10μM or 1μM RGYVYQGL. The concentrations of the peptide tested for antagonism, 10μM and 1μM, were used to saturate H-2K^b molecules available after SIINFEKL was loaded. As controls we included RMA/S cells individually loaded with 0.05μM SIINFEKL, 10μM

RGYVYQGL, 1μM RGYVYQGL, or no peptide. Measure of H-2K^b expression on RMA/S cells was performed using two distinct antibodies: an H-2K^b specific antibody and an H-2K^b-SIINFEKL specific antibody. RMA/S cells loaded with 0.05μM SIINFEKL alone, showed upregulation of H-2K^b as compared to the no peptide control. Cells that were incubated with 10μM RGYVYQGL, 1μM RGYVYQGL, 0.05μM SIINFEKL/10μM RGYVYQGL, and 0.05μM SIINFEKL/1μM RGYVYQGL, showed an increase in H-2K^b staining over RMA/S cells incubated with 0.05μM SIINFEKL alone (Figure 5-3A). Thus, RMA/S cells loaded with low concentration of agonist peptide, SIINFEKL, still show to be capable of loading additional peptides as it is demonstrated by the increase in H-2K^b staining in cells incubated with 10μM RGYVYQGL or 1μM RGYVYQGL following SIINFEKL incubation. As a control, RMA/S cells incubated with no peptide had a marked low H-2K^b expression, demonstrating the peptide requirement for stabilization of H-2K^b (Figure 5-3A). Measurement of H-2K^b-SIINFEKL complexes showed that RMA/S cells incubated with 0.05μM SIINFEKL, 0.05μM SIINFEKL/10μM RGYVYQGL and 0.05μM SIINFEKL/1μM RGYVYQGL have similar H-2K^b-SIINFEKL expression; whereas RMA/S cells incubated individually with 10μM RGYVYQGL, 1μM RGYVYQGL and no peptide, showed minimal staining (Figure 5-3B). Identification of H-2K^b-SIINFEKL complexes, demonstrates that stable H-2K^b-SIINFEKL complexes are formed during the loading RMA/S cells with SIINFEKL, and that the addition of a second peptide at high concentrations does not disrupt the formed H-2K^b-SIINFEKL complexes.

Functional assays were carried out using different ratios of $CD3^-$ $NK1.1^+Ly49C\&I^+$ effector cells and target RMA/S cells loaded with 0.05μM SIINFEKL, 0.05μM SIINFEKL/10μM RGYVYQGL, 0.05μM SIINFEKL/1μM RGYVYQGL, 10μM RGYVYQGL, 1μM RGYVYQGL and no peptide. Cytolytic activity of $CD3^-NK1.1^+Ly49C\&I^+$ cells was determined as percent specific lysis with the highest activity towards RMA/S cells with no peptide loaded reaching a plateau at the 0.5:1 effector to target cell ratio with 75% cytotoxicity, while the SIINFEKL loaded RMA/S cells showed a 53 % cytotoxicity at the same effector to target cell ratio (Figure 5-4A). To focus specifically on the influence of peptides on SIINFEKL mediated inhibition, we normalized the system, setting 53% from RMA/S-SIINFEKL as "0% Activation" and 75% from RMA/S-no peptide as "100% Activation" and used data points from the 0.5 to 1 effector to target cell ratio using the formula: $Activity=(\%SL_{(experiment)}-\%SL_{(RMA/S\text{-}SIINFEKL)})/(\%SL_{(NO\ PEPTIDE)}-\%SL_{(RMA/S\text{-}SIINFEKL)})X100$ to determine activity in each case. RMA/S cell incubated individually with 10μM RGYVYQGL and 1μM RGYVYQGL, showed a percent activity of 90.53% and 78.6% respectively. On the other hand, RMA/S cells co-incubated with 0.05μM SIINFEKL and 10μM RGYVYQGL or 1μM RGYVYQGL showed a percent increase of 23.3% and 21.17% over RMA/S cells incubated with 0.05μM SIINFEKL only (Figure 5-4B). This result suggests that in cells incubated with 0.05μM SIINFEKL/10μM RGYVYQGL and 0.05μM SIINFEKL/1μM RGYVYQGL, the H-$2K^b$-RGYVYQGL complexes weakly intervened in H-$2K^b$-SIINFEKL mediated inhibition. Therefore, a peptide bound to H-$2K^b$ that individually does not support H-$2K^b$ association with Ly49C, does not behave as a full antagonist when co-presented with agonist H-$2K^b$-SIINFEKL complexes.

Peptide supporting H-2K^b-Ly49C interaction at intermediate levels reduce NK inhibition by agonist H-2K^b complexes

For antagonism in KIR dependent NK cell activation, the antagonistic peptide by itself showed no detectable support of inhibitory KIR-MHC-I interactions, but co-expressed with an agonist peptide, it antagonized inhibitory signaling. However, using the RGYVYQGL, that does not confer Ly49C-H-2K^b association, we observed a relatively weak antagonism, suggesting that human and mouse NK cell antagonism may not be an identical phenomenon. Therefore, we next used a peptide that supports Ly49C-H-2K^b binding at an intermediate level to probe whether peptides had to induce a degree of Ly49C-H-2K^b association to function as an antagonist. Additional experiments to probe KIR-MHC-I antagonism showed that a peptide that supports KIR-MHC-I association at an intermediate level does not antagonize a strong agonist that supports KIR-MHC-I binding. Although KIR and Ly49 function is analogous, their structure and mode of MHC-I ligand recognition are different; therefore antagonism driven by the peptide bound to MHC-I, might be differentially regulated. The ISFKFDHL peptide confers an intermediate level of H-2K^b recognition by Ly49C, and can be probed to investigate if a low interaction is necessary between the ligand and receptor to trigger antagonism against the agonist H-2K^b-SIINFEKL complex.

We used cytotoxicity assays to investigate the effects of H-2K^b-ISFKFDHL co-presented with H-2K^b-SIINFEKL. Effector cells, CD3$^-$NK1.1$^+$Ly49C&I$^+$, were used at different ratios incubated with RMA/S target cells loaded with 0.05µM SIINFEKL followed by 10µM ISFKFDHL or 1µM ISFKFDHL. As controls we utilized RMA/S

cells loaded singly with 0.05μM SIINFEKL, 10μM ISFKFDHL, 1μM ISFKFDHL and no peptide. We determined H-2K^b expression by flow cytometry utilizing a H-2K^b specific antibody and a H-2K^b-SIINFEKL specific antibody. As previously shown, RMA/S cells incubated with 0.05μM SIINFEKL singly, display an increase in H-2K^b expression in contrast to RMA/S cells incubated with no peptide. Additionally, RMA/S cells that were loaded with 10μM ISFKFDHL, 1μM ISFKFDHL, 0.05μM SIINFEKL/10μM ISFKFDHL, and 0.05μM SIINFEKL/1μM ISFKFDHL, showed an moderate increase in H-2K^b expression compared to RMA/S cells incubated with 0.05μM SIINFEKL only (Figure 5-5A). An increase in the fluorescence intensity of cells incubated with the agonist peptide SIINFEKL and ISFKFDHL, demonstrates that upon SIINFEKL binding, ISFKFDHL can still occupy empty H-2K^b molecules during the sequential peptide loading procedure. RMA/S cells cultured with no peptide had a reduction in H-2K^b expression as expected for the lack of a stabilization peptide for H-2K^b (Figure 5-4A). Analysis of RMA/S cells incubated with 0.05μM SIINFEKL, 0.05μM SIINFEKL/10μM ISFKFDHL and 0.05μM SIINFEKL/1μM ISFKFDHL, using the H-2K^b-SIINFEKL specific antibody, show a similar fluorescence intensity. On the other hand, RMA/S cells incubated individually with 10μM ISFKFDHL, 1μM ISFKFDHL and no peptide, showed low fluorescence intensity that can be due to background staining (Figure 5-5B). Using the ISFKFDHL peptide at the relatively high concentrations of 10μM and 1μM during sequential loading experiments, using the low SIINFEKL concentration, shows that stable H-2K^b-SIINFEKL complexes remain at the cell surface.

In order to test antagonism using the ISFKFDHL peptide; we employed cytotoxicity assays with $CD3^{-}NK1.1^{+}Ly49C\&I^{+}$ effector cells and RMA/S targets incubated with 0.05μM SIINFEKL, 0.05μM SIINFEKL/10μM ISFKFDHL, 0.05μM SIINFEKL/1μM ISFKFDHL, 10μM ISFKFDHL, 1μM ISFKFDHL and no peptide. As a readout of $CD3^{-}NK1.1^{+}Ly49C\&I^{+}$ activity, we use percent specific lysis having the highest percent specific lysis against RMA/S cells incubated with no peptide, showing 75% cytotoxicity at the plateau at the 0.5 to 1 effector to target cell ratio, whereas we observed a 53% specific lysis in RMA/S incubated with SIINFEKL at the 0.5 to 1 effector to target cell ratio (Figure 5-6A). We used and normalized our experimental results at the 0.5 to 1 effector to target cell ratio by fixing 53% from RMA/S-SIINFEKL to "0% Activation" and 75% from RMA/S-no peptide to "100% Activation".To determine activity in each experiment setting, we calculated activity as: $Activity=(\%SL_{(experiment)}-\%SL_{(RMA/S\text{-}SIINFEKL)})/(\%SL_{(NO\ PEPTIDE)}-\%SL_{(RMA/S\text{-}SIINFEKL)})X100$. Target cells loaded separately with 10μM ISFKFDHL and 1μM ISFKFDHL, had a percent activity of 61% and 57% correspondingly; while, RMA/S loaded with 10μM ISFKFDHL or 1μM ISFKFDHL in addition to 0.05μM SIINFEKL, showed a percent increase of 51% and 48% over RMA/S cells incubated with 0.05μM SIINFEKL only (Figure 5-6B). Our data suggest that in cells incubated with 0.05μM SIINFEKL/10μM ISFKFDHL and 0.05μM SIINFEKL/1μM ISFKFDHL; the ISFKDFDHL peptide can depress the inhibition induced by $H\text{-}2K^{b}$-SIINFEKL. Therefore, our findings reveal that for peptides to act as antagonists, these are required to induce detectable $H\text{-}2K^{b}$ association with Ly49C.

Cooperative inhibition of NK cells by H-2K^b peptides that support H-2K^b*-Ly49C interaction*

When co-presented with SIINFEKL, ISFKFDHL, a peptide that supports Ly49C-H-2K^b interaction at an intermediate level, we observed a more marked antagonistic phenomenon than when using RGYVYQGL, a peptide that does not support Ly49C association with H-2K^b. Our data suggested that with murine NK cells, peptide leading to a stronger antagonist phenotype, also triggers partial H-2K^b-Ly49C recognition. The association between the peptide permissiveness towards H-2K^b-Ly49C association and antagonism when co-expressed with SIINFEKL; lead us to include as a control a peptide that is fully supportive of Ly49C association, KIITRYNL, during co-presentation with SIINFEKL. In addition, using peptides that support Ly49C recognition of H-2K^b at different levels (RGYVYQGL<ISFKFDHL<KIITYRNL) can allow us to gain a better understanding of how Ly49s respond to changes in pMHC-I expression at the cell surface.

In order to examine the role of H-2K^b-KIITYRNL when co-expressed with H-2K^b-SIINFEKL; we employed RMA/S cells and loaded them with 0.05μM SIINFEKL followed by 10μM KIITYRNL or 1μM KIITYRNL. At the concentrations of 10μM and 1μM, we saturated RMA/S cells already bearing SIINFEKL, in order to provide excess of peptide for binding empty H-2K^b molecules. For our controls we used RMA/S cells separately loaded with 0.05μM SIINFEKL, 10μM KIITYRNL, 1μM KIITYRNL and no peptide. We examined H-2K^b expression on RMA/S cells using H-2K^b specific antibody and H-2K^b-SIINFEKL specific antibody. RMA/S cells loaded singly with 0.05μM

SIINFEKL, showed upregulation of H-2K^b in contrast to the no peptide control. RMA/S cells that were incubated with 10μM KIITYRNL, 1μM KIITYRNL, 0.05μM SIINFEKL/10μM KIITYRNL, and 0.05μM SIINFEKL/1μM KIITYRNL, showed a moderate increase in H-2K^b expression over RMA/S cells incubated with 0.05μM SIINFEKL singly (Figure 5-7A). This indicates that RMA/S cells loaded with low concentration of SIINFEKL can bind additional peptides at the cell surface as shown by the upregulation in H-2K^b staining in cells incubated with 10μM or 1μM KIITYRNL following SIINFEKL incubation. Finally, our no peptide control had a pronounced decrease in H-2K^b expression, showing that a H-2K^b specific peptide is necessary to stabilize H-2K^b (Figure 5-7A). Examination of RMA/S cells staining for H-2K^b-SIINFEKL complexes demonstrated that RMA/S cells loaded with 0.05μM SIINFEKL, 0.05μM SIINFEKL/10μM KIITYRNL and 0.05μM SIINFEKL/1μM KIITYRNL have comparable H-2K^b-SIINFEKL expression; while RMA/S cells loaded independently with 10μM KIITYRNL, 1μM KIITYRNL and no peptide, showed minimal staining for H-2K^b-SIINFEKL (Figure 5-7B). Establishing the presence of H-2K^b-SIINFEKL complexes, shows that stable H-2K^b-SIINFEKL complexes are formed and preserved even after the loading of a second peptide at high concentrations.

Functional analysis of CD3$^-$NK1.1$^+$Ly49C&I$^+$ effector cells and RMA/S target cells were conducted to test the influence of KIITYRNL when co-expressed with SIINFEKL. Target cells were loaded with 0.05μM SIINFEKL, 0.05μM SIINFEKL/10μM KIITYRNL, 0.05μM SIINFEKL/1μM KIITYRNL, 10μM KIITYRNL, 1μM KIITYRNL and no peptide. Cytotoxicity of CD3$^-$NK1.1$^+$Ly49C&I$^+$

cells towards target cells was established as percent specific lysis. The highest activity of $CD3^{-}NK1.1^{+}Ly49C\&I^{+}$ cells reached at a plateau at the 0.5 to 1 effector to target cell ratio against RMA/S cells incubated with no peptide at 75% cytotoxicity (Figure 5-8A). On the other hand, RMA/S cells loaded with our control peptide SIINFEKL, demonstrated a 53 % cytotoxicity at the same effector to target cell ratio. We normalized our results by establishing the 53% cytotoxicity from RMA/S-SIINFEKL as "0% Activation" and 75% from RMA/S-no peptide as "100% Activation". Using our cytotoxicity results at the 0.5 to 1 effector to target cell ratio, we calculated activity using the formula: $Activity=(\%SL_{(experiment)}-\%SL_{(RMA/S\text{-}SIINFEKL)})/(\%SL_{(NO\ PEPTIDE)}-\%SL_{(RMA/S\text{-}SIINFEKL)})X100$. Target cells incubated separately with 10μM KIITYRNL and 1μM KIITYRNL, showed a percent activity of -43% and -31% (Figure 5-8B). The negative percentage indicates that the percent cytotoxicity using the KIITYRNL increased inhibition as compared to the SIINFEKL peptide, apparently meaning that KIITYRNL is a stronger agonist than SIINFEKL peptide at this concentration. Functional assays using RMA/S cells loaded with 0.05μM SIINFEKL/10μM KIITYRNL or 0.05μM SIINFEKL/1μM KIITYRNL showed a percent activity of -35% and -12% (Figure 5-8B). Our results suggest that the KIITYRNL peptide can positively influence inhibitory signals by the SIINFEKL peptide. This indicates that the presence of higher numbers of peptide agonists can cooperate to induce inhibitory NK cell function.

C. Discussion

NK cell inhibitory receptors KIRs and Ly49s, expressed in human and mouse respectively, can recognize their corresponding MHC-I ligands in a peptide dependent fashion. Alhough KIRs and Ly49s have similar functions, their structure and their association with their respective ligands is different. In general, KIRs are immunoglobulin-like proteins consisting 2 or 3 Ig-like extraceullular domains termed D1, D2 for membrane distal domains. Interaction with MHC-I occurs between KIR amino acids found at the hinge region between membrane distal Ig-like domains D1 and D2; and MHC-I residues at the α1, α2 regions and bound peptide residues at positions 7 and 8. Importantly, the crystal lattice produced in the co-crystalization of KIR2DL2 and its cognate ligand HLA-Cw3, showed KIR and MHC-I oligomeric aggregates that possibly resemble receptor and ligand clustering at the immune synapse (275). Still, KIR and MHC-I association takes place at a 1:1 ratio as confirmed by sedimentation experiments (275). On the other hand, murine Ly49s are C-type lectin-like receptors expressed as homodimers and associate with MHC-I utilizing regions L3/α3, L5, L6, β3 and β4 that form an interface with MHC-I at a site beneath the peptide binding groove, including residues within the α1, α2 and α3 regions as well as β2m. Using ultrafugation experiments, Ly49s have been shown to associate with MHC-I ligands at a 2 to 1 ratio, with one CTLD interacting with an individual MHC-I; but can also associate at a 1 to 1 ratio. In crystallographic data of Ly49 and MHC-I association, there is no reported evidence of receptor and ligand oligomerization, as observed with KIR and MHC-I (195, 275). However, it has been shown that both MHC-I and Ly49 aggregate at the synapse formed by target and effector cells (289, 290). Although the exact geometry of these

aggregates is not known, the accumulation of receptor and ligand at the synapse is also a critical event for murine NK cell function (289, 290). The clear differences in MHC-I association/recognition by KIR and Ly49s make peptide specificity an interesting trait to be conserved for NK cell function.

The peptide selective phenotype demonstrated by both KIR and Ly49 receptors, indicates that NK cells are capable of not only detecting lack or reduction of MHC-I molecules, but the presence of bound peptide residues is noted as well. This characteristic is important for the detection of tumor cells or viral infection, that do not trigger a decrease in MHC-I expression, but changes the pool of peptides for MHC-I binding. Studies using the co-presentation of both peptides that support and peptides that do not support KIR-MHC-I association, have further demonstrated the importance of peptide selective recognition of MHC-I. Association between KIR and MHC-I that results in NK cell inhibition, is characterized as an agonistic NK cell phenotype. Studies by Fadda *et al* showed that a peptide that individually does not support KIR binding to MHC-I, can cause antagonistic effects when co-presented with a peptide that strongly supports KIR-MHC-I interaction, leading to NK cell activation. This finding reveals that even peptides that do not support inhibitory receptor association with MHC-I, still have an active role in NK cell function and are not ignored by the NK cell. Although, in a different modality than as KIRs, Ly49s are peptide dependent in their recognition of MHC-I and we investigated whether peptide antagonism is also observed with murine NK cells. In addition, investigating if murine NK cells behave in a similar manner as human NK cells for peptide dependent activity may lead to supporting evidence for a

fundamental and universal mechanism of sensing cellular stress by surveying pMHC-I complexes to the advantage of the host.

We used functional assays in order to investigate the possibility of peptide antagonism by murine NK cells. The use of *ex vivo* mouse NK cells, allowed us to directly correlate expression of different pMHC-I complexes and their effects on NK cell inhibition. As target cells, we used RMA/S cells that can be loaded with peptides individually or when testing two peptides, can be loaded sequentially. From our previous studies, investigating the role of H-2K^b-peptide residues in Ly49C recognition, we can characterize peptides by the degree that these supported Ly49C recognition of H-2K^b into high, intermediate and low/null. For peptide antagonism experiments using murine *ex vivo* NK cells expressing Ly49C, we use SIINFEKL as the agonist peptide, since H-2K^b-SIINFEKL has been established to support Ly49C and H-2K^b association. To probe peptide antagonism we use two different peptides. The first peptide we employed is RGYVYQGL which does not support Ly49C-H-2K^b interaction when presented individually. In KIR-MHC-I antagonism studies, the peptide that acted as an antagonist, when co-presented with an agonist, did not confer detectable KIR-MHC-I interaction by itself. Therefore, the RGYVYQGL peptide served to probe whether the same phenomenon takes place in murine NK cells. Our results, using RMA/S cells co-presenting RGYVYQGL with SIINFEKL showed a weak antagonist phenotype that depressed inhibition of NK cells by 20% in our normalized data results. At least at the concentrations used in this study, the RGYVYQGL peptide only poorly acted as an apparent antagonist. In Fadda *et al* study with KIR and MHC-I association, the

antagonism assay was in part done using a 1 to 1 molar ratio between the agonist and the antagonist peptides. Therefore, for future studies a closer ratio between the SIINFEKL and RGYVYQGL can be employed to measure the reactivity of NK cells.

Since using the RGYVYQGL peptide only lead to weak apparent antagonism of H-2K^b-SIINFEKL; we hypothesized that murine NK cell antagonism perhaps required a minimal level of interaction between Ly49C and H-2K^b. As a result, we utilized a peptide that supports Ly49C-H-2K^b binding at an intermediate level: ISFKFDHL. In KIR studies on NK cell antagonism, a peptide that yielded an intermediate level of KIR-MHC-I recognition when singly presented on MHC-I, did not behave as an antagonist when co-expressed with an agonist peptide. Still, we tested ISFKFDHL to investigate if peptide dependent antagonism occurs differently between KIR and Ly49, since both receptors are peptide dependent and use different peptide "sensing" mechanisms. Our results suggest the ISFKFDHL peptide can suppress the inhibition induced by H-2K^b-SIINFEKL by 50%. These results indicate that peptide antagonism dependent on Ly49C and H-2K^b association requires an antagonist pMHC-I complex that can bind Ly49C at an intermediate level. In addition, comparing the antagonistic influence of H-2K^b-ISFKFDHL complexes to H-2K^b-RGYVYQGL showed that there might be a correlation between the level at which the peptide supports Ly49C interaction with H-2K^b and its antagonistic effects. Additionally, in order to have a complete picture of NK cell responses during the co-expression of different peptides, we tested a peptide that fully supports Ly49C association with H-2K^b, KIITYRNL, and its influence during functional assays when simultaneously presented on H-2K^b with SIINFEKL. Our results show that

KIITYRNL is as well an agonist compared to SIINFEKL. The SIINFEKL peptide at a concentration of 10μM and 1μM induces similar NK inhibition compared to KIITYRNL at a concentration of 10μM and 1μM. Our functional assays also indicated that the co-expression of SIINFEKL and KIITRYNL enhanced inhibition, over SIINFEKL alone, by 35% and 12% with 10μM and 1μM KIITYRNL, respectively. These results suggested that the presence of higher pMHC-I agonist complexes, H-2K^b-SIINFEKL and H-2K^b -KIITYRNL, can induce inhibitory NK cell function.

The mechanism of how peptides that support H-2K^b-Ly49C interaction at different levels antagonize or cooperate with agonist complexes has not been described. However, based on previous studies of the synapse between mouse NK and target cells, as well as the mode of H-2K^b-Ly49C binding, we can create a hypothetical model to describe our results. Synapse formation between NK cells expressing Ly49 and target cells expressing cognate ligand has been studied using confocal microscopy of molecules bearing fluorescent tags. During the engagement between effector and target cell, microscopy images show the aggregation of MHC-I molecules on the target cell at the site of contact with the effector cells (289, 290). Similarly, Ly49s aggregate at the site of contact with target cells leading to signaling events. We can therefore, hypothesize that H-2K^b-SIINFEKL complexes on RMA/S interact with Ly49C leading to recruitment and aggregation of Ly49C on effector cells and aggregation of H-2K^b-SIINFEKL on target cells, inhibiting NK cell activation. Association between Ly49C and H-2K^b-SIINFEKL occurs at a 1 to 2 ratio, according to crystal structural data and sedimentation analysis, with one CTLD of the Ly49C homodimer interacting with one

H-2K^b-SIINFEKL. Upon Ly49C binding with H-2K^b at the synapse between effector and target cells, we can hypothesize that a uniform lattice structure between complexes facilitates the signaling events that promote inhibitory signals in NK cells. Using this hypothesis, we can predict that the aggregation of agonist pMHC-I complex, H-2K^b-SIINFEKL, and cognate inhibitory receptor, Ly49C, lead to a uniform and stable interaction within the synapse between target and effector cell that leads to NK cell inhibitory signals (Figure 5-9). However, during expression of both H-2K^b-SIINFEKL and H-2K^b-RGYVYQGL our results suggested that a moderate decrease in inhibition was a direct result from the presence of H-2K^b-RGYVYQGL on target cells. In line with our hypothesis, H-2K^b-SIINFEKL and H-2K^b-RGYVYQGL can aggregate at the synapse between target and effector cells. In the presence of H-2K^b-RGYVYQGL however, a complex that has minimal interaction with Ly49C, the lattice structure between Ly49C-H-2K^b-SIINFEKL is not uniform due to the presence of H-2K^b-RGYVYQGL complexes, leading to attenuation of inhibitory signals in NK cells (Figure 5-10). Therefore, the H-2K^b-RGYVYQGL is not completely ignored by NK cells. Future experiments utilizing other peptides that resemble RGYVYQGL in their ability to abrogate Ly49C and H-2K^b association, when presented individually, such as AAYAYAAL, can be used to demonstrate whether an antagonistic phenomenon is also observed.

From our results using the ISFKFDHL peptide, that was a superior antagonist than RGYVYQGL, we can hypothesize that since H-2K^b-ISFKFDHL and H-2K^b-SIINFEKL can bind Ly49C at different levels, inhibitory signals can be hampered. The

Ly49C homodimer could bind one H-2K^b-ISFKFDHL leaving an additional CTLD domain to bind H-2K^b-SIINFEKL (Figure 5-11). This can be detrimental to signaling mediated by interactions between Ly49C and H-2K^b-SIINFEKL. An additional possibility is that the H-2K^b-ISFKFDHL complex may not fully support Ly49C conformational changes necessary for Ly49C receptor signaling. Taking this into account, we can hypothesize, in our theoretical uniform lattice structure of ligand and receptor, that by having an intermediate interaction with Ly49C, the ISFKFDHL can not only bind Ly49C that induces intermediate signaling events, but when bound to one CTLD of a Ly49C homodimer can also cause structural changes that abrogate or reduce the binding of H-2K^b-SIINFEKL by the additional CTLD. Therefore, co-presenting both pMHC-I complexes that have different topology at the site of binding under the peptide binding groove has a greater effect than co-presenting a peptide that does not interact with Ly49C such as RGYVYQGL.

Our results from the co-expression of agonist peptide complexes, SIINFEKL and KIITYRNL, demonstrated a cooperative effect that enhanced NK inhibition. Following the same line of reasoning with the analysis of the previous peptide, that Ly49C can bind two H-2K^b complexes, we can argue that H-2K^b-SIINFEKL and H-2K^b-KIITRYNL can be quiet similar for complex binding requirements to Ly49C (Figure 5-12). Both peptides SIINFEKL and KIITYRNL have Ile amino acids at positions 2 and 3 which, based on previous studies, we have demonstrated to be critical for the support of Ly49C interactions and we hypothesize that the region of Ly49C binding has a similar conformation. Therefore, H-2K^b-SIINFEKL and H-2K^b-KIITYRNL can bind Ly49C

and form stable lattices between the effector and target cell synapse that act to facilitate inhibitory signaling events.

Our experiments are a representation of cells *in vivo* with expression of a multitude of pMHC-I complexes that trigger a broad spectrum of Ly49C-dependent NK cell responses. Moreover, this study demonstrates the dynamic role of peptides in determining NK cell function. The diversity of peptides simultaneously presented on a cell can reach up to 2000 different peptides, with few prominently displayed (2). The peptide dependent regulation of an Ly49 receptor, will be dependent on signals received when Ly49C interacts with a multitude of co-expressed pMHC-I complexes. Therefore, it is the composite effect of those interactions between agonist and antagonist pMHC-I complexes, that contribute to NK cell activity. However, Ly49C is only one of multiple NK cell receptors that contribute to the net NK cell activation state. Our studies reveal that the pMHC-I mosaic can affect NK cell responses in an Ly49 dependent manner and that it should always be considered as a factor during studies of NK cell activity in mouse models of infection or tumorigenesis.

We have proposed that the observed phenotypes during the co-presentation of different pMHC-I complexes, can be due to modifications within the synapse between target and effector cells. However, experiments showing what the condition of the synapse is during co-expression of different sets of pMHC-I complexes remains to be established. Additionally, examination of the mechanism behind peptides antagonizing or acting in a cooperative manner needs to be addressed. Of particular importance are NK cell intrinsic mechanisms of activation. Upon engagement with cognate ligand,

immunoreceptor tyrosine-based inhibitory motifs (ITIMs) in the cytoplasmic tail of inhibitory Ly49 receptors become phosphorylated by Src kinases. Subsequent signaling events include the recruitment of phosphatases such as SHP-1 and SHP-2, followed by de-phosphorylation of Vav1 (291). On the other hand, the absence of inhibitory signals can lead to upregulation of signaling molecules Erk1 and Erk2 that are involved in the reorganization of cytoskeletal proteins required for NK cell degranulation (113, 291). Examination of early and late signaling molecules in the activation/inhibitory cascades in NK cells can provide more insight into the mechanism of peptide dependent NK cell activity.

A

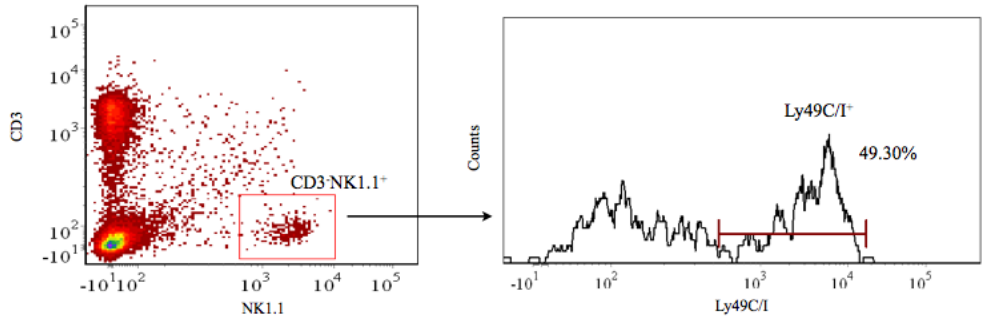

B

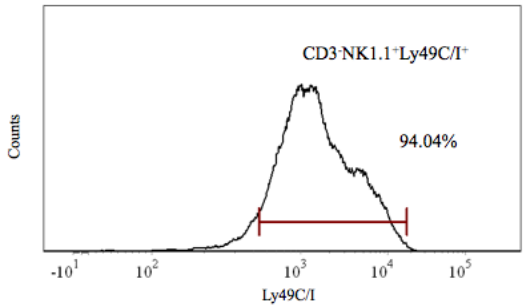

C

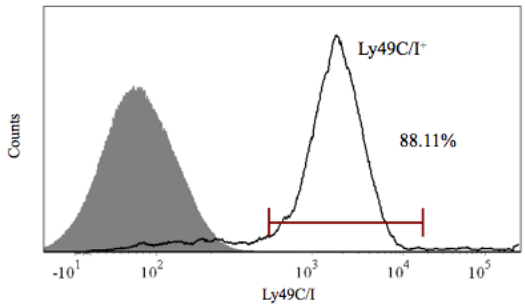

Figure 5-1. Analysis of *ex vivo* CD3$^-$NK1.1$^+$Ly49C&I$^+$ NK cells. (A) Gating strategy for the separation of CD3$^-$NK1.1$^+$ cell population expressing Ly49C&I **(B)** Purity levels of Ly49C&I$^+$ cells after sorting. **(C)** Expression of Ly49C&I is maintained after expansion of CD3$^-$NK1.1$^+$Ly49C&I$^+$ NK cells in the presence of IL-2 for 6 days. Examination of Ly49C&I expression was performed using 5E6 antibody, in black line, and isotype control in gray shaded curve.

H-2K^b Peptide	Recognized by Lv49C	Peptide Source
SIINFEKL	Yes	Chicken Ovalbumin (256-264)
RGYVYQGL	No	Vesicular Stomatitis Virus NP (52-59)
ISFKFDHL	Intermediate	F-actin capping protein alpha1 (93-100)
KIITYRNL	Yes	PCI domain-containing protein 2 (318-325)

Table 5-1. H-2K^b specific peptide sequences and effect on Ly49C recognition. Previous studies in our laboratory have demonstrated a varied range of Ly49C dependent NK cell responses against RMA/S bearing different peptides.

A

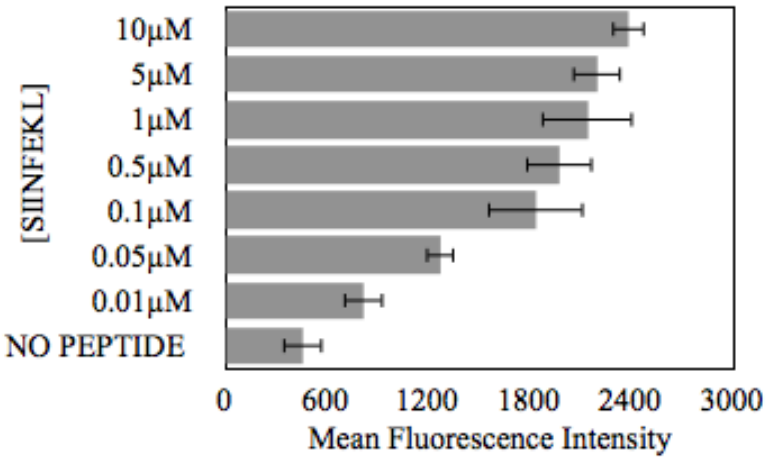
10μM
5μM
1μM
0.5μM
0.1μM
0.05μM
0.01μM
NO PEPTIDE
[SIINFEKL]
0
600
1200
1800
2400
3000
Mean Fluorescence Intensity

B

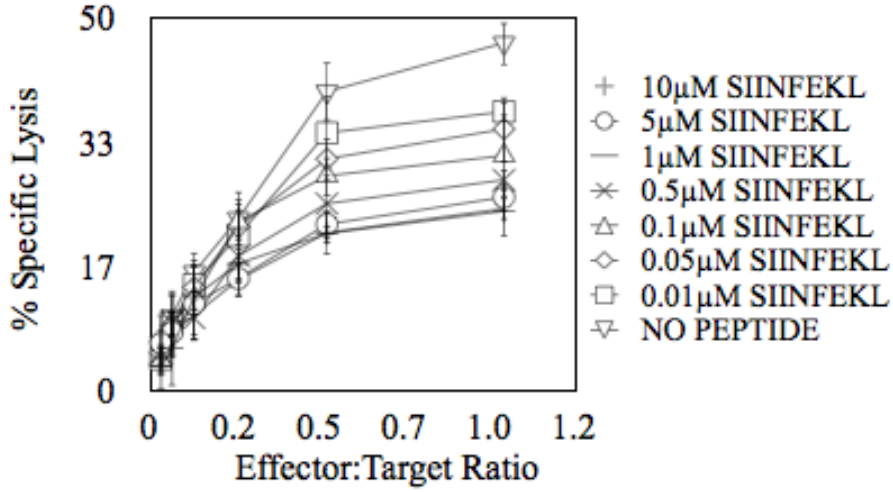
50
33
17
0
% Specific Lysis
0
0.2
0.5
0.7
1.0
1.2
Effector:Target Ratio
10μM SIINFEKL
5μM SIINFEKL
1μM SIINFEKL
0.5μM SIINFEKL
0.1μM SIINFEKL
0.05μM SIINFEKL
0.01μM SIINFEKL
NO PEPTIDE

C

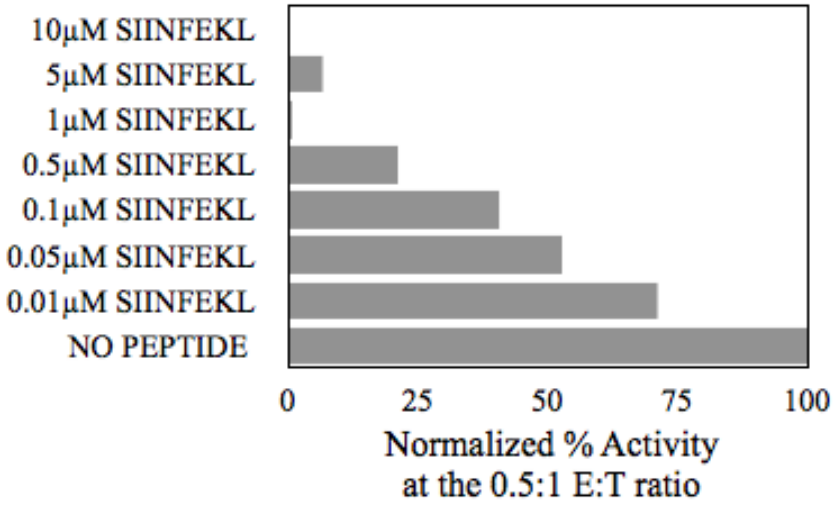
10μM SIINFEKL
5μM SIINFEKL
1μM SIINFEKL
0.5μM SIINFEKL
0.1μM SIINFEKL
0.05μM SIINFEKL
0.01μM SIINFEKL
NO PEPTIDE
0
25
50
75
100
Normalized % Activity
at the 0.5:1 E:T ratio

Figure 5-2. Low concentrations of SIINFEKL on RMA/S cells yield inhibition of $CD3^{-}NK1.1^{+}Ly49C\&I^{+}$ NK cells. (A) Detection of H-$2K^{b}$ on RMA/S cells after H-$2K^{b}$ stabilization assay in the presence of SIINFEKL at different concentrations and no peptide control. Expression of H-$2K^{b}$ was detected using the H-$2K^{b}$ specific antibody AF6-88.5.5.3 conjugated with APC. **(B)** Percent cytotoxicity of $CD3^{-}NK1.1^{+}Ly49C\&I^{+}$ NK cells against RMA/S cells loaded with the SIINFEKL peptide at the indicated concentrations. Data shown represents the mean of three different experiments with the error bars indicating the SD. **(C)** Normalized % activity utilizing the mean of three separate cytotoxicity assay results in Figure 5-2B at the 0.5:1 effector to target cell ratio. The formula to calculate the normalized activity is: % Activity=$(\%SL_{(experiment)}-\%SL_{(RMA/S\text{-}SIINFEKL)})/(\%SL_{(NO\ PEPTIDE)}-\%SL_{(RMA/S\text{-}SIINFEKL)})X100$.

A

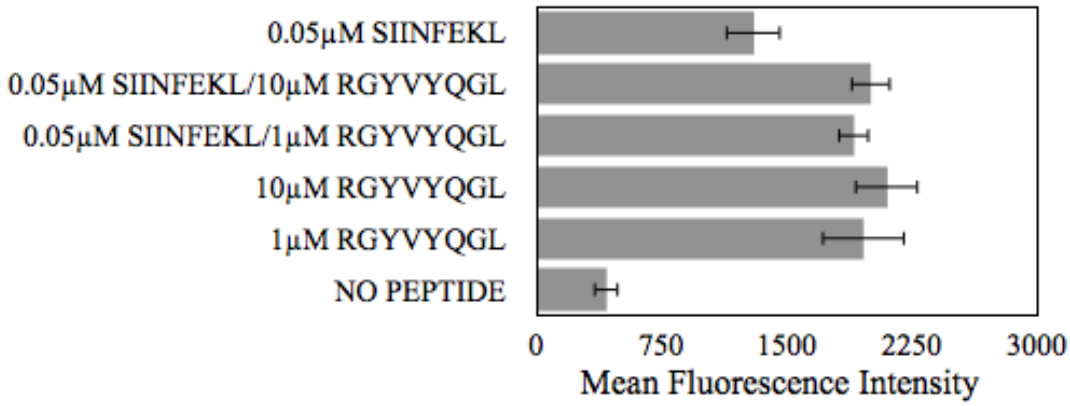

B

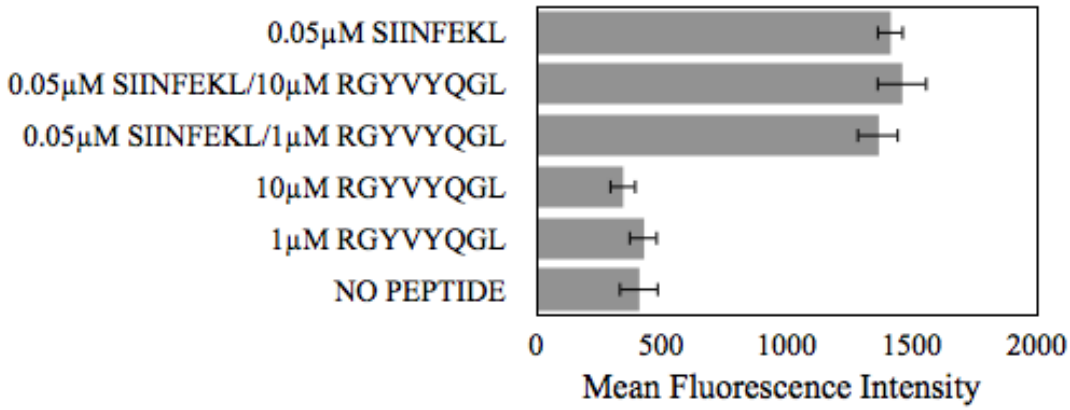

Figure 5-3. Expression levels of H-2K^b on RMA/S cells utilizing sequential peptide loading of SIINFEKL and RGYVYQGL. (A) Detection of H-2K^b on RMA/S cells after H-2K^b stabilization assay using sequential loading of peptides SIINFEKL and RGYVYQGL, individual loading of SIINFEKL or RGYVYQGL as controls, and no peptide control. Expression of H-2K^b was detected using the H-2K^b specific antibody AF6-88.5.5.3 conjugated with APC. **(B)** Detection of H-2K^b-SIINFEKL on RMA/S cells after H-2K^b stabilization assay using sequential loading of peptides SIINFEKL and RGYVYQGL, individual loading of SIINFEKL or RGYVYQGL as controls, and no peptide control. Expression of H-2K^b -SIINFEKL was detected using the H-2K^b-OVA specific antibody 25-D1.16 conjugated with APC. Data shown represents the mean of three different experiments with the error bars indicating the SD.

A

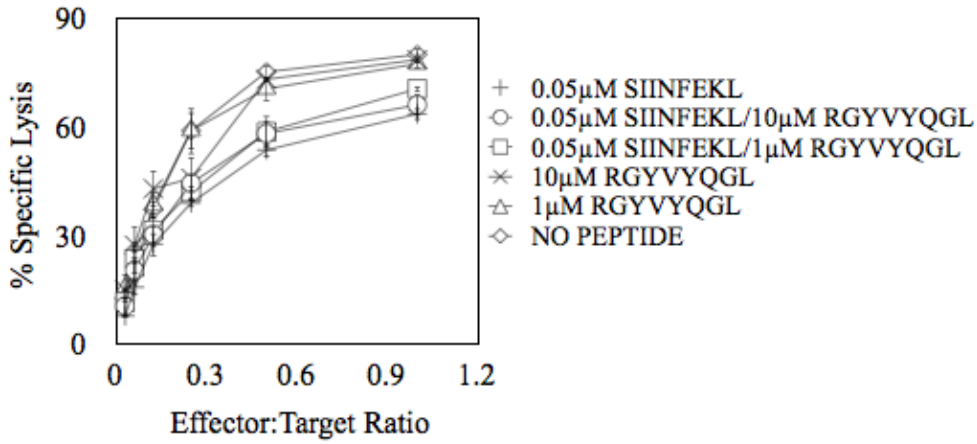

B

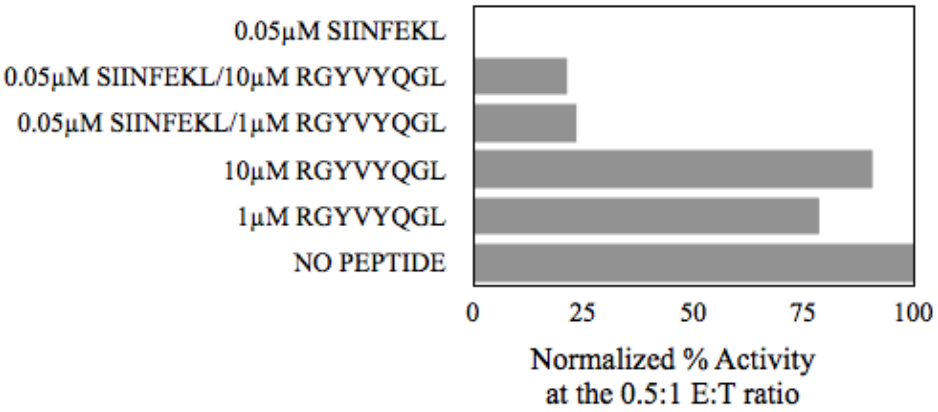

Figure 5-4. Peptide that does not supports Ly49C and H-2K^b interaction can act to weakly antagonize the inhibitory effect of H-2K^b-SIINFEKL. (A) Percent specific lysis of CD3$^-$NK1.1$^+$Ly49C&I$^+$ NK cells against RMA/S cells sequentially incubated with SIINFEKL followed by RGYVYQGL, individual incubated with SIINFEKL or RGYVYQGL as controls, and incubated with no peptide as a control. Data shown represents the mean of three different experiments with the error bars indicating the SD. **(B)** Normalized % activity utilizing the mean of three separate cytotoxicity assay results in Figure 5-4A at the 0.5:1 effector to target cell ratio. The formula to calculate the normalized activity is: % Activity=(%SL$_{(experiment)}$-%SL$_{(RMA/S-SIINFEKL)}$)/(%SL$_{(NO\ PEPTIDE)}$-%SL$_{(RMA/S-SIINFEKL)}$)X100.

A

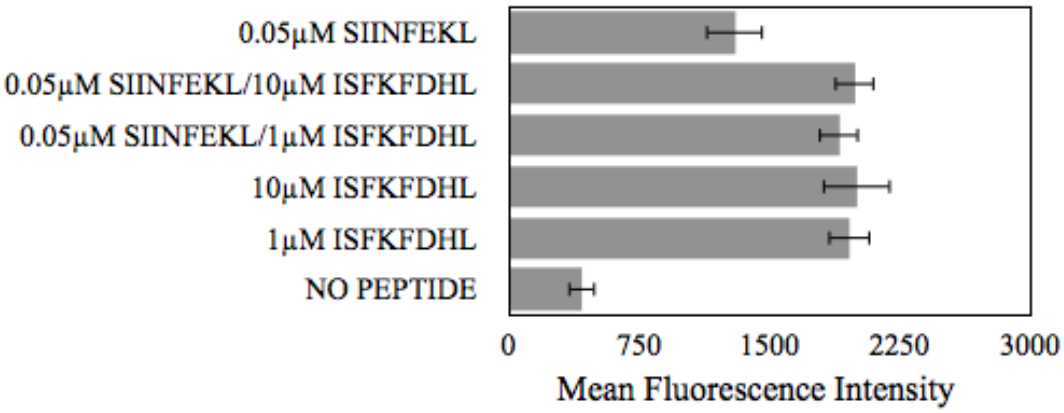

B

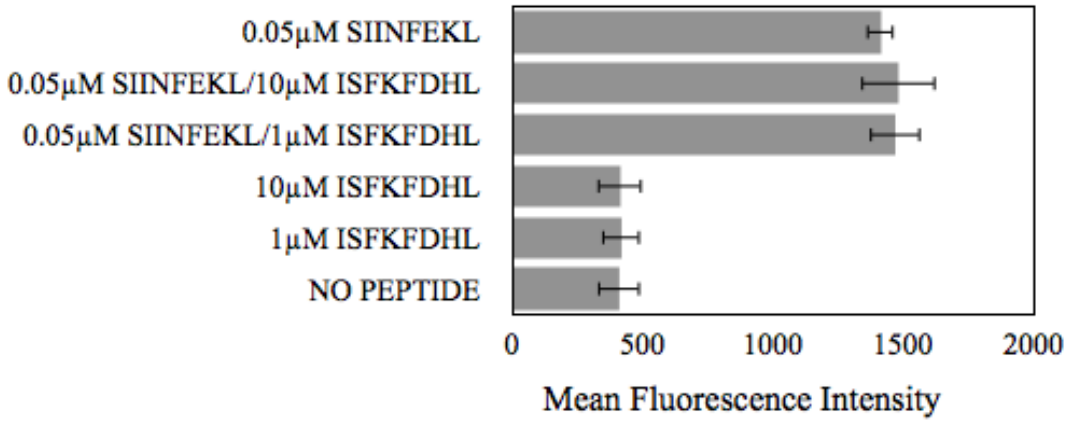

Figure 5-5. Expression levels of H-2K^b on RMA/S cells utilizing sequential peptide loading of SIINFEKL followed by ISFKFDHL. (A) Detection of H-2K^b on RMA/S cells after H-2K^b stabilization assay using sequential loading of peptides SIINFEKL and ISFKFDHL, individual loading of SIINFEKL or ISFKFDHL as controls, and no peptide control. Expression of H-2K^b was detected using the H-2K^b specific antibody AF6-88.5.5.3 conjugated with APC. **(B)** Detection of H-2K^b-SIINFEKL on RMA/S cells after H-2K^b stabilization assay using sequential loading of peptides SIINFEKL and ISFKFDHL, individual loading of SIINFEKL or ISFKFDHL as controls, and no peptide control. Expression of H-2K^b -SIINFEKL was detected using the H-2K^b-OVA specific antibody 25-D1.16 conjugated with APC. Data shown represents the mean of three different experiments with the error bars indicating the SD.

A

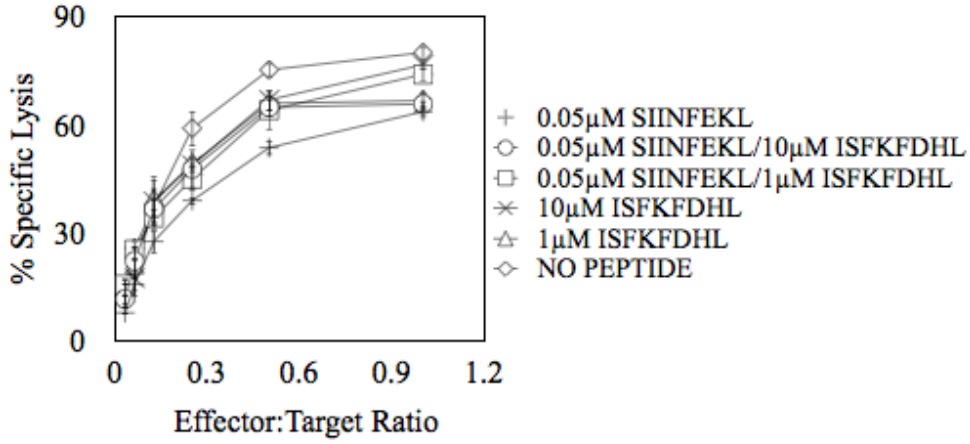

B

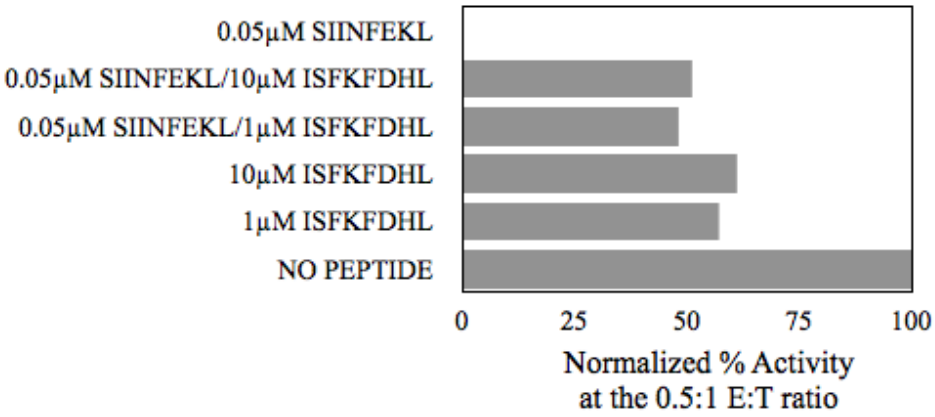

Figure 5-6. Peptide that supports Ly49C and H-2K^{b} interaction at a an intermediate level, can act to disrupt inhibition by H-2K^{b}-SIINFEKL complexes. **(A)** Percent specific lysis of CD3^{-}NK1.1^{+}Ly49C&I^{+} NK cells against RMA/S cells sequentially incubated with SIINFEKL followed by ISFKFDHL, individual incubated with SIINFEKL or ISFKFDHL as controls, and incubated with no peptide as a control. Data shown represents the mean of three different experiments with the error bars indicating the SD. **(B)** Normalized % activity utilizing the mean of three separate cytotoxicity assay results in Figure 5-6A at the 0.5:1 effector to target cell ratio. The formula to calculate the normalized activity is: % Activity=(%SL$_{(experiment)}$-%SL$_{(RMA/S-SIINFEKL)}$)/(%SL$_{(NO\ PEPTIDE)}$-%SL$_{(RMA/S-SIINFEKL)}$)X100.

A

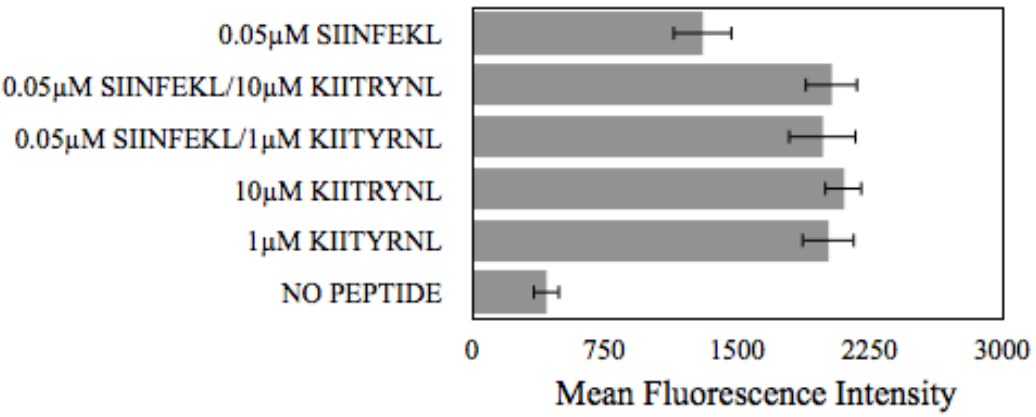

B

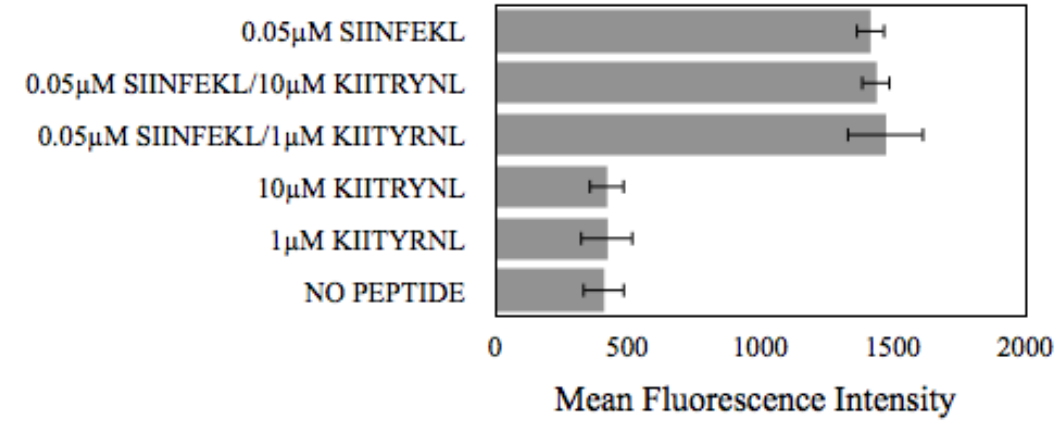

Figure 5-7. Expression levels of H-2K^b on RMA/S cells utilizing sequential peptide loading of peptides SIINFEKL and KIITYRNL. (A) Detection of H-2K^b on RMA/S cells after H-2K^b stabilization assay using sequential loading of peptides SIINFEKL and KIITYRNL, individual loading of SIINFEKL or KIITYRNL as controls, and no peptide control. Expression of H-2K^b was detected using the H-2K^b specific antibody AF6-88.5.5.3 conjugated with APC. **(B)** Detection of H-2K^b-SIINFEKL on RMA/S cells after H-2K^b stabilization assay using sequential loading of peptides SIINFEKL and KIITYRNL, individual loading of SIINFEKL or ISFKFDHL as controls, and no peptide control. Expression of H-2K^b -SIINFEKL was detected using the H-2K^b-OVA specific antibody 25-D1.16 conjugated with APC. Data shown represents the mean of three different experiments with the error bars indicating the SD.

A

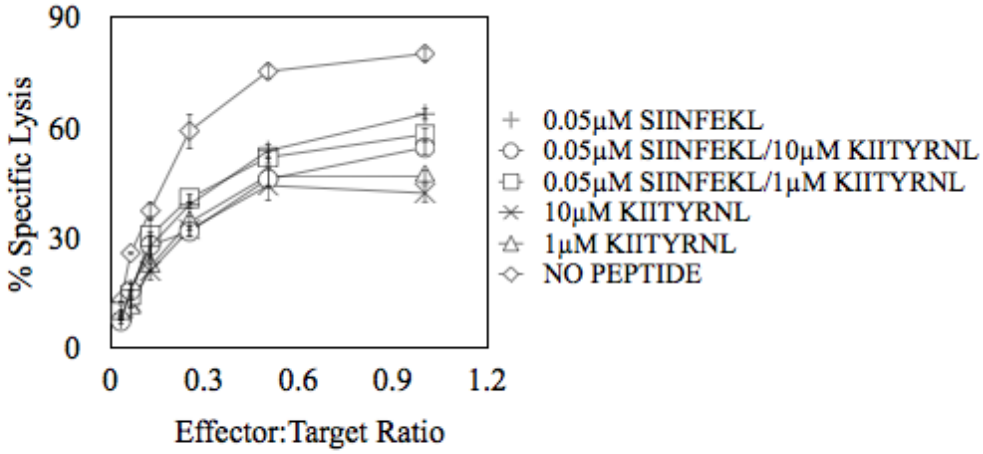

B

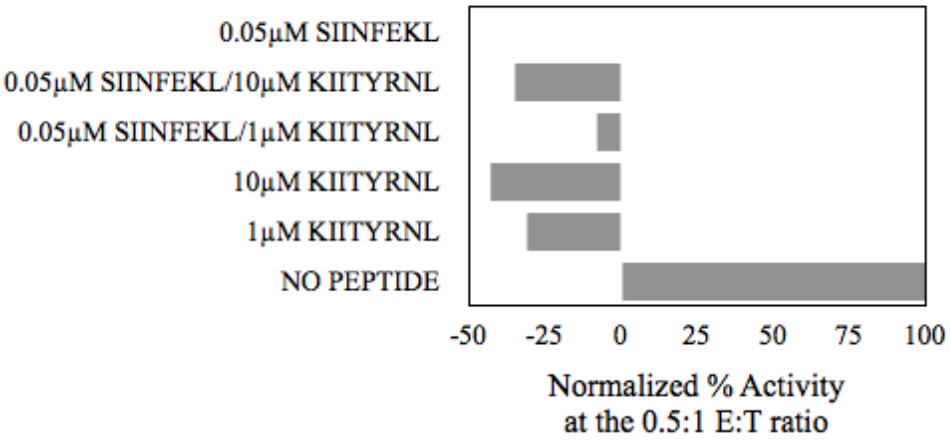

Figure 5-8. Peptide that supports Ly49C and H-2K^b interaction, can serve to enhance inhibition by H-2K^b-SIINFEKL complexes. (A) Percent specific lysis of CD3$^-$NK1.1$^+$Ly49C&I$^+$ NK cells against RMA/S cells sequentially incubated with SIINFEKL followed by KIITYRNL, individual incubated with SIINFEKL or KIITYRNL as controls, and incubated with no peptide as a control. Data shown represents the mean of three different experiments with the error bars indicating the SD. **(B)** Normalized % activity utilizing the mean of three separate cytotoxicity assay results in Figure 5-8A at the 0.5:1 effector to target cell ratio. The formula to calculate the normalized activity is: % Activity=(%SL$_{(experiment)}$-%SL$_{(RMA/S-SIINFEKL)}$)/(%SL$_{(NO\ PEPTIDE)}$-%SL$_{(RMA/S-SIINFEKL)}$)X100.

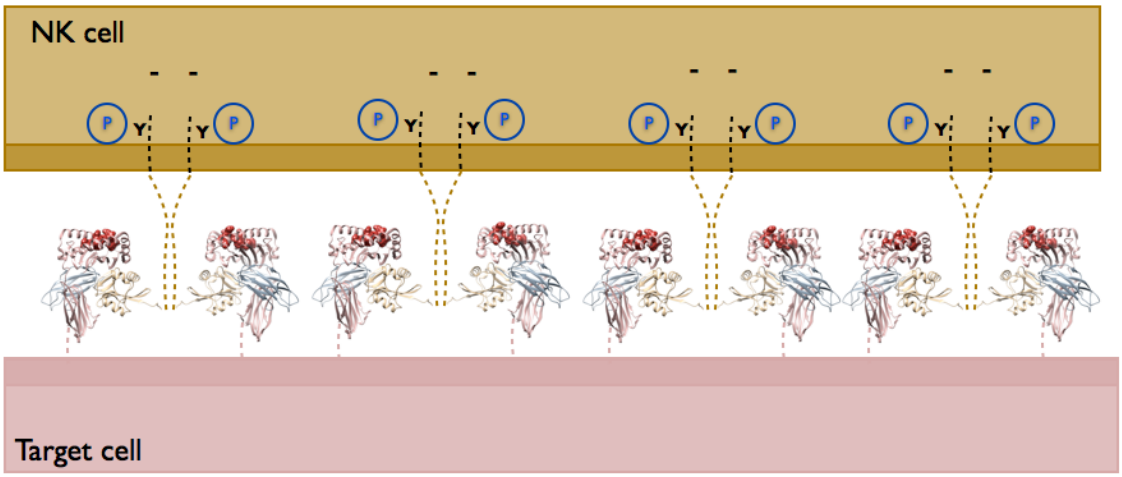

Figure 5-9. Hypothetical model for interaction of H-2K^b-SIINFEKL complexes with Ly49C at the immune synapse. Inhibitory Ly49s and MHC-I can aggregate at the site of contact between effector and target cells. Supportive inhibitory Ly49 and MHC-I association in the synapse, as during Ly49C and H-2K^b-SIINFEKL interaction, leads to inhibitory signaling events. In this theoretical model of the synapse, supportive Ly49C and H-2K^b-SIINFEKL association form a organized and uniform lattice structure between complexes that facilitates signaling events that substantiate inhibitory signals in NK cells. The H-2K^b heavy chain is shown in pink ribbon, the β2m is in grey ribbon and the peptide is in red surface representation. Proximal membrane amino acids connecting the α3 domain to the "target cell surface" are displayed as pink dashed lines. The C-type lectin-like domains (CTLD) of the Ly49C dimer are shown in gold ribbon. Stalk region of the Ly49C is represented as gold dashed lines; while transmembrane and cytoplasmic domains are displayed in black dashed lines. The immunoreceptor tyrosine-based inhibitory motif (ITIM) is represented by a Tyrosine (Y) in black. Phosphorylation of ITIM is noted with a blue circled P. Pictoral representations of receptor and ligand were generated using CHIMERA UCSF software with the PDB ID coordinates 3C8K for Ly49C/H-2K^b-SIINFEKL.

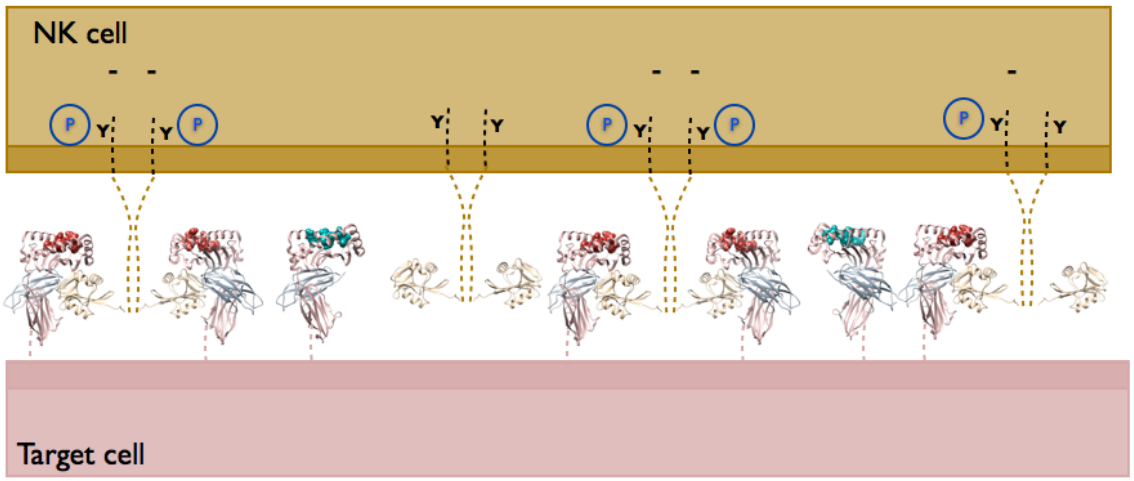

Figure 5-10. Theoretical display of the immune synapse during the co-presentation of peptide-H-2K^b complexes that support and complexes that abrogate Ly49C association with H-2K^b. Inhibitory Ly49s and MHC-I can aggregate at the site of contact between effector and target cells. During co-presentation of H-2K^b-SIINFEKL and H-2K^b-RGYVYQGL, complexes that support or abrogate Ly49C recognition of H-2K^b respectively, the uniform lattice structure between effective Ly49C and H-2K^b-SIINFEKL association loses uniformity due to the presence of H-2K^b-RGYVYQGL, leading to mild depression of inhibitory signals in NK cells. The H-2K^b heavy chain is shown in pink ribbon, the β2m is in grey ribbon and the peptides are in surface representation in red and teal for SIINFEKL and RGYVYQGL respectively. Proximal membrane amino acids connecting the α3 domain to the "target cell surface" are displayed as pink dashed lines. The C-type lectin-like domains (CTLD) of the Ly49C dimer are shown in gold ribbon. Stalk region of the Ly49C is represented as gold dashed lines; while transmembrane and cytoplasmic domains are displayed in black dashed lines. The immunoreceptor tyrosine-based inhibitory motif (ITIM) is represented by a Tyrosine (Y) in black. Phosphorylation of ITIM is noted with a blue circled P. Pictoral representations of receptor and ligand were generated using CHIMERA UCSF software with the PDB ID coordinates 3C8K for Ly49C/H-2K^b-SIINFEKL and IKPU for /H-2K^b-RGYVYQGL.

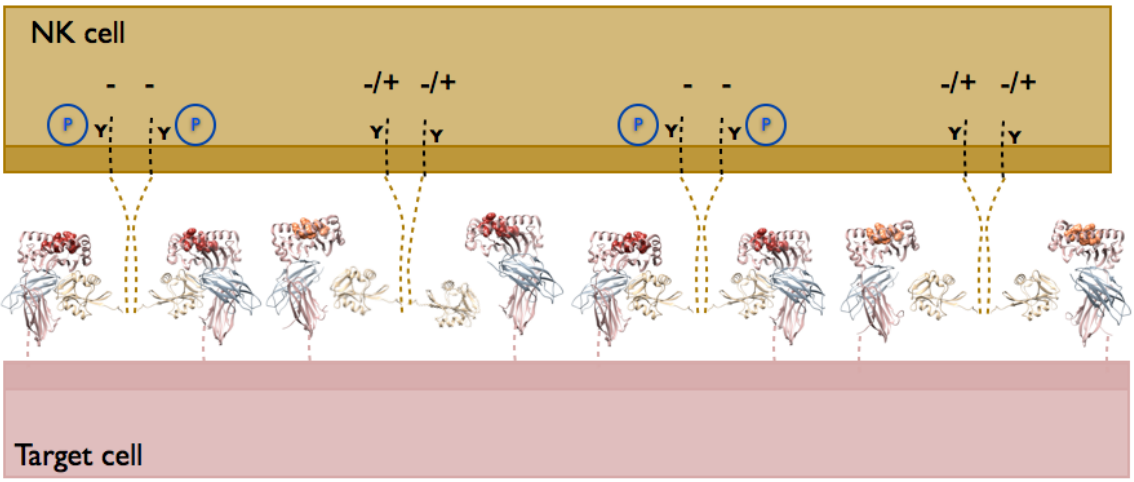

Figure 5-11. Hypothetical model of the immune synapse during the co-presentation of peptide-H-2K^b complexes that support Ly49C and H-2K^b interaction at high and intermediate levels. Inhibitory Ly49s and MHC-I can aggregate at the site of contact between effector and target cells. During co-presentation of H-2K^b-SIINFEKL and H-2K^b-ISFKFDHL, complexes that support Ly49C recognition of H-2K^b at a high and intermediate level, respectively, the uniform lattice structure between effective Ly49C and H-2K^b-SIINFEKL association does not retain uniformity due to the presence of H-2K^b-ISFKFDHL. The dimeric Ly49C can associate with 2 H-2K^b-ISFKFDHL complexes inducing intermediate signaling events; in addition, one H-2K^b-ISFKFDHL can bind to one Ly49C CTLD, causing structural changes that abrogate or reduce the binding of H-2K^b-SIINFEKL by the additional CTLD. As a result, moderate depression of inhibitory signals in NK cells occurs. The H-2K^b heavy chain is shown in pink ribbon, the β2m is in grey ribbon and the peptides are in surface representation in red and orange for SIINFEKL and "ISFKFDHL" respectively. Proximal membrane amino acids connecting the α3 domain to the "target cell surface" are displayed as pink dashed lines. The C-type lectin-like domains (CTLD) of the Ly49C dimer are shown in gold ribbon. Stalk region of the Ly49C is represented as gold dashed lines; while transmembrane and cytoplasmic domains are displayed in black dashed lines. The immunoreceptor tyrosine-based inhibitory motif (ITIM) is represented by a Tyrosine (Y) in black. Phosphorylation of ITIM is noted with a blue circled P. Pictoral representations of receptor and ligand were generated using CHIMERA UCSF software with the PDB ID coordinates 3C8K for Ly49C/H-2K^b-SIINFEKL, and 1VAC for H-2K^b-SIINFEKL utilized to represent H-2K^b-ISFKFDHL.

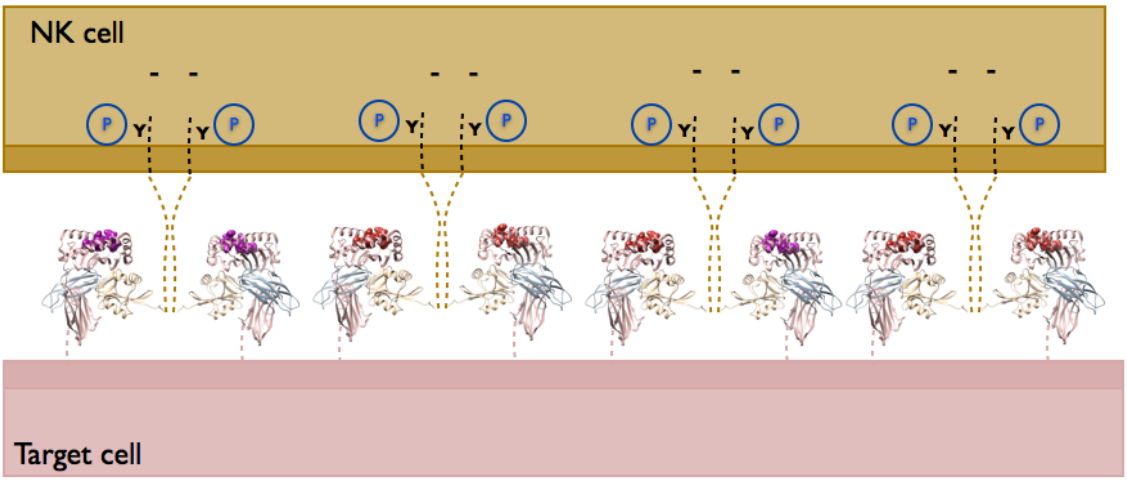

Figure 5-12. Theoretical display of the immune synapse during the co-presentation of peptide-H-2K^b complexes that fully support Ly49C association with H-2K^b. Inhibitory Ly49s and MHC-I can aggregate at the site of contact between effector and target cells. During co-presentation of H-2K^b-SIINFEKL and H-2K^b-KIITYRNL, complexes that highly support Ly49C recognition of H-2K^b, the uniform lattice structure between effective Ly49C and H-2K^b-SIINFEKL association is retained since H-2K^b-KIITYRNL lead to similar association between the receptor and the ligand. In consequence, inhibitory signaling events in NK cells are maintained. The H-2K^b heavy chain is shown in pink ribbon, the β2m is in grey ribbon and the peptides are in surface representation in red and purple for SIINFEKL and "KIITYRNL" respectively. Proximal membrane amino acids connecting the α3 domain to the "target cell surface" are displayed as pink dashed lines. The C-type lectin-like domains (CTLD) of the Ly49C dimer are shown in gold ribbon. Stalk region of the Ly49C is represented as gold dashed lines; while transmembrane and cytoplasmic domains are displayed in black dashed lines. The immunoreceptor tyrosine-based inhibitory motif (ITIM) is represented by a Tyrosine (Y) in black. Phosphorylation of ITIM is noted with a blue circled P. Pictoral representations of receptor and ligand were generated using CHIMERA UCSF software with the PDB ID coordinates 3C8K for Ly49C/H-2K^b-SIINFEKL and 1VAC for H-2K^b-SIINFEKL utilized to represent H-2K^b-KIITYRNL.

CHAPTER VI

DISCUSSION AND CONCLUSION

A. Overview of thesis

The study presented in this thesis was set out to investigate underlying principles of murine NK cell Ly49 receptor recognition of pMHC-I complexes. NK cells can be activated upon recognition of virus or tumorigenic cell stress; both states associated with changes in the self-peptide repertoire displayed by MHC-I. NK cell discrimination of peptide bound to MHC-I is therefore an important aspect to better define immunological responses during cell stress. We sought to answer specific questions with the intent of better defining self for NK cell recognition. First, we defined peptide specificity that conferred Ly49C binding to H-2K^b and second, we wanted to explore the possibility of peptide dependent antagonism of mouse NK cells. These studies shed more light on fundamental aspects of immune recognition by murine NK cells.

Rationale: H-2K^b peptide binding studies and H-2K^b peptide dependent Ly49C recognition

Murine NK cell inhibitory Ly49 receptors interact with MHC-I molecules at a site underneath the floor of the peptide binding groove involving amino acids in the α1 and α2 domains, as well as the α3 and β2m, with no direct contact with the peptide (Figure 6-1) (195). However, Ly49 recognition of MHC-I is dependent on the peptide bound and can be peptide selective. The inhibitory Ly49C receptor associates with a

cognate ligand, H-2K^b, in a peptide selective manner, a mechanism that has not been fully described. Studies by Franksson *et al.* first described the peptide selective interaction between Ly49C and H-2K^b. In addition, using SIINFEKL variants at positions 1, 2, 3, 6 and 7 of the peptide, this group demonstrated that amino acid at position 7 (P7) of the H-2K^b bound peptide had a partial influence in Ly49C recognition of H-2K^b, but not P1 or P6. However, using Ala SIINFEKL variants at P2 and P3, peptide variants did not stabilize H-2K^b molecules and their contribution to Ly49C recognition of H-2K^b was not determined (210). We had previously shown that the rat inhibitory Ly49i2 receptor associates with its cognate MHC-I ligand, RT1-A1^c, in a peptide selective manner (218). Moreover, we determined that this phenotype was dependent on the peptide anchor residue at P2. Peptide residues that make direct contact with the floor of the peptide binding groove, such as primary and auxiliary anchor residues, can more readily influence MHC-I-Ly49 interactions, since Ly49 recognition of MHC-I occurs in a cavity formed under the peptide binding groove. Therefore, we further investigated whether auxiliary anchor residues had an effect on Ly49C recognition of H-2K^b and determine whether peptide specificity is driven by residues directly acting on the peptide binding groove.

Summary: H-2K^b peptide binding studies

In order to study H-2K^b peptide dependent recognition by Ly49C, we firstly described a protocol that would allow us to test the peptide binding ability of several peptides to H-2K^b. RMA/S cells are a mouse T cell lymphoma cell line, deficient in TAP-2 thus lacking the ability to transport peptides in the cytosol to the ER for MHC-I

binding. As a result, RMA/S cell express low levels of MHC-I devoid of peptide. However, peptide-empty MHC-I molecules can be upregulated by decreasing culture temperature to 26°C and are further stabilized by exogenous MHC-I-specific peptide (230). Peptide binding and stabilization is corroborated by incubating cells at 37°C for 4 hours and detecting stable MHC-I complexes by flow cytometry. We probed peptide binding to H-2K^b on RMA/S cells utilizing peptides that have H-2K^b-specific anchor residues. The peptides in this group were identified by peptide elution studies and have canonical anchor and auxiliary anchor residues. Peptides tested for H-2K^b binding can be categorized by the identity of auxiliary anchor residues at P3 as peptides bearing non-polar aliphatic residues, KSPWFTTL, TTIHYKYM, TSINFVKI, KIITYRNL, KVITFIDL and YAMIYRNL, and peptides with aromatic auxiliary anchor residues EQYKFYSV, AQYKFIYV, RGYVYQGL, AAYAYAAL, ANYDFITV, ISFKFDHL and INFDFPKL. We determined the ability of a peptide to bind H-2K^b by comparing flow cytometry results of RMA/S loaded individually with each peptide to RMA/S incubated with SIINFEKL, a peptide that is known to bind H-2K^b and can stabilize peptide empty H-2K^b on RMA/S cells . Peptides with non-polar aliphatic auxiliary anchor residues, KSPWFTTL, TTIHYKYM and TSINFVKI, did not bind H-2K^b; while, KIITYRNL, KVITFIDL and YAMIYRNL stabilized H-2K^b at similar levels as SIINFEKL. Peptides with aromatic residues at P3, EQYKFYSV and AQYKFIYV did not bind H-2K^b; whereas, AAYAYAAL, ANYDFITV, ISFKFDHL, RGYVYQGL and INFDFPKL, similarly stabilized H-2K^b compared to SIINFEKL. Results on peptide binding to H-2K^b were confirmed by using 4 different antibodies that recognize H-2K^b molecules. In addition, we also employed recombinant mouse β2m to upregulate H-2K^b

and test whether excess of β2m would positively facilitate peptide binding. However, addition of β2m did not rescue peptide binding observed in the absence of β2m, suggesting that β2m does not enhance peptide binding on H-2K^b at the cell surface. Our experiments identified peptides that can bind and stabilize H-2K^b on RMA/S cells to be used in determining Ly49C recognition H-2K^b-peptide dependent studies.

Summary: H-2K^b peptide dependent Ly49C recognition

To determine the nature of peptide dependent recognition of H-2K^b by Ly49C, we used functional assays with RMA/S as target cells. As the effector cells, we used RNK-16, a rat leukemia cell line, stably expressing an engineered chimeric receptor Ly49W/C, RNK.49W/C. The chimeric receptor maintains inhibitory Ly49C specificity while responses are mediated through the activating Ly49W cytoplasmic and transmembrane domains. In this way, the specificity of an inhibitory Ly49 receptor is identified by a direct and positive readout. We initially tested peptides that stabilized H-2K^b on RMA/S cells in our previous study: SIINFEKL, KIITYRNL, KVITFIDL, YAMIYRNL, RGYVYQGL, AAYAYAAL, ANYDFITV, ISFKFDHL and INFDFPKL. The aforementioned peptides were loaded on RMA/S cells and were used as targets during cytotoxicity assays, with RNK.49W/C effector cells at different effector to target cell ratios. From our cytotoxicity assay results, we analyzed if there was a correlation between Ly49W/C dependent recognition and the identity of primary and auxiliary anchor residues. We found that peptides containing an Ile or Met at the P3 auxiliary anchor residue supported H-2K^b association with Ly49W/C; while, peptides bearing Tyr or Phe at P3 did not support H-2K^b interaction with Ly49W/C or did at low levels. We

further probed the role of P3 by using peptide variants of SIINFEKL, where we swapped Ile at P3 to a Val, similar to Ile, or to a Tyr, found in peptides that did not facilitate Ly49W/C recognition of H-2K^b, such as RGYVYQGL. Exchange of Ile to Tyr resulted in partial loss of Ly49W/C recognition of H-2K^b; on the other hand, Ile to Val exchange did not disturb H-2K^b-Ly49W/C interaction. In addition, we tested a gain of recognition phenotype using the AAYAYAAL peptide, that stabilized H-2K^b but did not support Ly49C recognition of H-2K^b. In order to form a peptide with Ile at P3, we resorted to exchanging P2 to Ile as well in AAYAYAAL, resulting in AIIAYAAL, that was fully supportive of Ly49W/C interaction. Our studies show that the identity of residues at P2 and P3 of the H-2K^b bound peptide are fundamental to Ly49W/C recognition. Finally, we also tested a LCMV glycoprotein derived immunodominant peptide, GP1 33-41, and GP1 33-41 CTL escape altered peptides that bind H-2K^b. The LCMV peptide, GP1 33-41 (KAVYNFATM), and CTL escape peptides that bind H-2K^b, KAVFNFATM and KAVYNYASM were tested for their ability to support H-2K^b recognition by Ly49W/C (272). We found that both wildtype and CTL escape variants poorly supported Ly49W/C recognition of H-2K^b, in line with our initial findings, peptides with a bulky aromatic residues at the auxiliary anchor position poorly support Ly49C recognition. Loss of recognition by inhibitory NK cell receptors, as observed with the LCMV immunodominant peptide and CTL escape variants, can lead to suppression of NK cell inhibition possibly resulting in NK cell activation against virally infected cells.

Rationale: MHC-I peptide dependent antagonism depresses NK cell inhibition

The role of peptide-MHC-I (pMHC-I) complexes, that do not detectably associate with cognate inhibitory receptors, can still have an active role affecting NK cell activity. Inhibitory KIRs in human, like Ly49 receptors, can recognize cognate MHC-I ligands in a peptide selective manner (50, 210, 266, 276). Still, peptides that do not contribute to detectable MHC-I association with KIR, have an active role when co-presented with a peptide agonist that supports MHC-I-KIR association, by antagonizing productive MHC-I-KIR interaction and resulting in an increase of NK cell activation (212). Peptide agonists with NK cells, are MHC-I complexes that support association with cognate inhibitory receptor and lead to NK inhibitory signals; while antagonist peptides, are MHC-I complexes that individually do not support detectable receptor-ligand interaction, but when co-presented with an agonist pMHC-I complex, lead to a decrease in inhibitory signals. Peptide dependent antagonism in murine NK cells has not been described. Defining whether this phenomenon is observed in murine NK cells is important to unlock an important aspect of NK cell activation in mouse and to find out if this feature is also shared between KIRs and Ly49 receptors.

Summary: MHC-I peptide dependent antagonism depresses NK cell inhibition

In our initial studies investigating the role of specific amino acid residues that contribute to Ly49C recognition of H-2K^b, we observed a range of Ly49C dependent recognition depending on the H-2K^b peptide bound, with peptides that fully supported ligand-receptor interaction, or did at an intermediate or poor level. We addressed the question of whether the co-presentation of a peptide that does not confer Ly49C-H-2K^b

interaction affected NK cell responses of a peptide that supports Ly49C-H-2K^b association in a similar manner as observed with KIR-MHC-I antagonism. We used functional assays with *ex vivo* mouse NK cells as effectors, and RMA/S target cells sequentially loaded with the SIINFEKL agonist peptide at low concentration, followed by a second peptide at high concentrations. We tested two peptides for antagonism, RGYVYQGL that does not support Ly49C-H-2K^b interaction and ISFKFDHL that supports Ly49C-H-2K^b interaction at an intermediate level. Our results using RMA/S cells co-presenting RGYVYQGL and SIINFEKL, showed a weak antagonist phenotype that moderately depressed NK cell of inhibition; while ISFKFDHL, showed a greater antagonistic effect by suppressing NK inhibition. These results suggested that murine NK cell peptide antagonism dependent on Ly49C and H-2K^b association requires an antagonist pMHC-I complex that can bind Ly49C at an intermediate level. Since we had tested peptides that do not confer Ly49C and H-2K^b association, or do so at an intermediate level, we also tested a peptide that fully supports receptor-ligand association, KIITYRNL, in order to have a more complete picture of the relationship between peptide dependent Ly49C-H-2K^b interaction and the antagonistic phenomenon. Results using KIITYRNL demonstrated that KIITYRNL is an agonist peptide and the co-expression of both agonist peptides, SIINFEKL and KIITYRNL, lead to inhibitory NK cell signals. Overall, our studies showed that peptides bound to H-2K^b are fundamental in the integration of NK cell signaling events that determine NK activity.

Overall Contributions Remarks and Research Significance

Collectively, our studies demonstrated underlaying aspects of NK cell recognition of pMHC-I complexes. We found that the identity of residues at P2 and P3 of the H-2K^b bound peptide are fundamental to form structural determinants for Ly49C binding. At the same time, H-2K^b bound peptides that contain optimal residues at P2 and P3 for Ly49C binding, can be categorized as agonists of Ly49C-H-2K^b interaction. On the other hand, peptides bearing P2 and P3 residues that lead to a decrease in Ly49C and H-2K^b association, can antagonize agonist H-2K^b-peptide interaction with Ly49C and NK cell inhibition to varying degrees. Therefore, the peptide repertoire expressed on MHC-I molecules may have a dramatic impact on NK function.

As innate immune lymphocytes, NK cells are among the first cells that respond to viral infections and tumorigenesis (99). During cell stress, cells can display peptides derived from virus-related or tumor-related origin on MHC-I (40, 292). Therefore, the capability of NK cells to sense peptides presented on MHC-I molecules, is of crucial importance to understand mechanisms related to NK cell recognition of target cells.

B. Discussion and Future Studies

MHC-I and peptide affinity

Mass spectrometry technology has made possible the identification of peptides bound to MHC-I molecules via peptide elution studies, allowing us to have a better understanding of peptides presented by MHC-I (278, 293, 294). Our studies utilizing peptides previously identified, allowed us to investigate their role in Ly49C recognition

when bound to H-2K^b. In addition to finding common features between peptides that supported Ly49C recognition of H-2K^b, P2 and P3 peptide residues, we also conjectured a molecular mechanism by which residues at P2 and P3 might exert the peptide selective interaction between the receptor and the ligand, using structural modeling software. We also hypothesized that perhaps residues at these positions, P2 and P3, were driving or determining peptide affinities for H-2K^b, where peptides that usually confer Ly49C-H-2K^b binding, have lower predicted affinity for H-2K^b, than those peptides that do not support receptor-ligand interaction. Using the algorithm NetMHCpan, we determined the theoretical peptide affinity for H-2K^b, expressed as an IC_{50} value (233). In general, we found that most of the peptides that did not confer Ly49C recognition of H-2K^b had higher theoretical affinity for H-2K^b, than those peptides that supported Ly49C interaction with H-2K^b. Therefore, self-peptides that supported Ly49C interaction with H-2K^b appear to have lower affinity for H-2K^b than virus derived peptides that did not confer Ly49C binding to H-2K^b. Additional experimental data is needed to corroborate viral-peptide vs self-peptide affinities for MHC-I and their effect on Ly49C interaction and regulation of NK cell mediated lysis.

Both viruses and their hosts have evolved in an arms race for survival. Many viruses abrogate MHC-I expression as a strategy to avoid T cell killing, making cells infected susceptible to NK cell cytotoxicity (46, 295-297). Other viruses do not change MHC-I expression or induce the upregulation of MHC-I at the cell surface, but still shifting the peptide repertoire for MHC-I binding (20). The battle is not over, and as viruses and humans exist, the development of new viral strategies and human evasion

mechanisms will continue. Thus, investigating viral proteins as peptide sources for MHC-I binding and their effect on NK cell recognition is important to study.

Cell changes: role of PTMs in MHC-I-bound peptides

During tumorigenesis changes in the peptide repertoire can occur due to the over-expression of tumor-related proteins or self-proteins containing post translational modifications (PTMs) that are not normally observed in healthy tissues. Although there are multiple PTMs related to disease, such as deamidation, oxidation and cysteinylation, the role of phosphopeptides and glycopeptides has been more extensively studied, allowing us to discuss these further in the context of immune receptor recognition (298-303). Peptides having carbohydrate or phosphate motifs as PTMs, may result in different peptide-MHC-I alterations that can affect MHC-I structure compared to peptides lacking these modifications (35, 304). Peptides bearing phosphate or carbohydrate motifs can be presented by MHC-I *in vitro* and *in vivo* eliciting specific $CD8^+$ T cell responses (39, 268, 301, 302, 305). In addition, phosphopeptides can be of importance to NK cell recognition. Upon addition of a phosphate moiety to the peptide bound to HLA-Cw4 at position 8, inhibitory KIR2DL1 recognition of HLA-Cw4 is abrogated, resulting in a reduction of NK cell inhibition (306). However, the effect of modified peptides bound to MHC-I has not been studied in Ly49 receptor recognition.

Studies in our laboratory demonstrated the essential role of P2 and P3 residues, that dock into the B-pocket and D-pocket of H-$2K^b$, respectively, in Ly49C recognition. Carbohydrate motifs of glycosylated peptides bound to MHC-I can be accommodated

within pockets in the peptide binding groove, or protrude from the peptide binding platform to the solvent (304, 307). In phosphopeptides, due to its hydrophilic nature, phosphate moieties are usually exposed to solvent, away from the peptide binding groove (35). Although both modalities of moiety binding can be at play, towards or away from the peptide binding platform, Ly49 binding properties can be assessed to determine functional effects. Based on our studies, we can hypothesize that PTM moieties accommodated within pockets of the peptide binding groove can have a dramatic effect on Ly49 recognition of MHC-I. The implications for studies revealing the discrimination of normally expressed peptides versus altered peptides is of great interest in immunesurveillance. If the ability of inhibitory Ly49 receptors to recognize MHC-I is lost in the presence of a glycopeptide bound to MHC-I, the result would be a depression of NK cell inhibition. More importantly, this can signify a mechanism by which NK cells detect changes in altered self and towards elimination of cancer cells. On the contrary, if inhibitory Ly49 receptors equally recognize self and altered-self peptides, bearing a carbohydrate motif resulting from cell transformation, NK cell inhibition is retained and transformed cells may not be eliminated. Therefore, further studies into Ly49 dependent NK cell recognition of MHC-I-bound peptides containing PTMs, is an interesting question to determine NK cell sensitivity.

Ly49 peptide specific recognition of MHC-I

Discrimination between self and non-self or altered-self can be of benefit to the host, where the identification of non-self or altered-self can lead to suppression of infection or tumorigenesis. NK cells can survey for normal expression of pMHC-I

complexes, making their ability to sense specific residues within the MHC-I peptide bound, an added and sophisticated element of NK recognition. Our studies focused on Ly49C, a receptor that has been identified to be peptide selective along with Ly49I, both forming part of Group I of Ly49 receptors that contain an alpha helix in the L3 loop that has contacts with MHC-I under the peptide binding groove (195). The inhibitory Ly49A, on the other hand, is not peptide specific and belongs to the group of Ly49 receptors that instead of forming an alpha helix at region L3, forms a disordered loop. Although more receptors need to be examined for their peptide specificity, it would be interesting to define what makes one Ly49 peptide specific as opposed to one that is not. For instance, we mentioned the obvious structural difference in the L3 region. As a loop in Ly49A, the flexibility of this region could allow for easier contacts with residues underneath the peptide binding groove; while an alpha helix at this site can be more restrictive/static/rigid on the amino acids it can bind on MHC-I. Studying the structural specificity of Ly49-MHC-I interactions can be of importance to understand the molecular basis of regulation controlling NK cell effector functions as well as NK cell development. In addition, and equally important, is the identification of natural peptides that are recognized as self by Ly49 molecules, when bound to MHC-I.

Peptide antagonism and NK cell activity

Recognition of pMHC-I molecules by Ly49 receptors is an important aspect for NK cell function as well as NK cell development. The role of peptide specific human NK cell responses was reinforced in recent studies by Fadda *et al.* where peptide antagonism was presented as a way to suppress NK cell inhibition. This study led more

insight into the active role that pMHC-I complexes, that are not recognized by KIRs individually, play in NK cell function (212). More importantly, NK cells can also be used as targets for the development of peptide therapies to enhance NK cell activity. Still, mouse NK cell studies can be utilized to understand principles of NK cell biology. In our studies on peptide antagonism depending on NK cell recognition of co-presented pMHC-I complexes; we found a similar phenotype that resembled antagonism. However, the mechanism of antagonism needs to be addressed. First, we need to establish events within the synapse formed by effector and target cells during antagonism. Second, intrinsic NK cell signaling events need to be investigated. Finally, since Ly49C can recognize other MHC-I molecules, it remains to be established if antagonism is also observed in other MHC-I alleles or if other Ly49 receptors also have this capability.

C. Concluding remarks

The studies presented in this thesis have provided more insight in specific details of Ly49-MHC-I interaction. We have identified bound peptide residues that are responsible for Ly49C peptide specific recognition of H-2K^b. In addition, we provided evidence for H-2K^b peptide dependent antagonism leading to partial suppression of NK cell inhibition. Collectively, these results describe the active role that MHC-I bound peptides play in NK cell functions.

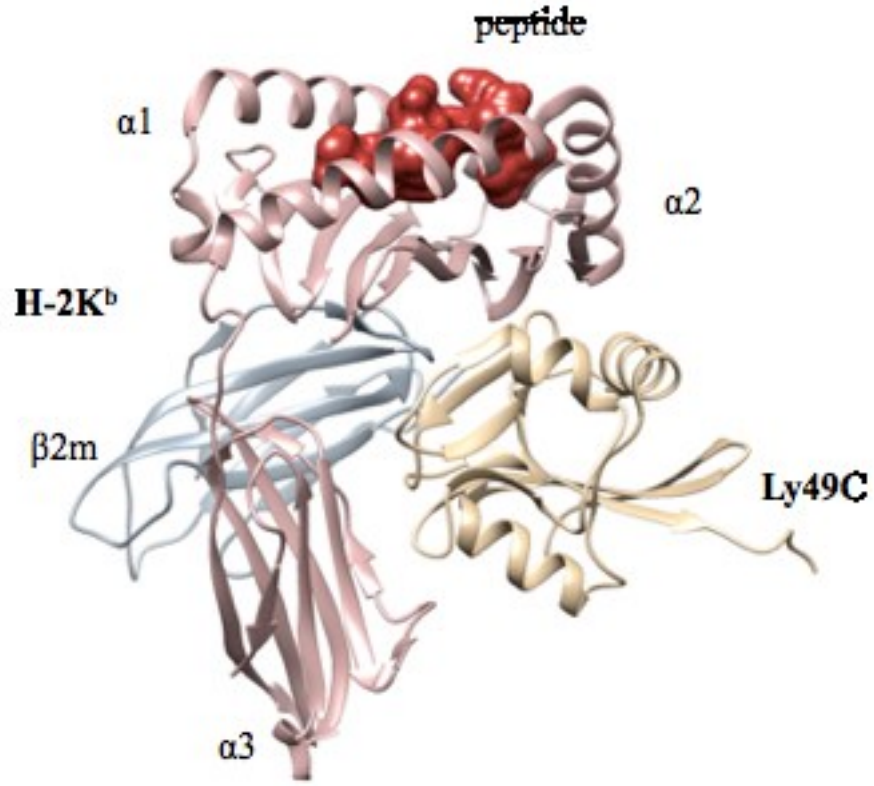

Figure 6-1. H-2K^b and Ly49C association. Interaction between Ly49C and H-2K^b includes amino acids within the α1, α2, α3 and β2m of H-2K^b, and amino acids within Ly49C regions α3/L3, L5, L6, β3 and β4. The H-2K^b heavy chain is represented in pink ribbon, β2m in blue, the SIINFEKL peptide in red surface model. The Ly49C CTLD is pictured as ribbon in gold. This figure was generated using UCSF CHIMERA with PDB coordinates 3C8K for Ly49C-H-2K^b-SIINFEKL.

References

1. Gunther, E., and T. Walter. 2000. Comparative genomic aspects of rat, mouse and human MHC class I gene regions. *Cytogenetics and Cell Genetics* 91: 107-112.
2. Yewdell, J. W., E. Reits, and J. Neefjes. 2003. Making sense of mass destruction: Quantitating MHC class I antigen presentation. *Nature Reviews Immunology* 3: 952-961.
3. Dohring, C., and M. Colonna. 1997. Major histocompatibility complex (MHC) class I recognition by natural killer cells. *Critical Reviews in Immunology* 17: 285-299.
4. Rodgers, J. R., and R. G. Cook. 2005. MHC class IB molecules bridge innate and acquired immunity. *Nature Reviews Immunology* 5: 459-471.
5. Blum, J. S., P. A. Wearsch, and P. Cresswell. 2013. Pathways of Antigen Processing. *Annual Review of Immunology, Vol 31* 31: 443-473.
6. Yu, C. Y., Z. Y. Yang, C. A. Blanchong, and W. Miller. 2000. The human and mouse MHC class III region: a parade of 21 genes at the centromeric segment. *Immunology Today* 21: 320-328.
7. Matsumura, M., D. H. Fremont, P. A. Peterson, and I. A. Wilson. 1992. Emerging principles for the recognition of peptide antigens by MHC class-I molecules. *Science* 257: 927-934.
8. Ruppert, J., J. Sidney, E. Celis, R. T. Kubo, H. M. Grey, and A. Sette. 1993. Prominent role of secondary anchor resiudes in peptide binding to HLA-A2.1 molecules. *Cell* 74: 929-937.
9. Garrett, T. P. J., M. A. Saper, P. J. Bjorkman, J. L. Strominger, and D. C. Wiley. 1989. Specificity pocktets for the side-chains of peptide antigens in HLA-AW68. *Nature* 342: 692-696.
10. Saper, M. A., P. J. Bjorkman, and D. C. Wiley. 1991. Refined structure of the human histocompatibility antigen HLA-A2 at 2.6A resolution. *Journal of Molecular Biology* 219: 277-319.
11. Sette, A., J. Sidney, B. D. Livingston, J. L. Dzuris, C. Crimi, C. M. Walker, S. Southwood, E. J. Collins, and A. L. Hughes. 2003. Class I molecules with similar peptide-binding specificities are the result of both common ancestry and convergent evolution. *Immunogenetics* 54: 830-841.
12. Reche, P. A., and E. L. Reinherz. 2004. Definition of MHC supertypes through clustering of MHC peptide binding repertoires. *Artificial Immune Systems, Proceedings* 3239: 189-196.
13. Sette, A., and J. Sidney. 1999. Nine major HLA class I supertypes account for the vast preponderance of HLA-A and -B polymorphism. *Immunogenetics* 50: 201-212.
14. Saito, Y., P. A. Peterson, and M. Matsumura. 1993. Quantitation of peptide anchor residue contributions to class-I major histocompatibility complex molecule-binding *Journal of Biological Chemistry* 268: 21309-21317.
15. Rock, K. L., I. A. York, T. Saric, and A. L. Goldberg. 2002. Protein degradation and the generation of MHC class I-presented peptides. In *Advances in Immunology, Vol 80*. 1-70.

16. Rock, K. L., C. Gramm, L. Rothstein, K. Clark, R. Stein, L. Dick, D. Hwang, and A. L. Goldberg. 1994. Inhibitors of the proteasome block the degradation of most cell-proteins and the generation of peptides presented on MHC class-I molecules. *Cell* 78: 761-771.
17. Parcej, D., and R. Tampe. 2010. ABC proteins in antigen translocation and viral inhibition. *Nature Chemical Biology* 6: 572-580.
18. van Endert, P. 2011. Post-proteasomal and proteasome-independent generation of MHC class I ligands. *Cellular and Molecular Life Sciences* 68: 1553-1567.
19. Shen, X. Z., S. Billet, C. T. Lin, D. Okwan-Duodu, X. Chen, A. E. Lukacher, and K. E. Bernstein. 2011. The carboxypeptidase ACE shapes the MHC class I peptide repertoire. *Nature Immunology* 12: 1078-U1083.
20. Blanchard, N., T. Kanaseki, H. Escobar, F. Delebecque, N. A. Nagarajan, E. Reyes-Vargas, D. K. Crockett, D. H. Raulet, J. C. Delgado, and N. Shastri. 2010. Endoplasmic Reticulum Aminopeptidase Associated with Antigen Processing Defines the Composition and Structure of MHC Class I Peptide Repertoire in Normal and Virus-Infected Cells. *Journal of Immunology* 184: 3033-3042.
21. Hearn, A., I. A. York, and K. L. Rock. 2009. The Specificity of Trimming of MHC Class I-Presented Peptides in the Endoplasmic Reticulum. *Journal of Immunology* 183: 5526-5536.
22. Cresswell, P., N. Bangia, T. Dick, and G. Diedrich. 1999. The nature of the MHC class I peptide loading complex. *Immunological Reviews* 172: 21-28.
23. Ortmann, B., J. Copeman, P. J. Lehner, B. Sadasivan, J. A. Herberg, A. G. Grandea, S. R. Riddell, R. Tampe, T. Spies, J. Trowsdale, and P. Cresswell. 1997. A critical role for tapasin in the assembly and function of multimeric MHC class I-TAP complexes. *Science* 277: 1306-1309.
24. Vigneron, N., D. R. Peaper, R. M. Leonhardt, and P. Cresswell. 2009. Functional significance of tapasin membrane association and disulfide linkage to ERp57 in MHC class I presentation. *European Journal of Immunology* 39: 2371-2376.
25. Shastri, N., S. Schwab, and T. Serwold. 2002. Producing nature's gene-chips: The generation of peptides for display by MHC class I molecules. *Annual Review of Immunology* 20: 463-493.
26. Androlewicz, M. J., K. S. Anderson, and P. Cresswell. 1993. Evidence that transporters associated with antigen-processing translocate a major histocompatibility complex class-I-binding peptide into the endoplasmic-reticulum in an ATP-dependent manner. *Proceedings of the National Academy of Sciences of the United States of America* 90: 9130-9134.
27. Ortmann, B., M. J. Androlewicz, and P. Cresswell. 1994. MHC class I/beta(2)-microglobulin complexes associate with TAP transporters before peptide binding *Nature* 368: 864-867.
28. Reits, E. A. J., J. C. Vos, M. Gromme, and J. Neefjes. 2000. The major substrates for TAP in vivo are derived from newly synthesized proteins. *Nature* 404: 774-778.
29. Schubert, U., L. C. Anton, J. Gibbs, C. C. Norbury, J. W. Yewdell, and J. R. Bennink. 2000. Rapid degradation of a large fraction of newly synthesized proteins by proteasomes. *Nature* 404: 770-774.

30. Mayrand, S. M., and W. R. Green. 1998. Non-traditionally derived CTL epitopes: exceptions that prove the rules? *Immunology Today* 19: 551-556.
31. Apcher, S., C. Daskalogianni, F. Lejeune, B. Manoury, G. Imhoos, L. Heslop, and R. Fahraeus. 2011. Major source of antigenic peptides for the MHC class I pathway is produced during the pioneer round of mRNA translation. *Proceedings of the National Academy of Sciences of the United States of America* 108: 11572-11577.
32. Boon, T., and A. Vanpel. 1989. T-cell-recognized antigenic peptides derived from the cellular genome are not protein-degradation products but can be generated directly by transcription and translation of short subgenic regions - a hypothesis *Immunogenetics* 29: 75-79.
33. Yewdell, J. W., L. C. Anton, and J. R. Bennink. 1996. Defective ribosomal products (DRiPs) - A major source of antigenic peptides for MHC class I molecules? *Journal of Immunology* 157: 1823-1826.
34. Dolan, B. P., L. Li, C. A. Veltri, C. M. Ireland, J. R. Bennink, and J. W. Yewdell. 2011. Distinct Pathways Generate Peptides from Defective Ribosomal Products for CD8(+) T Cell Immunosurveillance. *Journal of Immunology* 186: 2065-2072.
35. Mohammed, F., M. Cobbold, A. L. Zarling, M. Salim, G. A. Barrett-Wilt, J. Shabanowitz, D. F. Hunt, V. H. Engelhard, and B. E. Willcox. 2008. Phosphorylation-dependent interaction between antigenic peptides and MHC class I: a molecular basis for the presentation of transformed self. *Nature Immunology* 9: 1236-1243.
36. Lu, X. J., J. S. Gibbs, H. D. Hickman, A. David, B. P. Dolan, Y. T. Jin, D. M. Kranz, J. R. Bennink, J. W. Yewdell, and R. Varma. 2012. Endogenous viral antigen processing generates peptide-specific MHC class I cell-surface clusters. *Proceedings of the National Academy of Sciences of the United States of America* 109: 15407-15412.
37. Fortier, M. H., E. Caron, M. P. Hardy, G. Voisin, S. Lemieux, C. Perreault, and P. Thibault. 2008. The MHC class I peptide repertoire is molded by the transcriptome. *Journal of Experimental Medicine* 205: 595-610.
38. Hennessy, B. T., D. L. Smith, P. T. Ram, Y. L. Lu, and G. B. Mills. 2005. Exploiting the PI3K/AKT pathway for cancer drug discovery. *Nature Reviews Drug Discovery* 4: 988-1004.
39. Ryan, S. O., A. M. Vlad, K. Islam, J. Gariepy, and O. J. Finn. 2009. Tumor-associated MUC1 glycopeptide epitopes are not subject to self-tolerance and improve responses to MUC1 peptide epitopes in MUC1 transgenic mice. *Biological Chemistry* 390: 611-618.
40. Croft, N. P., S. A. Smith, Y. C. Wong, C. T. Tan, N. L. Dudek, I. E. A. Flesch, L. C. W. Lin, D. C. Tscharke, and A. W. Purcell. 2013. Kinetics of antigen expression and epitope presentation during virus infection. *Plos Pathogens* 9.
41. Qian, S.-B., E. Reits, J. Neefjes, J. M. Deslich, J. R. Bennink, and J. W. Yewdell. 2006. Tight linkage between translation and MHC class I peptide ligand generation implies specialized antigen processing for defective ribosomal products. *Journal of Immunology* 177: 227-233.

42. Dolan, B. P., L. Li, K. Takeda, J. R. Bennink, and J. W. Yewdell. 2010. Defective Ribosomal Products Are the Major Source of Antigenic Peptides Endogenously Generated from Influenza A Virus Neuraminidase. *Journal of Immunology* 184: 1419-1424.
43. Cardinaud, S., S. R. Starck, P. Chandra, and N. Shastri. 2010. The Synthesis of Truncated Polypeptides for Immune Surveillance and Viral Evasion. *Plos One* 5.
44. Goldwich, A., S. S. C. Hahn, S. Schreiber, S. Meier, E. Kaempgen, R. Wagner, M. B. Lutz, and U. Schubert. 2008. Targeting HIV-1 gag into the defective rihosomal product pathway enhances MHC class I antigen presentation and CD8(+) T cell activation. *Journal of Immunology* 180: 372-382.
45. Tissot, A. C., C. Ciatto, P. R. E. Mittl, M. G. Grutter, and A. Pluckthun. 2000. Viral escape at the molecular level explained by quantitative T-cell receptor/peptide/MHC interactions and the crystal structure of a peptide/MHC complex. *Journal of Molecular Biology* 302: 873-885.
46. Zhou, F. 2009. Molecular Mechanisms of Viral Immune Evasion Proteins to Inhibit MHC Class I Antigen Processing and Presentation. *International Reviews of Immunology* 28: 376-393.
47. Pircher, H., D. Moskophidis, U. Rohrer, K. Burki, H. Hengartner, and R. M. Zinkernagel. 1990. Viral escape by selection of cytotoxic T cell resistant virus variants in vivo. *Nature* 346: 629-633.
48. Biron, C. A. 1997. Activation and function of natural killer cell responses during viral infections. *Current Opinion in Immunology* 9: 24-34.
49. Peruzzi, M., N. Wagtmann, and E. O. Long. 1996. A p70 killer cell inhibitory receptor specific for several HLA-B allotypes discriminates among peptides bound to HLA-B*2705. *Journal of Experimental Medicine* 184: 1585-1590.
50. Hanke, T., H. Takizawa, C. W. McMahon, D. H. Busch, E. G. Pamer, J. D. Miller, J. D. Altman, Y. Liu, D. Cado, F. A. Lemonnier, P. J. Bjorkman, and D. H. Raulet. 1999. Direct assessment of MHC class I binding by seven Ly49 inhibitory NK cell receptors. *Immunity* 11: 67-77.
51. Ljunggren, H. G., and K. Karre. 1990. In search of the missing self - MHC molecules and NK cell recognition *Immunology Today* 11: 237-244.
52. Lian, R. H., and V. Kumar. 2002. Murine natural killer cell progenitors and their requirements for development. *Seminars in Immunology* 14: 453-460.
53. Freud, A. G., and M. A. Caligiuri. 2006. Human natural killer cell development. *Immunological Reviews* 214: 56-72.
54. Vivier, E., E. Tomasello, M. Baratin, T. Walzer, and S. Ugolini. 2008. Functions of natural killer cells. *Nature Immunology* 9: 503-510.
55. Colucci, F., M. A. Caligiuri, and J. P. Di Santo. 2003. What does it take to make a natural killer? *Nature Reviews Immunology* 3: 413-425.
56. Hayakawa, Y., and M. J. Smyth. 2006. CD27 dissects mature NK cells into two subsets with distinct responsiveness and migratory capacity. *Journal of Immunology* 176: 1517-1524.
57. Kim, S., K. Iizuka, H. S. P. Kang, A. Dokun, A. R. French, S. Greco, and W. M. Yokoyama. 2002. In vivo developmental stages in murine natural killer cell maturation. *Nature Immunology* 3: 523-528.

58. Cooper, M. A., T. A. Fehniger, and M. A. Caligiuri. 2001. The biology of human natural killer-cell subsets. *Trends in Immunology* 22: 633-640.
59. Lowin, B., M. C. Peitsch, and J. Tschopp. 1995. Perforin and granzymes: crucial effector molecules in cytolytic T lymphocyte and natural killer cell-mediated cytotoxicity. *Current topics in microbiology and immunology* 198: 1-24.
60. Smyth, M. J., K. Takeda, Y. Hayakawa, J. J. Peschon, M. R. M. van den Brink, and H. Yagita. 2003. Nature's TRAIL - On a path to cancer immunotherapy. *Immunity* 18: 1-6.
61. Chua, H. L., Y. Serov, and Z. Brahmi. 2004. Regulation of FasL expression in natural killer cells. *Human Immunology* 65: 317-327.
62. von Albertini, M., C. Ferran, C. Brostjan, F. H. Bach, and D. J. Goodman. 1998. Membrane-associated lymphotoxin on natural killer cells activates endothelial cells via an NF-kappa B-dependent pathway. *Transplantation* 66: 1211-1219.
63. Lieberman, J. 2003. The ABCs of granule-mediated cytotoxicity: New weapons in the arsenal. *Nature Reviews Immunology* 3: 361-370.
64. Cappello, P., F. Novelli, G. Forni, and M. Giovarelli. 2002. Death receptor ligands in tumors. *Journal of Immunotherapy* 25: 1-15.
65. Orange, J. S., B. P. Wang, C. Terhorst, and C. A. Biron. 1995. Requirement for natural-killer cell-produced interferon-gamma in defense against murine cytomegalovirus-infection and enhancement of this defense pathway by interleukin-12 administration. *Journal of Experimental Medicine* 182: 1045-1056.
66. Walzer, T., M. Dalod, S. H. Robbins, L. Zitvogel, and E. Vivier. 2005. Natural-killer cells and dendritic cells: "l' union fait la force". *Blood* 106: 2252-2258.
67. Nedvetzki, S., S. Sowinski, R. A. Eagle, J. Harris, F. Vely, D. Pende, J. Trowsdale, E. Vivier, S. Gordon, and D. M. Davis. 2007. Reciprocal regulation of human natural killer cells and macrophages associated with distinct immune synapses. *Blood* 109: 3776-3785.
68. Moretta, L., G. Ferlazzo, C. Bottino, M. Vitale, D. Pende, M. C. Mingari, and A. Moretta. 2006. Effector and regulatory events during natural killer-dendritic cell interactions. *Immunological Reviews* 214: 219-228.
69. Degli-Esposti, M. A., and M. J. Smyth. 2005. Close encounters of different kinds: Dendritic cells and NK cells take centre stage. *Nature Reviews Immunology* 5: 112-124.
70. Martin-Fontecha, A., L. L. Thomsen, S. Brett, C. Gerard, M. Lipp, A. Lanzavecchia, and F. Sallusto. 2004. Induced recruitment of NK cells to lymph nodes provides IFN-gamma for T(H)1 priming. *Nature Immunology* 5: 1260-1265.
71. Long, E. O. 2007. Ready for prime time: NK cell priming by dendritic cells. *Immunity* 26: 385-387.
72. Biron, C. A., K. B. Nguyen, G. C. Pien, L. P. Cousens, and T. P. Salazar-Mather. 1999. Natural killer cells in antiviral defense: Function and regulation by innate cytokines. *Annual Review of Immunology* 17: 189-220.
73. French, A. R., and W. M. Yokoyama. 2003. Natural killer cells and viral infections. *Current Opinion in Immunology* 15: 45-51.

74. Colonna, M., S. Jonjic, and C. Watzl. 2011. Natural killer cells: fighting viruses and much more. *Nature immunology* 12: 107-110.
75. Smith, H. R. C., J. W. Heusel, I. K. Mehta, S. Kim, B. G. Dorner, O. V. Naidenko, K. Iizuka, H. Furukawa, D. L. Beckman, J. T. Pingel, A. A. Scalzo, D. H. Fremont, and W. M. Yokoyama. 2002. Recognition of a virus-encoded ligand by a natural killer cell activation receptor. *Proceedings of the National Academy of Sciences of the United States of America* 99: 8826-8831.
76. Guma, M., M. Budt, A. Saez, T. Brckalo, H. Hengel, A. Angulo, and M. Lopez-Botet. 2006. Expansion of CD94/NKG2C(+) NK cells in response to human cytomegalovirus-infected fibroblasts. *Blood* 107: 3624-3631.
77. Siren, J., T. Sareneva, J. Pirhonen, M. Strengell, V. Veckman, L. Julkunen, and S. Matikainen. 2004. Cytokine and contact-dependent activation of natural killer cells by influenza A or Sendai virus-infected macrophages. *Journal of General Virology* 85: 2357-2364.
78. Alter, G., J. M. Malenfant, R. M. Delabre, N. C. Burgett, X. G. Yu, M. Lichterfeld, J. Zaunders, and M. Altfeld. 2004. Increased natural killer cell activity in viremic HIV-1 infection. *Journal of Immunology* 173: 5305-5311.
79. Warfield, K. L., J. G. Perkins, D. L. Swenson, E. M. Deal, C. M. Bosio, M. J. Aman, W. M. Yokoyama, H. A. Young, and S. Bavari. 2004. Role of natural killer cells in innate protection against lethal Ebola virus infection. *Journal of Experimental Medicine* 200: 169-179.
80. Ahlenstiel, G., R. H. Titerence, C. Koh, B. Edlich, J. J. Feld, Y. Rotman, M. G. Ghany, J. H. Hoofnagle, T. J. Liang, T. Heller, and B. Rehermann. 2010. Natural Killer Cells Are Polarized Toward Cytotoxicity in Chronic Hepatitis C in an Interferon-Alfa-Dependent Manner. *Gastroenterology* 138: 325-335.
81. Hoglund, P., J. Sundback, M. Y. OlssonAlheim, M. Johansson, M. Salcedo, C. Ohlen, H. G. Ljunggren, C. L. Sentman, and K. Karre. 1997. Host MHC class I gene control of NK-cell specificity in the mouse. *Immunological Reviews* 155: 11-28.
82. Waldhauer, I., and A. Steinle. 2008. NK cells and cancer immunosurveillance. *Oncogene* 27: 5932-5943.
83. Van Den Broek, M. F., D. Kagi, R. M. Zinkernagel, and H. Hengartner. 1995. Perforin dependence of natural killer cell-mediated tumor control in vivo. *European Journal of Immunology* 25: 3514-3516.
84. Smyth, M. J., K. Y. T. Thia, E. Cretney, J. M. Kelly, M. B. Snook, C. A. Forbes, and A. A. Scalzo. 1999. Perforin is a major contributor to NK cell control of tumor metastasis. *Journal of Immunology* 162: 6658-6662.
85. Smyth, M. J., J. M. Kelly, A. G. Baxter, H. Korner, and J. D. Sedgwick. 1998. An essential role for tumor necrosis factor in natural killer cell-mediated tumor rejection in the peritoneum. *Journal of Experimental Medicine* 188: 1611-1619.
86. Smyth, M. J., Y. Hayakawa, K. Takeda, and H. Yagita. 2002. New aspects of natural-killer-cell surveillance and therapy of cancer. *Nature Reviews Cancer* 2: 850-861.

87. Riccardi, C., A. Santoni, T. Barlozzari, P. Puccetti, and R. B. Herberman. 1980. In vivo natural reactivity of mice against tumor cells *International Journal of Cancer* 25: 475-486.
88. Gorelik, E., B. Rosen, D. Copeland, B. Weatherly, and R. B. Herberman. 1984. Evaluation of role of natural killer cells in radiation induced leukemogenesis in mice. *Journal of the National Cancer Institute* 72: 1397-1403.
89. Cheng, M., Y. Chen, W. Xiao, R. Sun, and Z. Tian. 2013. NK cell-based immunotherapy for malignant diseases. *Cellular & Molecular Immunology* 10: 230-252.
90. Kwak-Kim, J., S. H. Bao, S. K. Lee, J. W. Kim, and A. Gilman-Sachs. 2014. Immunological Modes of Pregnancy Loss: Inflammation, Immune Effectors, and Stress. *American Journal of Reproductive Immunology* 72: 129-140.
91. Gur, C., A. Porgador, M. Elboim, R. Gazit, S. Mizrahi, N. Stern-Ginossar, H. Achdout, H. Ghadially, Y. Dor, T. Nir, V. Doviner, O. Hershkovitz, M. Mendelson, Y. Naparstek, and O. Mandelboim. 2010. The activating receptor NKp46 is essential for the development of type 1 diabetes. *Nature Immunology* 11: 121-U137.
92. Kastrukoff, L. F., N. G. Morgan, D. Zecchini, R. White, A. J. Petkau, J. I. Satoh, and D. W. Paty. 1998. A role for natural killer cells in the immunopathogenesis of multiple sclerosis. *Journal of Neuroimmunology* 86: 123-133.
93. Henriques, A., L. Teixeira, L. Ines, T. Carvalheiro, A. Goncalves, A. Martinho, M. L. Pais, J. A. Pereira da Silva, and A. Paiva. 2013. NK cells dysfunction in systemic lupus erythematosus: relation to disease activity. *Clinical Rheumatology* 32: 805-813.
94. Dalbeth, N., and M. F. C. Callan. 2002. A subset of natural killer cells is greatly expanded within inflamed joints. *Arthritis and Rheumatism* 46: 1763-1772.
95. Yokoyama, W. M. 1995. Hybrid resistance and the Ly-49 family of natural killer cell receptors. *Journal of Experimental Medicine* 182: 273-277.
96. Ruggeri, L., M. Capanni, E. Urbani, K. Perruccio, W. D. Shlomchik, A. Tosti, S. Posati, D. Rogaia, F. Frassoni, F. Aversa, M. F. Martelli, and A. Velardi. 2002. Effectiveness of donor natural killer cell alloreactivity in mismatched hematopoietic transplants. *Science* 295: 2097-2100.
97. Ruggeri, L., A. Mancusi, M. Capanni, M. F. Martelli, and A. Velardi. 2005. Exploitation of alloreactive NK cells in adoptive immunotherapy of cancer. *Current Opinion in Immunology* 17: 211-217.
98. Kroemer, A., K. Edtinger, and X. C. Li. 2008. The innate natural killer cells in transplant rejection and tolerance induction. *Current Opinion in Organ Transplantation* 13: 339-343.
99. Lanier, L. L. 2005. NK cell recognition. *Annual Review of Immunology* 23: 225-274.
100. Colucci, F., J. P. Di Santo, and P. J. Leibson. 2002. Natural killer cell activation in mice and men: different triggers for similar weapons? *Nature Immunology* 3: 807-813.

101. Mace, E. M., S. J. Monkley, D. R. Critchley, and F. Takei. 2009. A Dual Role for Talin in NK Cell Cytotoxicity: Activation of LFA-1-Mediated Cell Adhesion and Polarization of NK Cells. *Journal of Immunology* 182: 948-956.
102. Davis, D. M., I. Chiu, M. Fassett, G. B. Cohen, O. Mandelboim, and J. L. Strominger. 1999. The human natural killer cell immune synapse. *Proceedings of the National Academy of Sciences of the United States of America* 96: 15062-15067.
103. Lou, Z. K., D. Jevremovic, D. D. Billadeau, and P. J. Leibson. 2000. A balance between positive and negative signals in cytotoxic lymphocytes regulates the polarization of lipid rafts during the development of cell-mediated killing. *Journal of Experimental Medicine* 191: 347-354.
104. Vyas, Y. M., K. M. Mehta, M. Morgan, H. Maniar, L. Butros, S. Jung, J. K. Burkhardt, and B. Dupont. 2001. Spatial organization of signal transduction molecules in the NK cell immune synapses during MHC class I-regulated noncytolytic and cytolytic interactions. *Journal of Immunology* 167: 4358-4367.
105. Vyas, Y. M., H. Maniar, and B. Dupont. 2002. Cutting edge: Differential segregation of the Src homology 2-containing protein tyrosine phosphatase-1 within the early NK cell immune synapse distinguishes noncytolytic from cytolytic interactions. *Journal of Immunology* 168: 3150-3154.
106. Orange, J. S., K. E. Harris, M. M. Andzelm, M. M. Valter, R. S. Geha, and J. L. Strominger. 2003. The mature activating natural killer cell immunologic synapse is formed in distinct stages. *Proceedings of the National Academy of Sciences of the United States of America* 100: 14151-14156.
107. Valiante, N. M., J. H. Phillips, L. L. Lanier, and P. Parham. 1996. Killer cell inhibitory receptor recognition of human leukocyte antigen (HLA) class I blocks formation of a pp36/PLC-gamma signaling complex in human natural killer (NK) cells. *Journal of Experimental Medicine* 184: 2243-2250.
108. Binstadt, B. A., K. M. Brumbaugh, C. J. Dick, A. M. Scharenberg, B. L. Williams, M. Colonna, L. L. Lanier, J. P. Kinet, R. T. Abraham, and P. J. Leibson. 1996. Sequential involvement of Lck and SHP-1 with MHC-recognizing receptors on NK cells inhibits FcR-initiated tyrosine kinase activation. *Immunity* 5: 629-638.
109. Binstadt, B. A., D. D. Billadeau, D. Jevremovic, B. L. Williams, N. Fang, T. L. Yi, G. A. Koretzky, R. T. Abraham, and P. J. Leibson. 1998. SLP-76 is a direct substrate of SHP-1 recruited to killer cell inhibitory receptors. *Journal of Biological Chemistry* 273: 27518-27523.
110. Palmieri, G., V. Tullio, A. Zingoni, M. Piccoli, L. Frati, M. Lopez-Botet, and A. Santoni. 1999. CD94/NKG2-A inhibitory complex blocks CD16-triggered Syk and extracellular regulated kinase activation, leading to cytotoxic function of human NK cells. *Journal of Immunology* 162: 7181-7188.
111. Stebbins, C. C., C. Watzl, D. D. Billadeau, P. J. Leibson, D. N. Burshtyn, and E. O. Long. 2003. Vav1 dephosphorylation by the tyrosine phosphatase SHP-1 as a mechanism for inhibition of cellular cytotoxicity. *Molecular and Cellular Biology* 23: 6291-6299.

112. Lanier, L. L., B. C. Corliss, J. Wu, C. Leong, and J. H. Phillips. 1998. Immunoreceptor DAP12 bearing a tyrosine-based activation motif is involved in activating NK cells. *Nature* 391: 703-707.
113. Vivier, E., J. A. Nunes, and F. Vely. 2004. Natural killer cell signaling pathways. *Science* 306: 1517-1519.
114. Vitale, M., C. Bottino, S. Sivori, L. Sanseverino, R. Castriconi, E. Marcenaro, R. Augugliaro, L. Moretta, and A. Moretta. 1998. NKp44, a novel triggering surface molecule specifically expressed by activated natural killer cells, is involved in non-major histocompatibility complex-restricted tumor cell lysis. *Journal of Experimental Medicine* 187: 2065-2072.
115. Cantoni, C., C. Bottino, M. Vitale, A. Pessino, R. Augugliaro, A. Malaspina, S. Parolini, L. Moretta, A. Moretta, and R. Biassoni. 1999. NKp44, a triggering receptor involved in tumor cell lysis by activated human natural killer cells, is a novel member of the immunoglobulin superfamily. *Journal of Experimental Medicine* 189: 787-795.
116. Pende, D., S. Parolini, A. Pessino, S. Sivori, R. Augugliaro, L. Morelli, E. Marcenaro, L. Accame, A. Malaspina, R. Biassoni, C. Bottino, L. Moretta, and A. Moretta. 1999. Identification and molecular characterization of NKp30, a novel triggering receptor involved in natural cytotoxicity mediated by human natural killer cells. *Journal of Experimental Medicine* 190: 1505-1516.
117. Pessino, A., S. Sivori, C. Bottino, A. Malaspina, L. Morelli, L. Moretta, R. Biassoni, and A. Moretta. 1998. Molecular cloning of NKp46: A novel member of the immunoglobulin superfamily involved in triggering of natural cytotoxicity. *Journal of Experimental Medicine* 188: 953-960.
118. Biassoni, R., A. Pessino, C. Bottino, D. Pende, L. Moretta, and A. Moretta. 1999. The murine homologue of the human NKp46, a triggering receptor involved in the induction of natural cytotoxicity. *European Journal of Immunology* 29: 1014-1020.
119. Sivori, S., D. Pende, C. Bottino, E. Marcenaro, A. Pessino, R. Biassoni, L. Moretta, and A. Moretta. 1999. NKp46 is the major triggering receptor involved in the natural cytotoxicity of fresh or cultured human NK cells. Correlation between surface density of NKp46 and natural cytotoxicity against autologous, allogeneic or xenogeneic target cells. *European Journal of Immunology* 29: 1656-1666.
120. Spaggiari, G. M., R. Carosio, D. Pende, S. Marcenaro, P. Rivera, M. R. Zocchi, L. Moretta, and A. Poggi. 2001. NK cell-mediated lysis of autologous antigen-presenting cells is triggered by the engagement of the phosphatidylinositol 3-kinase upon ligation of the natural cytotoxicity receptors NKp30 and NKp46. *European Journal of Immunology* 31: 1656-1665.
121. Mandelboim, O., N. Lieberman, M. Lev, L. Paul, T. I. Arnon, Y. Bushkin, D. M. Davis, J. L. Strominger, J. W. Yewdell, and A. Porgador. 2001. Recognition of haemagglutinins on virus-infected cells by NKp46 activates lysis by human NK cells. *Nature* 409: 1055-1060.
122. Gazit, R., R. Gruda, M. Elboim, T. I. Arnon, G. Katz, H. Achdout, J. Hanna, U. Qimron, G. Landau, E. Greenbaum, Z. Zakay-Rones, A. Porgador, and O.

Mandelboim. 2006. Lethal influenza infection in the absence of the natural killer cell receptor gene Ncr1. *Nature Immunology* 7: 517-523.

123. Arnon, T. I., H. Achdout, N. Lieberman, R. Gazit, T. Gonen-Gross, G. Katz, A. Bar-Ilan, N. Bloushtain, M. Lev, A. Joseph, E. Kedar, A. Porgador, and O. Mandelboim. 2004. The mechanisms controlling the recognition of tumor- and virus-infected cells by NKp46. *Blood* 103: 664-672.
124. Meyaard, L., G. J. Adema, C. W. Chang, E. Woollatt, G. R. Sutherland, L. L. Lanier, and J. H. Phillips. 1997. LAIR-1, a novel inhibitory receptor expressed on human mononuclear leukocytes. *Immunity* 7: 283-290.
125. Lebbink, R. J., T. de Ruiter, A. Verbrugge, W. S. Bril, and L. Meyaard. 2004. The mouse homologue of the leukocyte-associated Ig-like receptor-1 is an inhibitory receptor that recruits Src homology region 2-containing protein tyrosine phosphatase (SHP)-2, but not SHP-1. *Journal of Immunology* 172: 5535-5543.
126. Lebbink, R. J., T. de Ruiter, J. Adelmeijer, A. B. Brenkman, J. M. van Helvoort, M. Koch, R. W. Farndale, T. Lisman, A. Sonnenberg, P. J. Lenting, and L. Meyaard. 2006. Collagens are functional, high affinity ligands for the inhibitory immune receptor LAIR-1. *Journal of Experimental Medicine* 203: 1419-1425.
127. Lebbink, R. J., T. de Ruiter, G. J. A. Kaptijn, D. G. Bihan, C. A. Jansen, P. J. Lenting, and L. Meyaard. 2007. Mouse leukocyte-associated Ig-like receptor-1 (mLAIR-1) functions as an inhibitory collagen-binding receptor on immune cells. *International Immunology* 19: 1011-1019.
128. Martin, A. M., J. K. Kulski, C. Witt, P. Pontarotti, and F. T. Christiansen. 2002. Leukocyte Ig-like receptor complex (LRC) in mice and men. *Trends in Immunology* 23: 81-88.
129. Chapman, T. L., A. P. Heikema, and P. J. Bjorkman. 1999. The inhibitory receptor LIR-1 uses a common binding interaction to recognize class I MHC molecules and the viral homolog UL18. *Immunity* 11: 603-613.
130. Willcox, B. E., L. M. Thomas, and P. J. Bjorkman. 2003. Crystal structure of HLA-A2 bound to LIR-1, a host and viral major histocompatibility complex receptor. *Nature Immunology* 4: 913-919.
131. Cosman, D., N. Fanger, L. Borges, M. Kubin, W. Chin, L. Peterson, and M. L. Hsu. 1997. A novel immunoglobulin superfamily receptor for cellular and viral MHC class I molecules. *Immunity* 7: 273-282.
132. Kubagawa, H., C. C. Chen, L. H. Ho, T. Shimada, L. Gartland, C. Mashburn, T. Uehara, J. V. Ravetch, and M. D. Cooper. 1999. Biochemical nature and cellular distribution of the paired immunoglobulin-like receptors, PIR-A and PIR-B. *Journal of Experimental Medicine* 189: 309-317.
133. Burshtyn, D. N., A. M. Scharenberg, N. Wagtmann, S. Rajagopalan, K. Berrada, T. L. Yi, J. P. Kinet, and E. O. Long. 1996. Recruitment of tyrosine phosphatase HCP by the killer cell inhibitory receptor. *Immunity* 4: 77-85.
134. Winter, C. C., J. E. Gumperz, P. Parham, E. O. Long, and N. Wagtmann. 1998. Direct binding and functional transfer of NK cell inhibitory receptors reveal novel patterns of HLA-C allotype recognition. *Journal of Immunology* 161: 571-577.

135. Khakoo, S. I., R. Rajalingam, B. P. Shum, K. Weidenbach, L. Flodin, D. G. Muir, F. Canavez, S. L. Cooper, N. M. Valiante, L. L. Lanier, and P. Parham. 2000. Rapid evolution of NK cell receptor systems demonstrated by comparison of chimpanzees and humans. *Immunity* 12: 687-698.
136. Parham, P. 2005. MHC class I molecules and KIRs in human history, health and survival. *Nature Reviews Immunology* 5: 201-214.
137. Wilson, M. J., M. Torkar, A. Haude, S. Milne, T. Jones, D. Sheer, S. Beck, and J. Trowsdale. 2000. Plasticity in the organization and sequences of human KIR/ILT gene families. *Proceedings of the National Academy of Sciences of the United States of America* 97: 4778-4783.
138. Uhrberg, M., N. M. Valiante, B. P. Shum, H. G. Shilling, K. Lienert-Weidenbach, B. Corliss, D. Tyan, L. L. Lanier, and P. Parham. 1997. Human diversity in killer cell inhibitory receptor genes. *Immunity* 7: 753-763.
139. Raulet, D. H. 2003. Roles of the NKG2D immunoreceptor and its ligands. *Nature Reviews Immunology* 3: 781-790.
140. Bauer, S., V. Groh, J. Wu, A. Steinle, J. H. Phillips, L. L. Lanier, and T. Spies. 1999. Activation of NK cells and T cells by NKG2D, a receptor for stress-inducible MICA. *Science* 285: 727-729.
141. Cosman, D., J. Mullberg, C. L. Sutherland, W. Chin, R. Armitage, W. Fanslow, M. Kubin, and N. J. Chalupny. 2001. ULBPs, novel MHC class I-related molecules bind to CMV glycoprotein UL16 and stimulate NK cytotoxicity through the NKG2D receptor. *Immunity* 14: 123-133.
142. Diefenbach, A., E. Tomasello, M. Lucas, A. M. Jamieson, J. K. Hsia, E. Vivier, and D. H. Raulet. 2002. Selective associations with signaling proteins determine stimulatory versus costimulatory activity of NKG2D. *Nature Immunology* 3: 1142-1149.
143. Carayannopoulos, L. N., O. V. Naidenko, D. H. Fremont, and W. M. Yokoyama. 2002. Cutting edge: Murine UL16-binding protein-like transcript 1: A newly described transcript encoding a high-affinity ligand for marine NKG2D. *Journal of Immunology* 169: 4079-4083.
144. Toyama-Sorimachi, N., Y. Taguchi, H. Yagita, F. Kitamura, A. Kawasaki, S. Koyasu, and H. Karasuyama. 2001. Mouse CD94 participates in Qa-1-mediated self recognition by NK cells and delivers inhibitory signals independent of Ly-49. *Journal of Immunology* 166: 3771-3779.
145. Lazetic, S., C. Chang, J. P. Houchins, L. L. Lanier, and J. H. Phillips. 1996. Human natural killer cell receptors involved in MHC class I recognition are disulfide-linked heterodimers of CD94 and NKG2 subunits. *Journal of Immunology* 157: 4741-4745.
146. Vance, R. E., J. R. Kraft, J. D. Altman, P. E. Jensen, and D. H. Raulet. 1998. Mouse CD94/NKG2A is a natural killer cell receptor for the nonclassical major histocompatibility complex (MHC) class I molecule Qa-1(b). *Journal of Experimental Medicine* 188: 1841-1848.
147. Aramburu, J., M. A. Balboa, A. Ramirez, A. Silva, A. Acevedo, F. Sanchezmadrid, M. O. Delandazuri, and M. Lopezbotet. 1990. A novel functional cell-surface dimer (KP43) expressed by natural killer cells and T cell

receptor gamma delta T lymphocytes.1. Inhibition of the iL-2 dependent proliferation by anti-KP43 monoclonal antibody. *Journal of Immunology* 144: 3238-3247.

148. Braud, V. M., D. S. J. Allan, C. A. O'Callaghan, K. Soderstrom, A. D'Andrea, G. S. Ogg, S. Lazetic, N. T. Young, J. I. Bell, J. H. Phillips, L. L. Lanier, and A. J. McMichael. 1998. HLA-E binds to natural killer cell receptors CD94/NKG2A, B and C. *Nature* 391: 795-799.
149. Lee, N., D. R. Goodlett, A. Ishitani, H. Marquardt, and D. E. Geraghty. 1998. HLA-E surface expression depends on binding of TAP-dependent peptides derived from certain HLA class I signal sequences. *Journal of Immunology* 160: 4951-4960.
150. DeCloux, A., A. S. Woods, R. J. Cotter, M. J. Soloski, and J. Forman. 1997. Dominance of a single peptide bound to the class I-B molecule, Qa-1(b). *Journal of Immunology* 158: 2183-2191.
151. Kim, D. K., J. Kabat, F. Borrego, T. B. Sanni, C. H. You, and J. E. Coligan. 2004. Human NKG2F is expressed and can associate with DAP12. *Molecular Immunology* 41: 53-62.
152. Voigt, S., A. Mesci, J. Ettinger, J. H. Fine, P. Chen, W. Chou, and J. R. Carlyle. 2007. Cytomegalovirus evasion of innate immunity by subversion of the NKR-P1 B : Clr-b missing-self axis. *Immunity* 26: 617-627.
153. Poggi, A., P. Costa, E. Tomasello, and L. Moretta. 1998. IL-12-induced up-regulation of NKRP1A expression in human NK cells and consequent NIRP1A-mediated down-regulation of NK cell activation. *European Journal of Immunology* 28: 1611-1616.
154. Azzoni, L., O. Zatsepina, E. Abebe, I. M. Bennett, P. Kanakaraj, and B. Perussia. 1998. Differential transcriptional regulation of CD161 and a novel gene, 197/15a, by IL-2, IL-15, and IL-12 in NK and T cells. *Journal of Immunology* 161: 3493-3500.
155. Aldemir, H., V. Prod'homme, M. J. Dumaurier, C. Retiere, G. Poupon, J. Cazareth, F. Bih, and V. M. Braud. 2005. Cutting edge: Lectin-like transcript 1 is a ligand for the CD161 receptor. *Journal of Immunology* 175: 7791-7795.
156. Rosen, D. B., Y. Bettadapura, M. Alsharifi, P. A. Mathew, H. S. Warren, and L. L. Lanier. 2005. Cutting edge: Lectin-like transcript-1 is a ligand for the inhibitory human NKR-P1A receptor. *Journal of Immunology* 175: 7796-7799.
157. Lanier, L. L., C. W. Chang, and J. H. Phillips. 1994. Human NKR-P1A - a disulfide-linked homodimer of the C-type lectin superfamily expressed by a subset of NK and T lymphocytes. *Journal of Immunology* 153: 2417-2428.
158. Iizuka, K., O. V. Naidenko, B. F. M. Plougastel, D. H. Fremont, and W. M. Yokoyama. 2003. Genetically linked C-type lectin-related ligands for the NKRP1 family of natural killer cell receptors. *Nature Immunology* 4: 801-807.
159. Carlyle, J. R., A. M. Jamieson, S. Gasser, C. S. Clingan, H. Arase, and D. H. Raulet. 2004. Missing self-recognition of Ocil/Cir-b by inhibitory NKR-P1 natural killer cell receptors. *Proceedings of the National Academy of Sciences of the United States of America* 101: 3527-3532.

160. Smith, K. M., J. Wu, A. B. H. Bakker, J. H. Phillips, and L. L. Lanier. 1998. Cutting edge: Ly-49D and Ly-49H associate with mouse DAP12 and form activating receptors. *Journal of Immunology* 161: 7-10.
161. Westgaard, I. H., S. F. Berg, S. Orstavik, S. Fossum, and E. Dissen. 1998. Identification of a human member of the Ly-49 multigene family. *European Journal of Immunology* 28: 1839-1846.
162. Zohar, O., Y. Reiter, J. R. Bennink, A. Lev, S. Cavallaro, S. Paratore, C. G. Pick, G. Brooker, and J. W. Yewdell. 2008. MHC class I-Ly49 interaction regulates neuronal function. *Journal of Immunology* 180: 6447-6451.
163. Stenstrom, M., M. Skold, A. Ericcson, L. Beaudoin, S. Sidobre, M. Kronenberg, A. Lehuen, and S. Cardell. 2004. Surface receptors identify mouse NK1.1(+) T cell subsets distinguished by function and T cell receptor type. *European Journal of Immunology* 34: 56-65.
164. Coles, M. C., C. W. McMahon, H. Takizawa, and D. H. Raulet. 2000. Memory CD8 T lymphocytes express inhibitory MHC-specific Ly49 receptors. *European Journal of Immunology* 30: 236-244.
165. Gays, F., J. G. Aust, D. M. Reid, J. Falconer, N. Toyama-Sorimachi, P. R. Taylor, and C. G. Brooks. 2006. Ly49B is expressed on multiple subpopulations of myeloid cells. *Journal of Immunology* 177: 5840-5851.
166. Berry, R., N. Ng, P. M. Saunders, J. P. Vivian, J. Lin, F. A. Deuss, A. J. Corbett, C. A. Forbes, J. M. Widjaja, L. C. Sullivan, A. D. McAlister, M. A. Perugini, M. J. Call, A. A. Scalzo, M. A. Degli-Esposti, J. D. Coudert, T. Beddoe, A. G. Brooks, and J. Rossjohn. 2013. Targeting of a natural killer cell receptor family by a viral immunoevasin. *Nature Immunology* 14: 699-+.
167. Kielczewska, A., H.-S. Kim, L. L. Lanier, N. Dimasi, and S. M. Vidal. 2007. Critical residues at the ly49 natural killer receptor's homodimer interface determine functional recognition of m157, a mouse cytomegalovirus MHC class I-Like protein. *Journal of Immunology* 178: 369-377.
168. Arase, H., E. S. Mocarski, A. E. Campbell, A. B. Hill, and L. L. Lanier. 2002. Direct recognition of cytomegalovirus by activating and inhibitory NK cell receptors. *Science* 296: 1323-1326.
169. Wilhelm, B. T., L. Gagnier, and D. L. Mager. 2002. Sequence analysis of the Ly49 cluster in C57BL/6 mice: A rapidly evolving multigene family in the immune system. *Genomics* 80: 646-661.
170. Makrigiannis, A. P., A. T. Pau, P. L. Schwartzberg, D. W. McVicar, T. W. Beck, and S. K. Anderson. 2002. A BAC contig map of the Ly49 gene cluster in 129 mice reveals extensive differences in gene content relative to C57BL/6 mice. *Genomics* 79: 437-444.
171. Proteau, M. F., E. Rousselle, and A. P. Makrigiannis. 2004. Mapping of the BALB/c Ly49 cluster defines a minimal natural killer cell receptor gene repertoire. *Genomics* 84: 669-677.
172. Belanger, S., L. H. Tai, S. K. Anderson, and A. P. Makrigiannis. 2008. Ly49 cluster sequence analysis in a mouse model of diabetes: an expanded repertoire of activating receptors in the NOD genome. *Genes and Immunity* 9: 509-521.

173. Held, W., and B. Kunz. 1998. An allele-specific, stochastic gene expression process controls the expression of multiple Ly49 family genes and generates a diverse, MHC-specific NK cell receptor repertoire. *European Journal of Immunology* 28: 2407-2416.
174. Smith, H. R. C., H. H. Chuang, L. L. Wang, M. Salcedo, J. W. Heusel, and W. M. Yokoyama. 2000. Nonstochastic coexpression of activation receptors on murine natural killer cells. *Journal of Experimental Medicine* 191: 1341-1354.
175. Fernandez, N. C., E. Treiner, R. E. Vance, A. M. Jamieson, S. Lemieux, and D. H. Raulet. 2005. A subset of natural killer cells achieves self-tolerance without expressing inhibitory receptors specific for self-MHC molecules. *Blood* 105: 4416-4423.
176. Kim, S., J. Poursine-Laurent, S. M. Truscott, L. Lybarger, Y. J. Song, L. P. Yang, A. R. French, J. B. Sunwoo, S. Lemieux, T. H. Hansen, and W. M. Yokoyama. 2005. Licensing of natural killer cells by host major histocompatibility complex class I molecules. *Nature* 436: 709-713.
177. Roth, C., J. R. Carlyle, H. Takizawa, and D. H. Raulet. 2000. Clonal acquisition of inhibitory Ly49 receptors on developing NK cells is successively restricted and regulated by stromal class I MHC. *Immunity* 13: 143-153.
178. Sykes, M., M. W. Harty, F. M. Karlhofer, D. A. Pearson, G. Szot, and W. Yokoyama. 1993. Hematopoietic cells and radioresistant host elements inlfuence natural killer cell differentiation. *Journal of Experimental Medicine* 178: 223-229.
179. Jonsson, A. H., and W. M. Yokoyama. 2009. Natural Killer Cell Tolerance: Licensing and Other Mechanisms. *Advances in Immunology, Vol 101* 101: 27-+.
180. Orr, M. T., and L. L. Lanier. 2010. Natural Killer Cell Education and Tolerance. *Cell* 142: 847-856.
181. Liao, N. S., M. Bix, M. Zijlstra, R. Jaenisch, and D. Raulet. 1991. MHC class-I deficiency - susceptibility to natural killer (NK) cells and impaired NK activity *Science* 253: 199-202.
182. Raulet, D. H., and R. E. Vance. 2006. Self-tolerance of natural killer cells. *Nature Reviews Immunology* 6: 520-531.
183. Yokoyama, W. M., and S. Kim. 2006. How do natural killer cells find self to achieve tolerance? *Immunity* 24: 249-257.
184. Raulet, D. H. 2006. Missing self recognition and self tolerance of natural killer (NK) cells. *Seminars in Immunology* 18: 145-150.
185. Orr, M. T., W. J. Murphy, and L. L. Lanier. 2010. 'Unlicensed' natural killer cells dominate the response to cytomegalovirus infection. *Nature Immunology* 11: 321-U329.
186. Juelke, K., M. Killig, A. Thiel, J. Dong, and C. Romagnani. 2009. Education of hyporesponsive NK cells by cytokines. *European Journal of Immunology* 39: 2548-2555.
187. Wang, L. L., D. T. Chu, A. O. Dokun, and W. M. Yokoyama. 2000. Inducible expression of the gp49B inhibitory receptor on NK cells. *Journal of Immunology* 164: 5215-5220.

188. Dokun, A. O., S. Kim, H. R. C. Smith, H. S. P. Kang, D. T. Chu, and W. M. Yokoyama. 2001. Specific and nonspecific NK cell activation during virus infection. *Nature Immunology* 2: 951-956.
189. Elliott, J. M., J. A. Wahle, and W. M. Yokoyama. 2010. MHC class I-deficient natural killer cells acquire a licensed phenotype after transfer into an MHC class I-sufficient environment. *Journal of Experimental Medicine* 207: 2073-2079.
190. Joncker, N. T., N. Shifrin, F. Delebecque, and D. H. Raulet. 2010. Mature natural killer cells reset their responsiveness when exposed to an altered MHC environment. *Journal of Experimental Medicine* 207: 2065-2072.
191. Elliott, J. M., and W. M. Yokoyama. 2011. Unifying concepts of MHC-dependent natural killer cell eduction. *Trends in Immunology* 32: 364-372.
192. Kiessling, R., E. Klein, and H. Wigzell. 1975. Natural killer cells in mouse. 1.Cytotoxic cells with specificity for mouse moloeny leukemia cells - specificity and distribution according to genotype. *European Journal of Immunology* 5: 112-117.
193. Karre, K., H. G. Ljunggren, G. Piontek, and R. Kiessling. 1986. Selective rejection of H-2-deficient lymphoma variants suggests alternative immune defense strategy *Nature* 319: 675-678.
194. Karlhofer, F. M., R. K. Ribaudo, and W. M. Yokoyama. 1992. MHC class-I alloantigen specificity of Ly-49^{+} IL-2-activated natural killer cells *Nature* 358: 66-70.
195. Deng, L., S. Cho, E. L. Malchiodi, M. C. Kerzic, J. Dam, and R. A. Mariuzza. 2008. Molecular architecture of the major histocompatibility complex class I-binding site of Ly49 natural killer cell receptors. *Journal of Biological Chemistry* 283: 16840-16849.
196. Tormo, J., K. Natarajan, D. H. Margulies, and R. A. Marluzza. 1999. Crystal structure of a lectin-like natural killer cell receptor bound to its MHC class I ligand. *Nature* 402: 623-631.
197. Dam, J., R. J. Guan, K. Natarajan, N. Dimasi, L. K. Chlewicki, D. M. Kranz, P. Schuck, D. H. Margulies, and R. A. Mariuzza. 2003. Variable MHC class I engagement by Ly49 natural killer cell receptors demonstrated by the crystal structure of Ly49C bound to H-2K(b). *Nature Immunology* 4: 1213-1222.
198. Berry, R., J. Rossjohn, and A. G. Brooks. 2014. The Ly49 natural killer cell receptors: a versatile tool for viral self-discrimination. *Immunol. Cell Biol.* 92: 214-220.
199. Dimasi, N., and R. Biassoni. 2005. Structural and functional aspects of the Ly49 natural killer cell receptors. *Immunol. Cell Biol.* 83: 1-8.
200. Wang, J., M. C. Whitman, K. Natarajan, J. Tormo, R. A. Mariuzza, and D. H. Margulies. 2002. Binding of the natural killer cell inhibitory receptor Ly49A to its major histocompatibility complex class I ligand - Crucial contacts include both H-2D(d) and beta(2)-microglobulin. *Journal of Biological Chemistry* 277: 1433-1442.
201. Dimasi, N., M. W. Sawicki, L. A. Reineck, Y. L. Li, K. Natarajan, D. H. Margulies, and R. A. Mariuzza. 2002. Crystal structure of the Ly49I natural

killer cell receptor reveals variability in dimerization mode within the Ly49 family. *Journal of Molecular Biology* 320: 573-585.
202. Natarajan, K., N. Dimasi, J. Wang, D. H. Margulies, and R. A. Mariuzza. 2002. MHC class I recognition by Ly49 natural killer cell receptors. *Molecular Immunology* 38: 1023-1027.
203. Michaelsson, J., A. Achour, A. Rolle, and K. Karre. 2001. MHC class I recognition by NK receptors in the Ly49 family is strongly influenced by the beta(2)-microglobulin subunit. *Journal of Immunology* 166: 7327-7334.
204. Biassoni, R., E. Ugolotti, and A. De Maria. 2009. NK Cell Receptors and Their Interactions with MHC. *Current Pharmaceutical Design* 15: 3301-3310.
205. Sundback, J., A. Achour, J. Michaelsson, H. Lindstrom, and K. Karre. 2002. NK cell inhibitory receptor Ly-49C residues involved in MHC class I binding. *Journal of Immunology* 168: 793-800.
206. Doucey, M. A., L. Scarpellino, J. Zimmer, P. Guillaume, I. F. Luescher, C. Bron, and W. Held. 2004. Cis association of Ly49A with MHC class I restricts natural killer cell inhibition. *Nature Immunology* 5: 328-336.
207. Scarpellino, L., F. Oeschger, P. Guillaume, J. D. Coudert, F. Levy, G. Leclercq, and W. Held. 2007. Interactions of Ly49 family receptors with MHC class I ligands in trans and cis. *Journal of Immunology* 178: 1277-1284.
208. Dam, J., J. Baber, A. Grishaev, E. L. Malchiodi, P. Schuck, A. Bax, and R. A. Mariuzza. 2006. Variable dimerization of the Ly49A natural killer cell receptor results in differential engagement of its MHC class I ligand. *Journal of Molecular Biology* 362: 102-113.
209. Thananchai, H., G. Gillespie, M. P. Martin, A. Bashirova, N. Yawata, M. Yawata, P. Easterbrook, D. W. McVicar, K. Maenaka, P. Parham, M. Carrington, T. Dong, and S. Rowland-Jones. 2007. Cutting edge: Allele-specific and peptide-dependent interactions between KIR3DL1 and HLA-A and HLA-B. *Journal of Immunology* 178: 33-37.
210. Franksson, L., J. Sundback, A. Achour, J. Bernlind, R. Glas, and K. Karre. 1999. Peptide dependency and selectivity of the NK cell inhibitory receptor Ly-49C. *European Journal of Immunology* 29: 2748-2758.
211. Long, E. O., and S. Rajagopalan. 2000. HLA class I recognition by killer cell Ig-like receptors. *Seminars in Immunology* 12: 101-108.
212. Fadda, L., G. Borhis, P. Ahmed, K. Cheent, S. V. Pageon, A. Cazaly, S. Stathopoulos, D. Middleton, A. Mulder, F. H. J. Claas, T. Elliott, D. M. Davis, M. A. Purbhoo, and S. I. Khakoo. 2010. Peptide antagonism as a mechanism for NK cell activation. *Proceedings of the National Academy of Sciences of the United States of America* 107: 10160-10165.
213. Bachmann, M. F., D. E. Speiser, A. Zakarian, and P. S. Ohashi. 1998. Inhibition of TCR triggering by a spectrum of altered peptide ligands suggests the mechanism for TCR antagonism. *European Journal of Immunology* 28: 3110-3119.
214. Kalergis, A. M., and S. G. Nathenson. 2000. Altered peptide ligand-mediated TCR antagonism can be modulated by a change in a single amino acid residue

within the CDR3 beta of an MHC class I-Restricted TCR. *Journal of Immunology* 165: 280-285.
215. Sykulev, Y., Y. Vugmeyster, A. Brunmark, H. L. Ploegh, and H. N. Eisen. 1998. Peptide antagonism and T cell receptor interactions with peptide-MHC complexes. *Immunity* 9: 475-483.
216. Matsumoto, N., W. M. Yokoyama, S. Kojima, and K. Yamamoto. 2001. The NK cell MHC class I receptor Ly49A detects mutations on H-2D(d) inside and outside of the peptide binding groove. *Journal of Immunology* 166: 4422-4428.
217. Matsumoto, N., M. Mitsuki, K. Tajima, W. M. Yokoyama, and K. Yamamoto. 2001. The functional binding site for the C-type lectin-like natural killer cell receptor Ly49A spans three domains of its major histocompatibility complex class I ligand. *Journal of Experimental Medicine* 193: 147-157.
218. Ma, B. J., and K. P. Kane. 2011. Recognition of Class I MHC by a Rat Ly49 NK Cell Receptor Is Dependent on the Identity of the P2 Anchor Amino Acid of Bound Peptide. *Journal of Immunology* 187: 3267-3276.
219. Brennan, J., G. Mahon, D. L. Mager, W. A. Jefferies, and F. Takei. 1996. Recognition of class I major histocompatibility complex molecules by Ly-49: Specificities and domain interactions. *Journal of Experimental Medicine* 183: 1553-1559.
220. Orihuela, M., D. H. Margulies, and W. M. Yokoyama. 1996. The natural killer cell receptor Ly-49A recognizes a peptide-induced conformational determinant on its major histocompatibility complex class I ligand. *Proceedings of the National Academy of Sciences of the United States of America* 93: 11792-11797.
221. Matsumoto, N., R. K. Ribaudo, J. P. Abastado, D. H. Margulies, and W. M. Yokoyama. 1998. The lectin-like NK cell receptor Ly-49A recognizes a carbohydrate-independent epitope on its MHC class I ligand. *Immunity* 8: 245-254.
222. Sundback, J., M. C. Nakamura, M. Waldenstrom, E. C. Niemi, W. E. Seaman, J. C. Ryan, and K. Karre. 1998. The alpha(2) domain of H-2D(d) restricts the allelic specificity of the murine NK cell inhibitory receptor Ly-49A. *Journal of Immunology* 160: 5971-5978.
223. Kane, K. P. 1994. Ly-49 mediates EL4 lymphoma adhesion to isolated class-I major histocompatibility complex molecules *Journal of Experimental Medicine* 179: 1011-1015.
224. Sentman, C. L., M. Y. Olsson, M. Salcedo, P. Hoglund, U. Lendahl, and K. Karre. 1994. H-2 allele-specific protection from NK cell lysis in vitro for lymphoblasts but not tumor targets protection mediated by alpha-1/alpha-2 domains. *Journal of Immunology* 153: 5482-5490.
225. Waldenstrom, M., J. Sundback, M. Y. Olsson-Alheim, A. Achour, and K. Karre. 1998. Impaired MHC class I (H-2D(d))-mediated protection against Ly-49A(+) NK cells after amino acid substitutions in the antigen binding cleft. *European Journal of Immunology* 28: 2872-2881.
226. Mitsuki, M., N. Matsumoto, and K. Yamamoto. 2004. A species-specific determinant on beta(2)-microglobulin required for Ly49A recognition of its MHC class I ligand. *International Immunology* 16: 197-204.

227. Lavender, K. J., and K. P. Kane. 2006. Cross-species dependence of Ly49 recognition on the supertype defining B-pocket of a class I MHC molecule. *Journal of Immunology* 177: 8578-8586.
228. Ljunggren, H. G., and K. Karre. 1985. Host-resistance directed selectively against H-2-deficient lymphoma variants-analysis of the mechanism. *Journal of Experimental Medicine* 162: 1745-1759.
229. Reynolds, C. W., E. W. Bere, and J. M. Ward. 1984. Natural-killer activity in the rat. 3.Characterization of transplantable large granular lymphocyte (LGL) leukemias in the F344 rat *Journal of Immunology* 132: 534-540.
230. Ljunggren, H. G., N. J. Stam, C. Ohlen, J. J. Neefjes, P. Hoglund, M. T. Heemels, J. Bastin, T. N. M. Schumacher, A. Townsend, K. Karre, and H. L. Ploegh. 1990. Empty MHC class-I molecules come out in the cold *Nature* 346: 476-480.
231. Nuchtern, J. G., J. S. Bonifacino, W. E. Biddison, and R. D. Klausner. 1989. Brefeldin-A implicates egress from endoplasmic reticulum in class-I restricted antigen presentation. *Nature* 339: 223-226.
232. Yewdell, J. W., and J. R. Bennink. 1989. Brefeldin-A specifically inhibits presentation of protein antigens to cytotoxic lymphocytes T. *Science* 244: 1072-1075.
233. Hoof, I., B. Peters, J. Sidney, L. E. Pedersen, A. Sette, O. Lund, S. Buus, and M. Nielsen. 2009. NetMHCpan, a method for MHC class I binding prediction beyond humans. *Immunogenetics* 61: 1-13.
234. Neefjes, J., M. L. M. Jongsma, P. Paul, and O. Bakke. 2011. Towards a systems understanding of MHC class I and MHC class II antigen presentation. *Nature Reviews Immunology* 11: 823-836.
235. Mellman, I., and P. Cresswell. 2010. Antigen processing. *Current Opinion in Immunology* 22: 78-80.
236. Kloetzel, P. M. 2001. Antigen processing by the proteasome. *Nature Reviews Molecular Cell Biology* 2: 179-187.
237. Peaper, D. R., and P. Cresswell. 2008. Regulation of MHC class I assembly and peptide binding. In *Annual Review of Cell and Developmental Biology*. 343-368.
238. Dong, G., P. A. Wearsch, D. R. Peaper, P. Cresswell, and K. M. Reinisch. 2009. Insights into MHC Class I Peptide Loading from the Structure of the Tapasin-ERp57 Thiol Oxidoreductase Heterodimer. *Immunity* 30: 21-32.
239. Wearsch, P. A., and P. Cresswell. 2008. The quality control of MHC class I peptide loading. *Current Opinion in Cell Biology* 20: 624-631.
240. Yewdell, J. W. 2007. Plumbing the sources of endogenous MHC class I peptide ligands. *Current Opinion in Immunology* 19: 79-86.
241. Hickman, H. D., A. D. Luis, R. Buchli, S. R. Few, M. Sathiamurthy, R. S. VanGundy, C. F. Giberson, and W. H. Hildebrand. 2004. Toward a definition of self: Proteomic evaluation of the class I peptide repertoire. *Journal of Immunology* 172: 2944-2952.
242. Schirle, M., W. Keilholz, B. Weber, C. Gouttefangeas, T. Dumrese, H. D. Becker, S. Stevanovic, and H. G. Rammensee. 2000. Identification of tumor-

associated MHC class I ligands by a novel T cell-independent approach. *European Journal of Immunology* 30: 2216-2225.

243. de Verteuil, D., D. P. Granados, P. Thibault, and C. Perreault. 2012. Origin and plasticity of MHC I-associated self peptides. *Autoimmunity Reviews* 11: 627-635.
244. Falk, K., O. Rotzschke, S. Stevanovic, G. Jung, and H. G. Rammensee. 1991. Allele-specific motifs revealed by sequencing of self-peptides eluted from MHC molecules. *Nature* 351: 290-296.
245. Fremont, D. H., E. A. Stura, M. Matsumura, P. A. Peterson, and I. A. Wilson. 1995. Crystal structure of an H-2Kb-Ovalbumin peptide complex reveals the interplay of primary and secondary anchor positions in the major histocompatibility complex binding groove. *Proceedings of the National Academy of Sciences of the United States of America* 92: 2479-2483.
246. Jameson, S. C., and M. J. Bevan. 1992. Dissection of major histocompatibility complex (MHC) and T cell receptor contact residues in a Kb-restricted ovalbumin peptide and an assessment of the predictive power of MHC-binding motifs *European Journal of Immunology* 22: 2663-2667.
247. Hogquist, K. A., A. G. Grandea, and M. J. Bevan. 1993. Peptide variants reveal how antibodies recognize major histocompatibility complex class-I. *European Journal of Immunology* 23: 3028-3036.
248. Haemmerling, G. J., E. Ruesch, N. Tada, S. Kimura, and U. Haemmerling. 1982. Localization of allodeterminnats on H-2Kb antigens determined with monoclonal antibodies and H-2 mutant mice. *Proceedings of the National Academy of Sciences of the United States of America* 79: 4737-4741.
249. Sadovnikova, E., and H. J. Stauss. 1996. Peptide-specific cytotoxic T lymphocytes restricted by nonself major histocompatibility complex class I molecules: Reagents for tumor immunotherapy. *Proceedings of the National Academy of Sciences of the United States of America* 93: 13114-13118.
250. Obst, R., N. Netuschil, K. Klopfer, S. Stevanovic, and H. G. Rammensee. 2000. The role of peptides in T cell alloreactivity is determined by self-major histocompatibility complex molecules. *Journal of Experimental Medicine* 191: 805-812.
251. Tallquist, M. D., T. J. Yun, and L. R. Pease. 1996. A single T cell receptor recognizes structurally distinct MHC/peptide complexes with high specificity. *Journal of Experimental Medicine* 184: 1017-1026.
252. Guimezanes, A., G. A. Barrett-Wilt, P. Gulden-Thompson, J. Shabanowitz, V. H. Engelhardt, D. F. Hunt, and A. M. Schmitt-Verhulst. 2001. Identification of endogenous peptides recognized by in vivo or in vitro generated alloreactive cytotoxic T lymphocytes: distinct characteristics correlated with CD8 dependence. *European Journal of Immunology* 31: 421-432.
253. Malarkannan, S., T. Serwold, V. Nguyen, L. A. Sherman, and N. Shastri. 1996. The mouse mammary tumor virus env gene is the source of a CD8(+) T-cell-stimulating peptide presented by a major histocompatibility complex class I molecule in a murine thymoma. *Proceedings of the National Academy of Sciences of the United States of America* 93: 13991-13996.

254. Liu, L. Z., E. Flano, E. J. Usherwood, S. Surman, M. A. Blackman, and D. L. Woodland. 1999. Lytic cycle T cell epitopes are expressed in two distinct phases during MHV-68 infection. *Journal of Immunology* 163: 868-874.
255. Hogquist, K. A., A. J. Tomlinson, W. C. Kieper, M. A. McGargill, M. C. Hart, S. Naylor, and S. C. Jameson. 1997. Identification of a naturally occurring ligand for thymic positive selection. *Immunity* 6: 389-399.
256. Rotzschke, O., K. Falk, S. Stevanovic, G. Jung, P. Walden, and H. G. Rammensee. 1991. Exact prediction of a natural T cell epitope. *European Journal of Immunology* 21: 2891-2894.
257. Vanbleek, G. M., and S. G. Nathenson. 1990. Isolation of an endogenously processed immunodominant viral peptide from the class-I H-2Kb molecule. *Nature* 348: 213-216.
258. Sijts, A., F. Ossendorp, E. A. M. Mengede, P. J. Vandenelsen, and C. J. M. Melief. 1994. Immunodominant MINK cell focus-inducing murine leukemia-versus (MULV)- encoded CTL epitope, identified by its MHC class-I-binding motif, explains MULV-type specificity of MCF-directed cytotoxic T-lymphocytes. *Journal of Immunology* 152: 106-116.
259. McCoy, W. H., X. Wang, W. M. Yokoyama, T. H. Hansen, and D. H. Fremont. 2012. Structural Mechanism of ER Retrieval of MHC Class I by Cowpox. *Plos Biology* 10.
260. Loken, M. R., and A. M. Stall. 1982. Flow-cytometry as an analytical and preparative tool in immunology. *Journal of Immunological Methods* 50: R85-R112.
261. Ajitkumar, P., S. S. Geier, K. V. Kesari, F. Borriello, M. Nakagawa, J. A. Bluestone, M. A. Saper, D. C. Wiley, and S. G. Nathenson. 1988. Evidence that multiple residues on both the alpha-helices of the class-I MHC molecule are simultaneously recognized by the T cell receptor *Cell* 54: 47-56.
262. Stallcup, K. C., T. A. Springer, and M. F. Mescher. 1981. Characterization of an anti-H-2 monoclonal antibody and its use in large scale antigen purification. *Journal of Immunology* 127: 923-930.
263. Cerwenka, A., and L. L. Lanier. 2001. Natural killer cells, viruses and cancer. *Nature Reviews Immunology* 1: 41-49.
264. Natarajan, K., N. Dimasi, J. Wang, R. A. Mariuzza, and D. H. Margulies. 2002. Structure and function of natural killer cell receptors: Multiple molecular solutions to self, nonself discrimination. *Annual Review of Immunology* 20: 853-885.
265. Michaelsson, J., A. Achour, M. Salcedo, A. Kase-Sjostrom, J. Sundback, R. A. Harris, and K. Karre. 2000. Visualization of inhibitory Ly49 receptor specificity with soluble major histocompatibility complex class I tetramers. *European Journal of Immunology* 30: 300-307.
266. Malnati, M. S., M. Peruzzi, K. C. Parker, W. E. Biddison, E. Ciccone, A. Moretta, and E. O. Long. 1995. Peptide specificity in the recognition of MHC class-I by natural killer cell clones *Science* 267: 1016-1018.
267. Meiring, H. D., E. C. Soethout, M. C. M. Poelen, D. Mooibroek, R. Hoogerbrugge, H. Timmermans, C. J. Boog, A. J. R. Heck, A. de Jong, and C.

van Els. 2006. Stable isotope tagging of epitopes - A highly selective strategy for the identification of major histocompatibility complex class I-associated peptides induced upon viral infection. *Molecular & Cellular Proteomics* 5: 902-913.
268. Zarling, A. L., S. B. Ficarro, F. M. White, J. Shabanowitz, D. F. Hunt, and V. H. Engelhard. 2000. Phosphorylated peptides are naturally processed and presented by major histocompatibility complex class I molecules in vivo. *Journal of Experimental Medicine* 192: 1755-1762.
269. Rammensee, H. G., K. Falk, and O. Rotzschke. 1993. Peptides naturally presented by MHC class-I molecules. *Annual Review of Immunology* 11: 213-244.
270. Hudrisier, D., M. B. A. Oldstone, and J. E. Gairin. 1997. The signal sequence of lymphocytic choriomeningitis virus contains an immunodominant cytotoxic T cell epitope that is restricted by both H-2D(b) and H-2K(b) molecules. *Virology* 234: 62-73.
271. Lewicki, H., A. Tishon, P. Borrow, C. F. Evans, J. E. Gairin, K. M. Hahn, D. A. Jewell, I. A. Wilson, and M. B. A. Oldstone. 1995. CTL escape viral variants 1. Generation and molecular characterization. *Virology* 210: 29-40.
272. Achour, A., J. Michaelsson, R. A. Harris, J. Odeberg, P. Grufman, J. K. Sandberg, V. Levitsky, K. Karre, T. Sandalova, and G. Schneider. 2002. A structural basis for LCMV immune evasion: Subversion of H-2D(b) and H-2K(b) presentation of gp33 revealed by comparative crystal structure analyses. *Immunity* 17: 757-768.
273. Fremont, D. H., M. Matsumura, E. A. Stura, P. A. Peterson, and I. A. Wilson. 1992. Crystal structures of 2 viral peptides in complex with murine MHC class-I H-2Kb. *Science* 257: 919-927.
274. Allerbring, E. B., A. D. Duru, H. Uchtenhagen, C. Madhurantakam, M. B. Tomek, S. Grimm, P. A. Mazumdar, R. Friemann, M. Uhlin, T. Sandalova, P.-A. Nygren, and A. Achour. 2012. Unexpected T-cell recognition of an altered peptide ligand is driven by reversed thermodynamics. *European Journal of Immunology* 42: 2990-3000.
275. Boyington, J. C., S. A. Motyka, P. Schuck, A. G. Brooks, and P. D. Sun. 2000. Crystal structure of an NK cell immunoglobulin-like receptor in complex with its class I MHC ligand. *Nature* 405: 537-543.
276. Rajagopalan, S., and E. O. Long. 1997. The direct binding of a p58 killer cell inhibitory receptor to human histocompatibility leukocyte antigen (HLA)-Cw4 exhibits peptide selectivity. *Journal of Experimental Medicine* 185: 1523-1528.
277. Peruzzi, M., K. C. Parker, E. O. Long, and M. S. Malnati. 1996. Peptide sequence requirements for the recognition of HLA-B*2705 by specific natural killer cells. *Journal of Immunology* 157: 3350-3356.
278. Caron, E., K. Vincent, M.-H. Fortier, J.-P. Laverdure, A. Bramoulle, M.-P. Hardy, G. Voisin, P. P. Roux, S. Lemieux, P. Thibault, and C. Perreault. 2011. The MHC I immunopeptidome conveys to the cell surface an integrative view of cellular regulation. *Molecular Systems Biology* 7.
279. Granados, D. P., W. Yahyaoui, C. M. Laumont, T. Daouda, T. L. Muratore-Schroeder, C. Cote, J.-P. Laverdure, S. Lemieux, P. Thibault, and C. Perreault.

2012. MHC I-associated peptides preferentially derive from transcripts bearing miRNA response elements. *Blood* 119: E181-E191.

280. Johansson, S., M. Johansson, E. Rosmaraki, G. Vahlne, R. Mehr, M. Salmon-Divon, F. Lemonnier, K. Karre, and P. Hoglund. 2005. Natural killer cell education in mice with single or multiple major histocompatibility complex class I molecules. *Journal of Experimental Medicine* 201: 1145-1155.
281. Pyzik, M., B. Charbonneau, E. M. Gendron-Pontbriand, M. Babic, A. Krmpotic, S. Jonjic, and S. M. Vidal. 2011. Distinct MHC class I-dependent NK cell-activating receptors control cytomegalovirus infection in different mouse strains. *Journal of Experimental Medicine* 208: 1105-1117.
282. Silver, E. T., D. E. Gong, C. S. Chang, A. Amrani, P. Santamaria, and K. P. Kane. 2000. Ly-49P activates NK-mediated lysis by recognizing H-2D(d). *Journal of Immunology* 165: 1771-1781.
283. Silver, E. T., D. E. Gong, B. Hazes, and K. P. Kane. 2001. Ly-49W, an activating receptor of nonobese diabetic mice with close homology to the inhibitory receptor Ly-49G, recognizes H-2D(k) and H-2D(d). *Journal of Immunology* 166: 2333-2341.
284. Lanier, L. L. 2008. Up on the tightrope: natural killer cell activation and inhibition. *Nature Immunology* 9: 495-502.
285. Lanier, L. L. 1998. NK cell receptors. *Annual Review of Immunology* 16: 359-393.
286. Yokoyama, W. M., S. J. Kim, and A. R. French. 2004. The dynamic life of natural killer cells. *Annual Review of Immunology* 22: 405-429.
287. Zappacosta, F., F. Borrego, A. G. Brooks, K. C. Parker, and J. E. Coligan. 1997. Peptides isolated from HLA-Cw*0304 confer different degrees of protection from natural killer cell-mediated lysis. *Proceedings of the National Academy of Sciences of the United States of America* 94: 6313-6318.
288. Vivian, J. P., R. C. Duncan, R. Berry, G. M. O'Connor, H. H. Reid, T. Beddoe, S. Gras, P. M. Saunders, M. A. Olshina, J. M. L. Widjaja, C. M. Harpur, J. Lin, S. M. Maloveste, D. A. Price, B. A. P. Lafont, D. W. McVicar, C. S. Clements, A. G. Brooks, and J. Rossjohn. 2011. Killer cell immunoglobulin-like receptor 3DL1-mediated recognition of human leukocyte antigen B. *Nature* 479: 401-U155.
289. Back, J., A. Chalifour, L. Scarpellino, and W. Held. 2007. Stable masking by H-2D(d) cis ligand limits Ly49A relocalization to the site of NK cell/target cell contact. *Proceedings of the National Academy of Sciences of the United States of America* 104: 3978-3983.
290. Back, J., E. L. Malchiodi, S. Cho, L. Scarpellino, P. Schneider, M. C. Kerzic, R. A. Mariuzza, and W. Held. 2009. Distinct Conformations of Ly49 Natural Killer Cell Receptors Mediate MHC Class I Recognition in Trans and Cis. *Immunity* 31: 598-608.
291. Lanier, L. L. 2003. Natural killer cell receptor signaling. *Current Opinion in Immunology* 15: 308-314.
292. Zarling, A. L., J. M. Polefrone, A. M. Evans, L. M. Mikesh, J. Shabanowitz, S. T. Lewis, V. H. Engelhardt, and D. F. Hunt. 2006. Identification of class I MHC-

associated phosphopeptides as targets for cancer immunotherapy. *Proceedings of the National Academy of Sciences of the United States of America* 103: 14889-14894.

293. Hunt, D. F., R. A. Henderson, J. Shabanowitz, K. Sakaguchi, H. Michel, N. Sevilir, A. L. Cox, E. Appella, and V. H. Engelhard. 1992. CHARACTERIZATION OF PEPTIDES BOUND TO THE CLASS-I MHC MOLECULE HLA-A2.1 BY MASS-SPECTROMETRY. *Science* 255: 1261-1263.
294. Fricker, L. D., J. Y. Lim, H. Pan, and F. Y. Che. 2006. Peptidomics: identification and quantification of endogenous peptides in neuroendocrine tissues. *Mass Spectrometry Reviews* 25: 327-344.
295. Piguet, V., L. Wan, C. Borel, A. Mangasarian, N. Demaurex, G. Thomas, and D. Trono. 2000. HIV-1 Nef protein binds to the cellular protein PACS-1 to downregulate class I major histocompatibility complexes. *Nature Cell Biology* 2: 163-167.
296. Ishido, S., C. Y. Wang, B. S. Lee, G. B. Cohen, and J. U. Jung. 2000. Downregulation of major histocompatibility complex class I molecules by Kaposi's sarcoma-associated herpesvirus K3 and K5 proteins. *Journal of Virology* 74: 5300-5309.
297. Lybarger, L., X. L. Wang, M. Harris, and T. H. Hansen. 2005. Viral immune evasion molecules attack the ER peptide-loading complex and exploit ER-associated degradation pathways. *Current Opinion in Immunology* 17: 71-78.
298. Chen, W. S., J. W. Yewdell, R. L. Levine, and J. R. Bennink. 1999. Modification of cysteine residues in vitro and in vivo affects the immunogenicity and antigenicity of major histocompatibility complex class I-restricted viral determinants. *Journal of Experimental Medicine* 189: 1757-1764.
299. Andersen, M. H., J. E. Bonfill, A. Neisig, G. Arsequell, I. Sondergaard, J. Neefjes, J. Zeuthen, T. Elliott, and J. S. Haurum. 1999. Phosphorylated peptides can be transported by TAP molecules, presented by class I MHC molecules, and recognized by phosphopeptide-specific CTL. *Journal of Immunology* 163: 3812-3818.
300. Petersen, J., S. J. Wurzbacher, N. A. Williamson, S. H. Ramarathinam, H. H. Reid, A. K. N. Nair, A. Y. Zhao, R. Nastovska, G. Rudge, J. Rossjohn, and A. W. Purcell. 2009. Phosphorylated self-peptides alter human leukocyte antigen class I-restricted antigen presentation and generate tumor-specific epitopes. *Proceedings of the National Academy of Sciences of the United States of America* 106: 2776-2781.
301. Kastrup, I. B., S. Stevanovic, G. Arsequell, G. Valencia, J. Zeuthen, H. G. Rammensee, T. Elliott, and J. S. Haurum. 2000. Lectin purified human class I MHC-derived peptides: evidence for presentation of glycopeptides in vivo. *Tissue Antigens* 56: 129-135.
302. Haurum, J. S., I. B. Hoier, G. Arsequell, A. Neisig, G. Valencia, J. Zeuthen, J. Neefjes, and T. Elliott. 1999. Presentation of cytosolic glycosylated peptides by human class I major histocompatibility complex molecules in vivo. *Journal of Experimental Medicine* 190: 145-150.

303. Karve, T. M., and A. K. Cheema. 2011. Small changes huge impact: the role of protein posttranslational modifications in cellular homeostasis and disease. *Journal of amino acids* 2011: 207691-207691.
304. Apostolopoulos, V., E. Yuriev, P. A. Ramsland, J. Halton, C. Osinski, W. J. Li, M. Plebanski, H. Paulsen, and I. F. C. McKenzie. 2003. A glycopeptide in complex with MHC class I uses the GaINAc residue as an anchor. *Proceedings of the National Academy of Sciences of the United States of America* 100: 15029-15034.
305. Petersen, J., A. W. Purcell, and J. Rossjohn. 2009. Post-translationally modified T cell epitopes: immune recognition and immunotherapy. *Journal of Molecular Medicine-Jmm* 87: 1045-1051.
306. Betser-Cohen, G., G. Katz, T. Gonen-Gross, N. Stern, T. I. Arnon, H. Achdout, R. Gazit, and O. Mandelboim. 2006. Reduced KIR2DL1 recognition of MHC class I molecules presenting phosphorylated peptides. *Journal of Immunology* 176: 6762-6769.
307. Speir, J. A., U. M. Abdel-Motal, M. Jondal, and I. A. Wilson. 1999. Crystal structure of an MHC class I presented glycopeptide that generates carbohydrate-specific CTL. *Immunity* 10: 51-61.